

**GENERALIZED MODAL IDENTIFICATION
OF LINEAR AND NONLINEAR DYNAMIC SYSTEMS**

**Thesis by
Chia-Yen Peng**

**In Partial Fulfillment of the Requirements
for the Degree of
Doctor of Philosophy**

**California Institute of Technology
Pasadena, California**

1988

(Submitted September 1987)

To My Parents

Acknowledgments

I would like to express my appreciation to my advisor, Professor W. D. Iwan, for his guidance and for the opportunity he has given me to investigate various challenging engineering problems. The experience and knowledge obtained from these investigations have taught me how to solve new problems with confidence.

To my former advisor, Professor Chau-Shioung Yeh of the National Taiwan University who first encouraged me to pursue my graduate study at the California Institute of Technology, I am grateful for the concern and encouragement he has given me all these years.

I am grateful to all my teachers at the National Taiwan University and California Institute of Technology for the excellent education that I received. The willingness of members of the examining committee, Professors Paul C. Jennings, James K. Knowles, John F. Hall and James L. Beck to spend their time reviewing the dissertation is much appreciated.

Particular thanks are due to Professor Beck and P. Jayakumar for generously providing the U.S.-Japan pseudo-dynamic test data. The assistance of Crista Potter and Sharon Beckenbach in preparing this manuscript is appreciated. The support of the National Science Foundation is also acknowledged.

This thesis is dedicated to my parents, my first tutors in life and science, and all my family for their constant support and encouragement throughout my education. I especially wish to express my deep gratitude to my beloved wife, Wan-Shiun, who has been to me the most lovely, encouraging and understanding person involved in this educational endeavor. The happiness of living with her has always been the driven force of my career.

Abstract

This dissertation is concerned with the problem of determining the dynamic characteristics of complicated engineering systems and structures from the measurements made during dynamic tests or natural excitations. Particular attention is given to the identification and modeling of the behavior of structural dynamic systems in the nonlinear hysteretic response regime. Once a model for the system has been identified, it is intended to use this model to assess the condition of the system and to predict the response to future excitations.

A new identification methodology based upon a generalization of the method of modal identification for multi-degree-of-freedom dynamical systems subjected to base motion is developed. The situation considered herein is that in which only the base input and the response of a small number of degrees-of-freedom of the system are measured. In this method, called the generalized modal identification method, the response is separated into "modes" which are analogous to those of a linear system. Both parametric and nonparametric models can be employed to extract the unknown nature, hysteretic or nonhysteretic, of the generalized restoring force for each mode.

In this study, a simple four-term nonparametric model is used first to provide a nonhysteretic estimate of the nonlinear stiffness and energy dissipation behavior. To extract the hysteretic nature of nonlinear systems, a two-parameter distributed-element model is then employed. This model exploits the results of the nonparametric identification as an initial estimate for the model parameters. This approach greatly improves the convergence of the subsequent optimization process.

The capability of the new method is verified using simulated response data from a three-degree-of-freedom system. The new method is also applied to the analysis of response data obtained from the U.S.-Japan cooperative pseudo-dynamic test of

a full-scale six-story steel-frame structure.

The new system identification method described has been found to be both accurate and computationally efficient. It is believed that it will provide a useful tool for the analysis of structural response data.

Table of Contents

ACKNOWLEDGMENTS		iii
ABSTRACT		iv
CHAPTER 1	INTRODUCTION	1
	References	5
CHAPTER 2	GENERALIZED MODAL IDENTIFICATION METHOD	9
	2.1 Introduction	9
	2.2 Nonlinear System	10
	2.3 Modal Representation	11
	2.4 Identification Problem	15
	2.5 Minimization Criterion	16
	2.6 Identification Methodology	17
	2.6.1 Single-Mode Identification	17
	2.6.2 Estimation of the Modal Response	19
	2.6.3 Estimation of the Modal Restoring Force	23
	2.6.4 Estimation of the Modal Participation Factor	24
	2.7 Summary	25
	References	27
CHAPTER 3	GENERALIZED MODAL IDENTIFICATION USING NONHYSTERETIC MODELS	29
	3.1 Introduction	29
	3.2 Nonparametric Identification Techniques	29
	3.3 Nonhysteretic Restoring Force Models	30
	3.3.1 Linear Models	30
	3.3.2 Nonparametric Models	31
	3.4 Four-Parameter Nonparametric Model	35
	3.4.1 Model Considerations	35
	3.4.2 General Description	38
	3.4.3 Parameter Estimation	39
	3.5 Verification with Simulated Data	40
	3.5.1 Data Generation	40
	3.5.2 Model Identification—Parameter Calibration	49
	3.5.3 Model Validation—Response Prediction	58
	3.6 Summary	66
	References	67

CHAPTER 4	GENERALIZED MODAL IDENTIFICATION USING HYSTERETIC MODELS	69
4.1	Introduction	69
4.2	The Backbone Curve	70
4.3	Hysteretic Restoring Force Models	73
4.3.1	The Elasto-Plastic Model	73
4.3.2	The Bilinear Model	75
4.3.3	Smooth Backbone Models	75
4.4	Two-Parameter Distributed-Element Model	80
4.4.1	Model Considerations	80
4.4.2	General Description	82
4.4.3	Specification of k_i^r and y_i^{r*}	83
4.4.4	Parameter Estimation	84
4.5	Verification with Simulated Data	85
4.5.1	Model Identification—Parameter Calibration	85
4.5.2	Model Validation—Response Prediction	91
4.6	Summary	99
	References	100
CHAPTER 5	APPLICATION TO PSEUDO-DYNAMIC TEST DATA	103
5.1	Introduction	103
5.2	Pseudo-Dynamic Testing Method	104
5.2.1	General Features	104
5.2.2	Test Procedures	105
5.3	BRI Testing Program	108
5.4	Four-Parameter Nonhysteretic Model	113
5.5	Two-Parameter Hysteretic Model	121
5.6	Summary	130
	References	131
CHAPTER 6	CONCLUSIONS	134

Chapter 1

Introduction

The determination of mathematical models of dynamic systems from vibration measurements is a problem, commonly called system identification, of considerable importance in the area of applied mechanics. One major reason for this importance is the fact that it is not always possible to develop realistic, reliable theoretical and computational models for today's complicated engineering systems and structures. In situations where a more accurate interpretation/prediction of the behavior of systems is required, it is often necessary to develop an experimentally verified model. For example, in order to describe the response of structures to damaging excitations like earthquakes, consideration must be given to proper understanding and modeling of nonlinear structural behavior during strong ground motions. The rapid advance in high-speed digital computation and the increasing use of dynamic testing of complex systems have led to a growing interest in the development of new methodologies for efficient system identification [1-27].

Analytical modeling of dynamical systems is usually carried out at the design stage. Because of a priori knowledge, the dynamic response of many physical systems is typically described by a set of second order ordinary differential equations [28-30]. This set of equations represents a discrete model for the physical system of interest and may, for conceptual purposes, be thought of in terms of a system of mass or nodal points interconnected by elements whose behavior depends upon the relative motion between these points. Many analytical techniques, such as finite difference and finite element methods, [31-33] are available to derive such dynamic models for complex engineering systems and structures. These analytical models are used for response prediction during design. However, there are uncertainties involved in determining analytical models and assumptions have to be made accordingly.

In order to evaluate the assumptions made in design or to improve analytical models, it is often necessary, after the system has been built, to determine its actual characteristics experimentally based on response and/or excitation data measured during dynamic tests or natural excitations [34-37]. This gives rise to the development of various techniques for analyzing measured vibration data. Though any method used to determine the dynamic characteristics of a system from test data may, in a broad sense, be considered a system identification method, usually only those methods that use systematic mathematical techniques in the analysis are so designated [1-4]. The models derived from system identification may not only be used to assess the engineering practice in developing design models but can also themselves be taken as more realistic models for predicting the system response to future excitations.

In applications in the field of structural dynamics [38-41], most system identification performed so far has assumed that the structure is linear and that its properties are independent of the characteristics of the excitation or the response. It is further assumed that all the energy dissipation of the structural system may be represented by classical viscous damping. Thus, the analysis reduces to the problem of identifying the parameters of a structural model from its response, and excitation if available. Since a linear viscoously damped system may be represented by its physical parameters (mass, stiffness and damping matrices), or by its modal parameters (natural frequency, modal damping, modal participation factors), there is a choice of which parameters can be identified reliably in a given situation [42-52].

Two problems are common to all the efforts of structural identification. First, the number of response measurements is usually small. Frequently, only two records may be available, one at the base of the structure and the other near the top of the structure. Because of this problem and noise in the measurements [42-47], it is necessary in practice to estimate the parameters of the dominant modes in the response, rather than the physical parameters [48-49]. The process of characterizing the dynamic properties of an elastic stru-

culture by identifying its modes of vibration is commonly referred as modal identification [50-52]. Second, nonlinear behavior is observed for many cases of strong shaking [8-14]. Thus, linear time-invariant models cannot be used successfully to treat the entire duration of response. The absence of a well-established analytical technique for determining nonlinear structural models from vibration measurements has seriously limited the utility of these data.

The objective of the research described in this dissertation is to solve some of the above-mentioned problems by developing a relatively simple approach to the identification of nonlinear dynamic systems that is suitable for application to seismically excited structures. For this purpose, particular attention is given to the identification and modeling of the response behavior of nonlinear hysteretic systems under the action of base motion.

The problem is formulated in Chapter 2 through a generalization of the method of modal identification for multi-degree-of-freedom nonlinear dynamical systems subjected to base motion. This method, called the generalized modal identification method, considers the situation in which only the support excitation and the response at a small number of points in the system are measured. Both parametric and nonparametric models can be employed with the method. The error measure employed throughout is the difference between the actual system and model response at peaks only.

In Chapter 3 consideration is given to the generalized modal identification method incorporating nonhysteretic restoring force models. First, a class of nonparametric models which is suitable for nonlinear memoryless systems is reviewed. Subsequently, a model with only four parameters is proposed based on model simplicity and computational considerations. The identification algorithm together with the model are tested with simulated data generated for a nonlinear hysteretic system. The results provide insight into the use of nonparametric methods in the preliminary identification studies of hysteretic systems.

In order to extract the hysteretic response behavior of a nonlinear structural system, Chapter 4 is concerned with the generalized modal identification method incorporating

hysteretic restoring force models. A discussion of available models for hysteretic systems is presented with emphasis on the mathematical form of the backbone curve. Based on this investigation and the insight obtained in Chapter 3, a physically motivated model with a backbone curve characterized by only two parameters is proposed. This model employs the results of the nonparametric identification as an initial estimate for the backbone parameters. This approach greatly improves the convergence and efficiency of the subsequent parameter optimization process.

Finally, in Chapter 5 the generalized modal identification method is applied to the analysis of response data obtained from the U.S.-Japan cooperative pseudo-dynamic test of a full-scale six-story steel-frame structure. In marked contrast to most nonlinear system identification techniques, the roof response and base input only are employed in the analysis. This example is intended to illustrate that the method proposed in this dissertation is capable of providing an accurate representation of the hysteretic response of a real structure. Both nonhysteretic and hysteretic models are identified using the generalized modal identification method. The nonparametric model proposed in Chapter 3 is employed initially to give a nonhysteretic estimate of the nonlinear stiffness and energy dissipation behavior. Subsequently, the parametric model introduced in Chapter 4 is used to obtain the final hysteretic model which characterizes the nonlinear behavior of the test structure.

General conclusions and recommendations for further study are presented in Chapter 6.

References

- [1] G. A. Bekey, "System Identification, an Introduction and a Survey," *Simulation*, October 1970.
- [2] P. Eykhoff, *System Identification*, John Wiley & Sons, Inc., 1974.
- [3] R. K. Mehra and D. G. Lainiotis (editors), *System Identification: Advances and Case Studies*, Mathematics in Science and Engineering, Vol. 126, Academic Press, New York, 1976.
- [4] J. V. Beck and K. J. Aenold, *Parameter Estimation in Engineering and Science*, John Wiley & Sons, Inc., 1977.
- [5] N. Distefano and R. Todeschini, "Modeling, Identification and Prediction of a Class of Nonlinear Viscoelastic Materials," *International Journal of Solids and Structures*, Vol. 9, 1976.
- [6] W. D. Pilkey and R. Cohen (editors), "System Identification of Vibrating Structures: Mathematical Models from Test Data," ASME publications, 1972.
- [7] P. Ibanez, "Identification of Dynamic Parameters of Linear and Nonlinear Structural Models from Experimental Data," *Journal of Nuclear Engineering and Design*, Vol. 25, 1975.
- [8] F. E. Udawadia and M. D. Trifunac, "Time and Amplitude Dependent Response of Structures," *International Journal of Earthquake Engineering and Structural Dynamics*, Vol. 2, 1974.
- [9] H. Iemura and P. C. Jennings, "Hysteretic Response of a Nine-Storey Reinforced Concrete Building," *International Journal of Earthquake Engineering and Structural Dynamics*, Vol. 3, 1974.
- [10] A. M. Abdel-Ghaffar and R. F. Scott, "Experimental Investigation of the Dynamic Response Characteristics of an Earth Dam," *Proceedings of the 2nd U.S. National Conference on Earthquake Engineering*, 1979.
- [11] A. M. Abdel-Ghaffar and R. F. Scott, "Vibration Tests of Full-Scale Earth Dam," *ASCE Journal of Geotechnical Engineering Division*, 1981.
- [12] S. Toussi and J. Yao, "Identification of Hysteretic Behavior for Existing Structures," Report No. CE-STR-80-19, School of Civil Engineering, Purdue University, December 1980.
- [13] S. Toussi and J. Yao, "Hysteretic Identification of Multi-Story Buildings," Report No. CE-STR-81-15, School of Civil Engineering, Purdue University, May 1981.
- [14] A. O. Cifuentes, "System Identification of Hysteretic Structures," Earthquake

Engineering Research Laboratory, Report No. EERL 84-04, California Institute of Technology, September 1984.

- [15] P. Eykhoff (editor), *Trends and Progress in System Identification*, Pergamon Press, New York, 1981.
- [16] B. J. Heieh, C. A. Kot, and M. G. Srinivasan, "Evaluation of System Identification Methodology and Application," U. S. Nuclear Regulatory Committee Report NUREG/CR-3388, Argonne National Laboratory ANL-83-38, Washington, D. C., May 1983.
- [17] T. K. Caughey, "Nonlinear Analysis, Synthesis and Identification Theory," *Proceedings of the Symposium on Testing and Identification of Nonlinear Systems*, California Institute of Technology, March 1975.
- [18] S. F. Masri, T. K. Caughey, "A Nonparametric Identification Technique for Nonlinear Dynamic Problems," *ASME Journal of Applied Mechanics*, Vol. 46, June 1979.
- [19] S. F. Masri, H. Sassi, and T. K. Caughey, "Nonparametric Identification of Nearly Arbitrary Nonlinear Systems," *ASME Journal of Applied Mechanics*, Vol. 11, January 1981.
- [20] S. F. Masri, G. A. Bekey, H. Sassi, and T. K. Caughey, "Nonparametric Identification of a Class of Nonlinear Multidegree Dynamic Systems," *Journal of Earthquake Engineering and Structural Dynamics*, Vol. 10, 1982.
- [21] F. E. Udawadia and C-P Kuo, "Nonparametric Identification of a Class of Nonlinear Close-Coupled Dynamic Systems," *International Journal of Earthquake Engineering and Structural Dynamics*, Vol. 9, 1981.
- [22] M. B. Priestley, *Spectral Analysis and Time Series*, Vol. 1 and 2, Academic Press, Inc., 1981.
- [23] M. Hoshiya and E. Saito, "Structural Identification by Extended Kalman Filter," *ASCE Journal of Engineering Mechanics Division*, Vol. 110, No. 12, 1984.
- [24] M. H. A. Davis, "New Approach to Filtering for Nonlinear Systems," *IEE Proc.*, Vol. 128, PT. D, No. 5, September 1981.
- [25] S. A. Billings, "Identification of Nonlinear Systems - A Survey," *IEE Proc.*, Vol. 127, PT. D, No. 6, November 1980.
- [26] J. L. Beck and P. Jayakumar, "Pseudo-Dynamic Testing and Model Identification," *Proceedings of the 3rd U.S. National Conference on Earthquake Engineering*, Charleston, South Carolina, August, 1986.
- [27] J. L. Beck and P. Jayakumar, "Application of System Identification to Pseudo-Dynamic Test Data from a Full-Scale Six-Story Steel Structure," *Proceedings*

- of the International Conference on Vibration Problems in Engineering, Xian, China, June 1986.*
- [28] Lectures by Professor W. D. Iwan on Dynamics and Vibrations, California Institute of Technology, Pasadena, California, 1982-83.
 - [29] Lectures by Professor P. C. Jennings on Earthquake Engineering, California Institute of Technology, Pasadena, California, 1983-84.
 - [30] Lectures by Professor T. K. Caughey on Advanced Dynamics, California Institute of Technology, Pasadena, California, 1984-85.
 - [31] Lectures by Professor J. F. Hall on Finite Element Method, California Institute of Technology, Pasadena, California, 1983-84.
 - [32] O. C. Zienkiewicz, *The Finite Element Method in Engineering Science*, McGraw-Hill, London, 1971.
 - [33] K. J. Bathe and E. L. Wilson, *Numerical Methods in Finite Element Analysis*, Prentice-Hall, Englewood Cliffs, N.J., 1976.
 - [34] J. L. Beck, "System Identification Applied to Strong Motion Records from Structures," *Earthquake Ground Motion and Its Effects on Structures*, S. K. Datta (ed.) ASME, AMD-Vol. 53, New York, 1982.
 - [35] M. G. Srinivasan, C. A. Kot, and B. J. Hsieh, "Dynamic Testing of As-Built Civil Engineering Structures - A Review and Evaluation," U. S. Nuclear Regulatory Committee Report NUREG/CR-36, Argonne National Laboratory ANL-83-20, Washington, D. C., January 1983.
 - [36] M. G. Srinivasan, C. A. Kot, B. J. Hsieh, and H. H. Chung, "Feasibility of Dynamic Testing of As-Built Nuclear Power Plant Structures: An Interim Evaluation," U. S. Nuclear Regulatory Committee Report NUREG/CR-1937, Argonne National Laboratory ANL-CT-81-5, Washington, D. C., May 1981.
 - [37] E. C. Ting, S. J. H. Chen, and J. T. P. Yao, "System Identification, Damage Assessment and Reliability Evaluation of Structures," School of Civil Engineering, GE-STR-78-1, Purdue University, W. Lafayette, Indiana, 1978.
 - [38] S. D. Werner, J. L. Beck, and M. B. Levine, "Seismic Response Evaluation of Meloland Road Overpass Using 1979 Imperial Valley Earthquake Records," *International Journal of Earthquake Engineering and Structural Dynamics*, Vol. 15, 1987.
 - [39] P. Ibanez, "Review of Analytical and Experimental Techniques for Improving Structural Dynamic Models," *Welding Research Council Bulletin*, No. 249, June 1979.
 - [40] G. C. Hart and J. T. P. Yao, "System Identification in Structural Dynamics," *ASCE Journal of Engineering Mechanics Division*, Vol. 103, No. 6,

December 1977.

- [41] F. E. Udwadia and P. Z. Marmarelis, "System Identification of Building Structural Systems" *Bulletin of Seismological Society of America*, Vol. 66, February, 1976.
- [42] J. S. Bendat and K. J. Arnold, *Random Data: Analysis and Measurement Procedures*, John Wiley & Sons, Inc., 1977.
- [43] J. S. Bendat and A. G. Piersol, *Engineering Applications of Correlation and Spectral Analysis*, John Wiley & Sons, Inc., 1980.
- [44] M. D. Trifunac and V. Lee, "Routine Computer Processing of Strong-Motion Accelerograms," Earthquake Engineering Research Laboratory, Report No. EERL 73-03, California Institute of Technology, Pasadena, California, October 1973.
- [45] D. E. Hudson, *Reading and Interpreting Strong Motion Accelerograms*, Earthquake Engineering Research Institute, Berkeley, California, 1979.
- [46] V. W. Lee and M. D. Trifunac, "Current Developments in Data Processing of Strong Motion Accelerograms," University of Southern California, Department of Civil Engineering, Report No. CE-84-01, Los Angeles, California, August 1984.
- [47] W. D. Iwan, M. A. Moser, and C. Y. Peng, "Some Observations on Strong-Motion Earthquake Measurement Using a Digital Accelerograph," *Bulletin of Seismological Society of America*, Vol. 75, October 1985.
- [48] F. E. Udwadia, D. K. Sharma, and P. C. Shah, "Uniqueness of Damping and Stiffness Distribution in the Identification of Soil and Structural Systems," *ASME Journal of Applied Mechanics*, Vol. 45, March 1978.
- [49] J. L. Beck and P. C. Jennings, "Structural Identification Using Linear Models and Earthquake Records," *International Journal of Earthquake Engineering and Structural Dynamics*, Vol. 8, 1980.
- [50] "Modal Analysis - A Special Supplement to Experimental Techniques Supplied by the SEM Modal Analysis/Dynamic Systems Technical Activity Committee," *Experimental Techniques*, October 1985.
- [51] S. R. Ibrahim, "Modal Identification Techniques Assessment and Comparison," *Proceedings of the 3rd International Modal Analysis Conference*, Orlando, Florida, January 1985.
- [52] R. Schmidtberg, "Solving Vibration Problems Using Modal Analysis," *Sound and Vibration*, March 1986.

Chapter 2

Generalized Modal Identification Method

2.1 Introduction

In this Chapter a generalization of the method of modal identification for multi-degree-of-freedom nonlinear dynamical systems subjected to base excitation is presented. The case considered here is that in which only the base input and the response at a small number of points in the system are measured.

For the case of linear systems, the method of modal identification has been developed in both the time and frequency domains. References [1] and [2] are examples of two fundamentally equivalent approaches in the time and frequency domains, respectively. In general, linear models are only sufficient to describe and predict the dynamic response resulting from low-level excitations. However, the response of many systems during strong excitations is highly nonlinear and hysteretic. This reveals the inadequacies of many assumptions made in conventional modal identification methods using linear models, and the need for a well-established identification technique for nonlinearly responding systems. This motivates the present development.

Herein, an appropriate form of the equations of motion for a nonlinear system is derived. This form is then used to develop a new identification methodology. In this methodology, the response is decomposed into "modes" which are analogous to those for a linear system. The generalized restoring force for each mode is identified by employing nonparametric or parametric models. Consequently, the methodology reduces the identification problem to the determination of the effective participation factor for each mode which is performed by means of a one-dimensional optimization algorithm. The error minimization criterion selected is the difference between the

peaks of actual system and corresponding model response. This approach is motivated by the observation that peaks are generally the points of greatest significance in the response time history.

The new identification methodology proposed results in considerable computational efficiency. The information obtained is useful for characterizing the nonlinear behavior of structures and for predicting structural response to future excitations.

2.2 Nonlinear System

In this section the equations of motion which describe the response of a time-invariant nonlinear dynamical system are considered.

Although most engineering systems are continuous, in some cases, including building structures, the dynamics can be represented adequately by assuming the systems as an assemblage of lumped masses which are interconnected by discrete elements with arbitrary nonlinear characteristics. The motion of each lumped mass is governed by Newton's second law. This will yield one equation for each degree-of-freedom of each mass in the system. Combined, the equations of motion of the entire system are obtained and can be written in matrix form as

$$M\ddot{\underline{y}} + \underline{f}(\underline{y}, \dot{\underline{y}}) = \underline{p}(t) , \quad (2.1)$$

where a dot above a variable denotes differentiation with respect to the temporal variable t . M is a constant $n \times n$ inertia matrix, \underline{y} represents the state vector, \underline{f} is the nonlinear restoring force vector, and $\underline{p}(t)$ is the dynamic forcing vector.

For systems with complex geometries, material properties or boundary conditions, many analytical tools have been developed to derive equation (2.1). One of the most powerful and popular techniques is the finite element method. In this method, M and \underline{f} are assembled systematically by summing the contributions from each of the subcomponents of the system, called the finite elements. However, there

are uncertainties involved in determining the nature of the loading conditions and material properties and in modeling of certain physical aspects. These uncertainties impose limitations on the method and require other techniques to determine an experimentally verified model (2.1). One of the techniques is system identification.

For seismically excited structures, equation (2.1) may be expressed as

$$M\ddot{\underline{y}} + \underline{f}(\underline{y}, \dot{\underline{y}}) = -M\underline{1}\ddot{\underline{z}}(t), \quad (2.2)$$

where M is the mass matrix of order n , \underline{y} is the relative displacement vector with respect to the base, \underline{f} is the nonlinear restoring force vector and $\ddot{\underline{z}}(t)$ is the base acceleration. All the components of $\underline{1}$ are unity.

Equation (2.2), representing an open system (i.e., no feedback of the output of the system as input to the system), is the basic mathematical model used in almost all system identification methodologies for analyzing the seismic response of a structure.

2.3 Modal Representation

Consider the response of a representative six-story steel frame structure which was excited pseudo-dynamically into the inelastic range [3,4]. Figure 2.1 shows the Fourier amplitude spectrum for the relative acceleration at the roof with respect to the base. From the figure, the dominance of a number of frequencies and corresponding "modes" is clearly observed. The somewhat erratic appearance around each dominant frequency peak is partly due to the nonlinearity of the system. A similar response frequency spectrum is also observed for the nonlinear response of structures excited by actual earthquakes. For example, Figure 2.2 shows the Fourier amplitude spectrum of acceleration for the N11E component of the Bank of California building [5]. Based on these observations of nonlinear response in the frequency domain, it is assumed that the nonlinear response can be decomposed

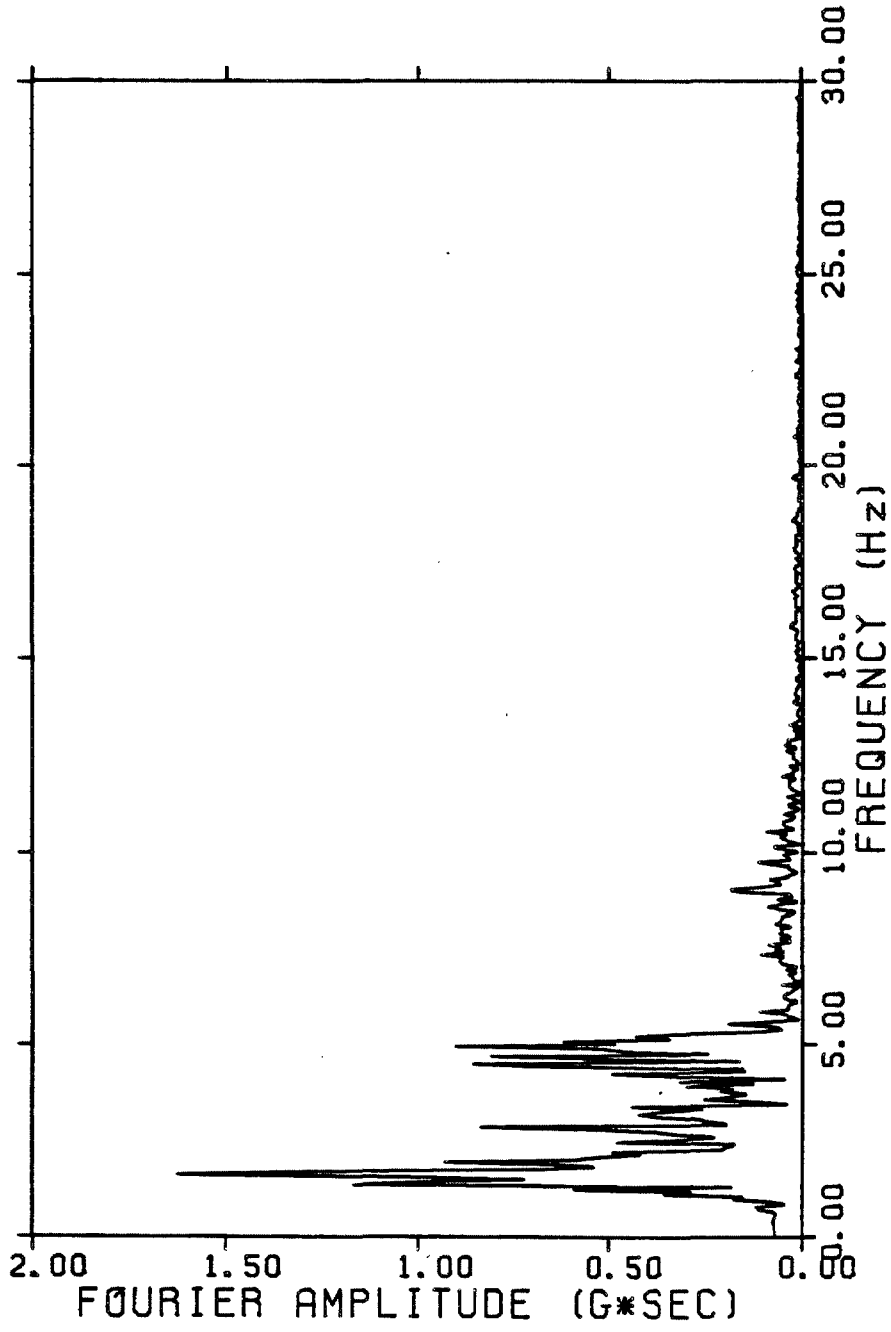


Figure 2.1 Fourier amplitude spectrum of relative acceleration for the roof response of a steel structure tested pseudo-dynamically.

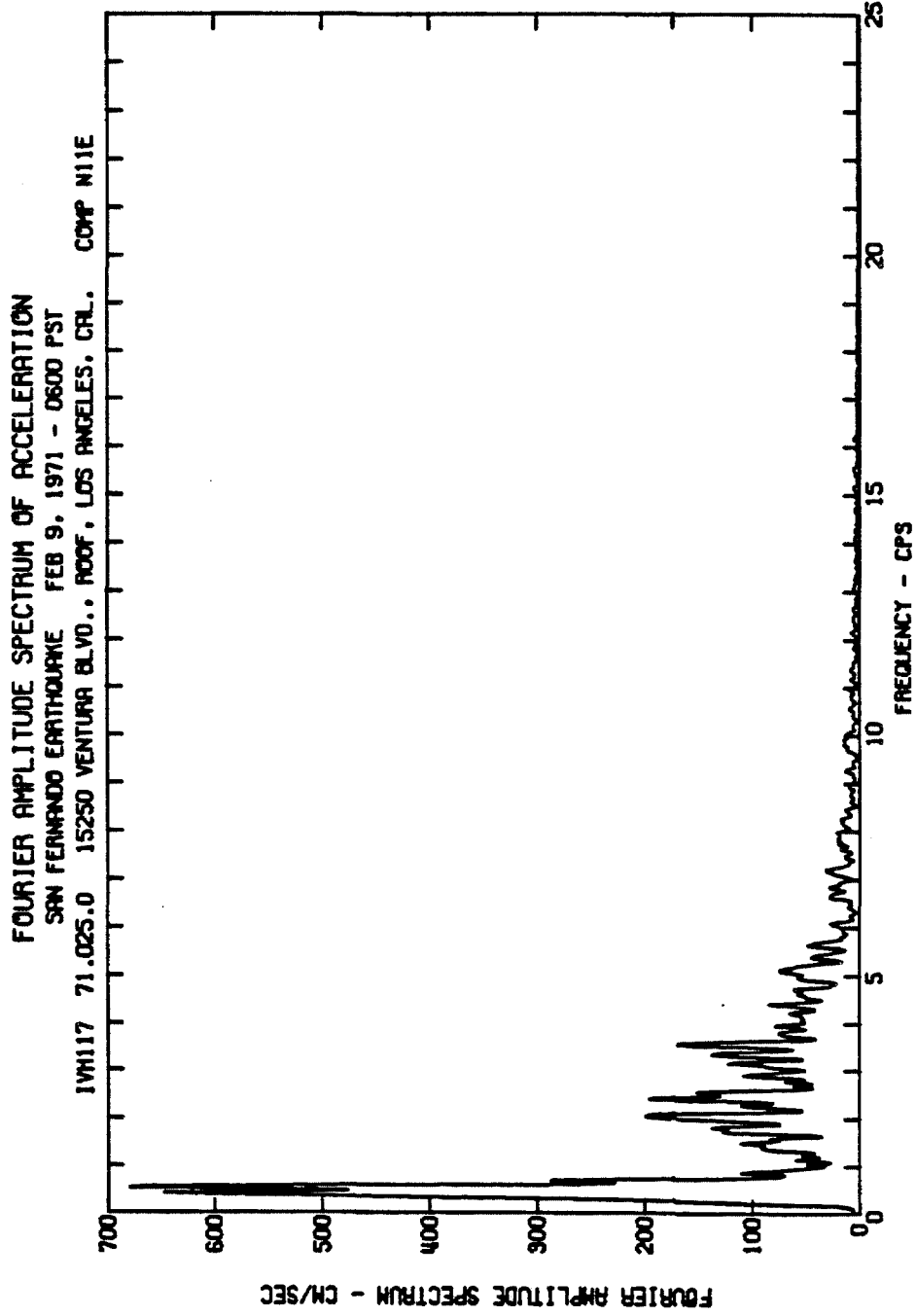


Figure 2.2 Fourier amplitude spectrum of acceleration for the N11E component of the Bank of California building to the San Fernando earthquake of 1971 [5].

into "modes" which are analogous to those of a linear system. Accordingly, a more appropriate form of the nonlinear system (2.2) is necessary to describe these modes. This form is an analogy to the modal equations of a linear system, and is derived from equation (2.2) by a similar transformation procedure.

Consider a nonlinear dynamic system whose motion is governed by (2.2).

Let

$$\underline{y}(t) = \Phi \underline{u}(t) , \quad (2.3)$$

where Φ is an $n \times m$ transformation matrix whose columns are a set of appropriate orthonormal "modal vectors" for the system (2.2). It will be assumed that m is less than or equal to n . Substituting (2.3) into (2.2) and pre-multiplying by Φ^T yields

$$\underline{\tilde{u}} + \underline{g}(\underline{u}, \underline{\dot{u}}) = -\underline{\alpha} \underline{\tilde{z}}(t) , \quad (2.4)$$

where $\underline{g} = \Phi^T \underline{f}$ and $\underline{\alpha} = \Phi^T \underline{1}$. In component form, equation (2.4) becomes

$$\tilde{u}_r + g_r(\underline{u}, \underline{\dot{u}}) = -\alpha_r \tilde{z}(t) ; \quad r = 1, 2, \dots, m . \quad (2.5)$$

Equations (2.5) are analogous to the modal equations for a linear system.

Next, define $y_i^r(t)$ as

$$y_i^r(t) = \phi_{ir} u_r(t) . \quad (2.6)$$

y_i^r may be considered to be the r^{th} generalized modal displacement at station i . Then, the total displacement at station i may be expressed as

$$y_i(t) = \sum_{r=1}^m y_i^r(t) , \quad (2.7)$$

where the y_i^r satisfies the equation

$$\ddot{y}_i^r + h_i^r(\dot{y}_i^r, y_i^r) = -\beta_i^r \tilde{z}(t) ; \quad s = 1, 2, \dots, m . \quad (2.8)$$

h_i^r is herein referred to as the generalized modal restoring force and β_i^r as the effective modal participation factor. In general, h_i^r is coupled as shown in equation

(2.8) since $h_i^r = \phi_{i,r} g_r$ and g_r is coupled in \underline{u} and $\dot{\underline{u}}$. Equation (2.7) represents a kind of modal superposition.

Equations (2.7) and (2.8) are the basic equations used to describe the response of the i^{th} degree of freedom. They are fundamental to the development and application of the method.

2.4 Identification Problem

The problem of system identification is to determine a model that describes input-output data obtained from a given system. The choice of model parameters is, as a rule, made based on some optimality criterion. The criterion is that the prediction error is minimized. The prediction error is usually defined as a function of the difference between the response predicted by the model and that actually measured from the system. Minimization criteria based on the prediction error are employed throughout in this dissertation to develop both parametric and nonparametric identification methods in a unified framework. This framework is described below.

As applied to dynamical systems, the identification problem can be formulated as minimizing the prediction error P according to the criterion

$$P(\underline{\theta}) = P(\underline{x}(t) - \hat{\underline{x}}(t; \underline{\theta})) = \text{minimum w.r.t. } \underline{\theta} \quad (2.9)$$

subject to

$$\frac{d\hat{\underline{x}}(t; \underline{\theta})}{dt} = \underline{f}(\hat{\underline{x}}, \underline{z}(t), t; \underline{\theta}) \quad (2.10)$$

and

$$\underline{g}(\underline{\theta}) \geq \underline{0}. \quad (2.11)$$

In this formulation, the function P needs to be specified in each case in terms the difference between the measured response \underline{x} and the predicted response $\hat{\underline{x}}$. A common definition of P is given in the next section. $\underline{\theta}$ is the vector of model

parameters. Note that in the case of nonparametric identification, $\underline{\theta}$ is a vector of unknown functions rather than unknown parameters. The model state $\hat{\underline{x}}$ is described by a state equation expressed in the general first-order form (2.10) in which $\underline{z}(t)$ represents the input to the system and the model. The parameter constraints are specified through (2.11). Any solution must satisfy both the dynamic constraints (2.10) and the static constraints (2.11).

2.5 Minimization Criterion

A simple mathematical model can never represent every detail of an actual system, and vibration measurements are inevitably contaminated by noise. Therefore, it is impossible that the parameters of an assumed model will ever result in a perfect match between the measured and computed responses. In the present formulation, the discrepancy between the state of the model and system is measured by the prediction error P . The parameters $\underline{\theta}$ are considered being determined if the prediction error P is minimized to an acceptable degree.

A variety of different error minimization criteria may be employed. The root-mean-squares criterion has been used by many researchers [6-8]. A common definition is

$$P(\underline{\theta}) = \frac{\frac{1}{T_o} \int_0^{T_o} [\underline{z}(t) - \hat{\underline{x}}(t; \underline{\theta})]^T [\underline{z}(t) - \hat{\underline{x}}(t; \underline{\theta})] dt}{\frac{1}{T_o} \int_0^{T_o} \underline{z}(t)^T \underline{z}(t) dt} = \text{minimum } \omega.r.t. \underline{\theta}, \quad (2.12)$$

where T_o is the time interval for which data are available. $\hat{\underline{x}}$ is the response predicted by the model and \underline{z} is the measured response of the system.

It has been found that an alternative criterion which minimizes the root-mean-square of the difference between the measured and model response at peaks only is adequate for structural systems. This approach is motivated by the observation that peaks are generally the points of greatest significance in the response time history. The error minimization criterion employed in this work is therefore defined

in this way. Hence,

$$P(\underline{\theta}) = \frac{\text{r.m.s. of } [\underline{x}(t_p) - \hat{\underline{x}}(t_p; \underline{\theta})]}{|\underline{x}|_{\max}} = \text{minimum } \omega.r.t. \underline{\theta}, \quad (2.13)$$

where $|\underline{x}|_{\max}$ is the maximum of the absolute value of the components of $\underline{x}(t)$. The peak $x(t_p)$ is the local extremum of the measured response which occurs at a time t_p , and $\hat{\underline{x}}(t_p; \underline{\theta})$ is the corresponding model response at time t_p . All the peaks so defined are checked and used in (2.13). The implicit dependence of the model response on the parameters of the model, $\underline{\theta}$, has been shown in equation (2.13).

In general, P is a nonlinear scalar function in the parameters $\underline{\theta}$. Therefore, the task of finding parameters that minimize P is a nonlinear optimization problem in which the initial guess for $\underline{\theta}$ is crucial. When the initial guess is far away from the minimum value, some algorithms will either not converge at all, or will converge to a local minimum or to a nonphysical set of parameters [9].

2.6 Identification Methodology

2.6.1 Single-Mode Identification

The case considered here is that in which the base excitation $z(t)$ and the parallel component of the response $y_i(t)$ at some point in the structure are measured. The subscript i will be omitted from this point on because the response of only one coordinate is used. The problem is to identify a nonlinear model for the system from the measured response and base excitation. The model used is defined by (2.7) and (2.8) which for only one response measurement may be written as

$$y(t) = \sum_{r=1}^m y^r(t) \quad (2.14)$$

$$\ddot{y}^r + h^r(y^s, \dot{y}^s) = -\beta^r \ddot{z}(t); \quad s = 1, 2, \dots, m. \quad (2.15)$$

The generalized restoring force function $\underline{h} = [h^1, h^2, \dots, h^m]^T$ and effective participation factor $\underline{\beta} = [\beta^1, \beta^2, \dots, \beta^m]^T$ are estimated optimally according to

$$P(\underline{h}, \underline{\beta}) = P(y(t) - \hat{y}(t; \underline{h}, \underline{\beta})) = \text{minimum } \omega.r.t. \underline{h}, \underline{\beta} \quad (2.16)$$

subject to (2.14) and (2.15).

This is a complex multi-variable nonlinear optimization problem. The difficulties involved in solving such a problem are:

- (1) It is difficult to get good initial estimates for all parameters but these are crucial for the minimization algorithm to converge. Otherwise, the algorithm may diverge or converge to some nonphysical parameters.
- (2) Even if the algorithm converges to some minimum, it is difficult to assure this is a global minimum.
- (3) If there are too many parameters to be optimized at one time, P may be insensitive to the change in a single parameter. Also, if noise exists in the measurement, some parameters may be determined by identifying noise. Both situations result in unreliable answers.

The generalized modal identification method presented herein alleviates the aforementioned problems associated with nonlinear optimization by determining the modal properties mode by mode, sequentially. Single-mode identification is the "building block" of the identification methodology (2.16). Each single-mode identification problem is performed based on

$$P(h^r, \beta^r) = P(y^r(t) - \hat{y}^r(t; h^r, \beta^r)) = \text{minimum } \omega.r.t. h^r, \beta^r \quad (2.17)$$

subject to (2.15).

It is convenient to formulate the single-mode identification problem in three parts:

- (1) estimation of the modal response y^r , \dot{y}^r and \ddot{y}^r ,
- (2) estimation of the modal restoring force h^r , and
- (3) estimation of the modal participation factor β^r .

2.6.2 Estimation of the Modal Response

Recall that it was assumed that the nonlinear response can be decomposed into modes based on an analogy to the modes of a linear system. Initially, the modes are separated by band-pass filtering based on the information contained in the frequency domain. A similar approach has been used to extract the modal parameters of a linear system, [10-11], and to study the fundamental mode behavior of the response of a nonlinear system [12-15].

Consider that the r^{th} dominant mode is under identification. The modal response y^r is estimated initially by applying a band-pass filter to the response data over a frequency band selected for this mode. The motivation for this operation is to define each dominant mode by an appropriate frequency band and to eliminate the influence of other modes by band-pass filtering. Consequently, the coupling in modes is effectively eliminated.

The determination of the appropriate frequency band is made by inspection of the Fourier amplitude spectrum of the response acceleration. The nonlinear effect may cause some erratic appearance around each dominant peak which makes the choice more difficult. However, any mistake made in choosing the frequency band can be corrected later if it is found that some parameters identified are nonphysical or the identification algorithm does not converge.

In practice, the band-pass filtering is performed in two stages: low-pass filtering of the signal and high-pass filtering of the filtered signal. The ideal low-, high- and band-pass filters have amplitude response of unity within the passband and zero elsewhere. The passbands for low-, high- and band-pass filters are as shown in Figure 2.3. The frequencies ω_L and ω_H are the cutoff frequencies. The response functions in the figure are those of ideal filters, and will have to be approximated in practice [16-20]. The attention will focus herein on a specific low-pass filter, the Ormsby filter, which provides the "building block" for band-pass filters.

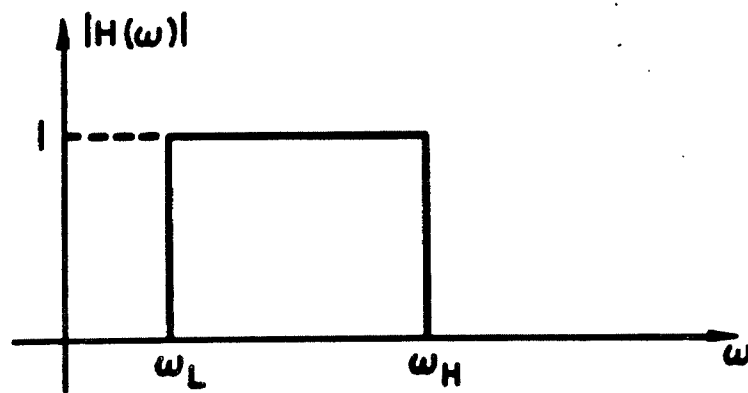
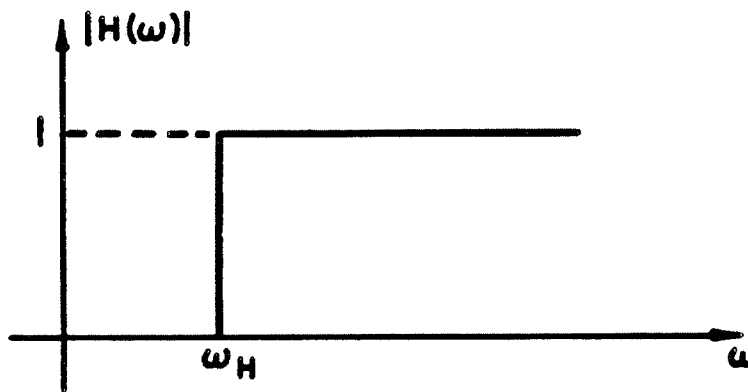
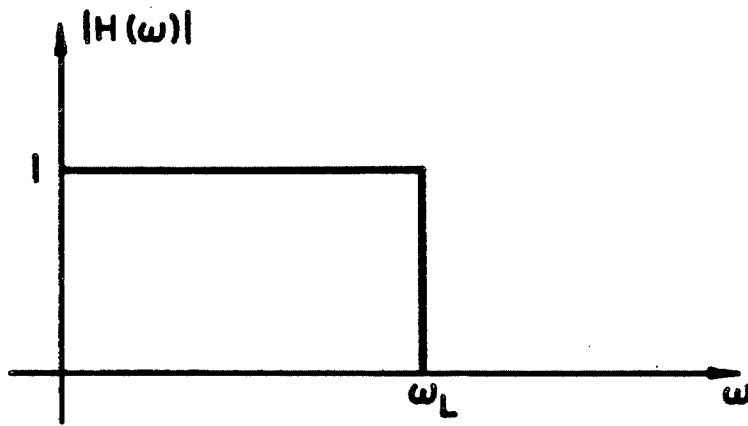


Figure 2.3 Ideal low-pass (top), high-pass (center) and band-pass (bottom) filters [19].

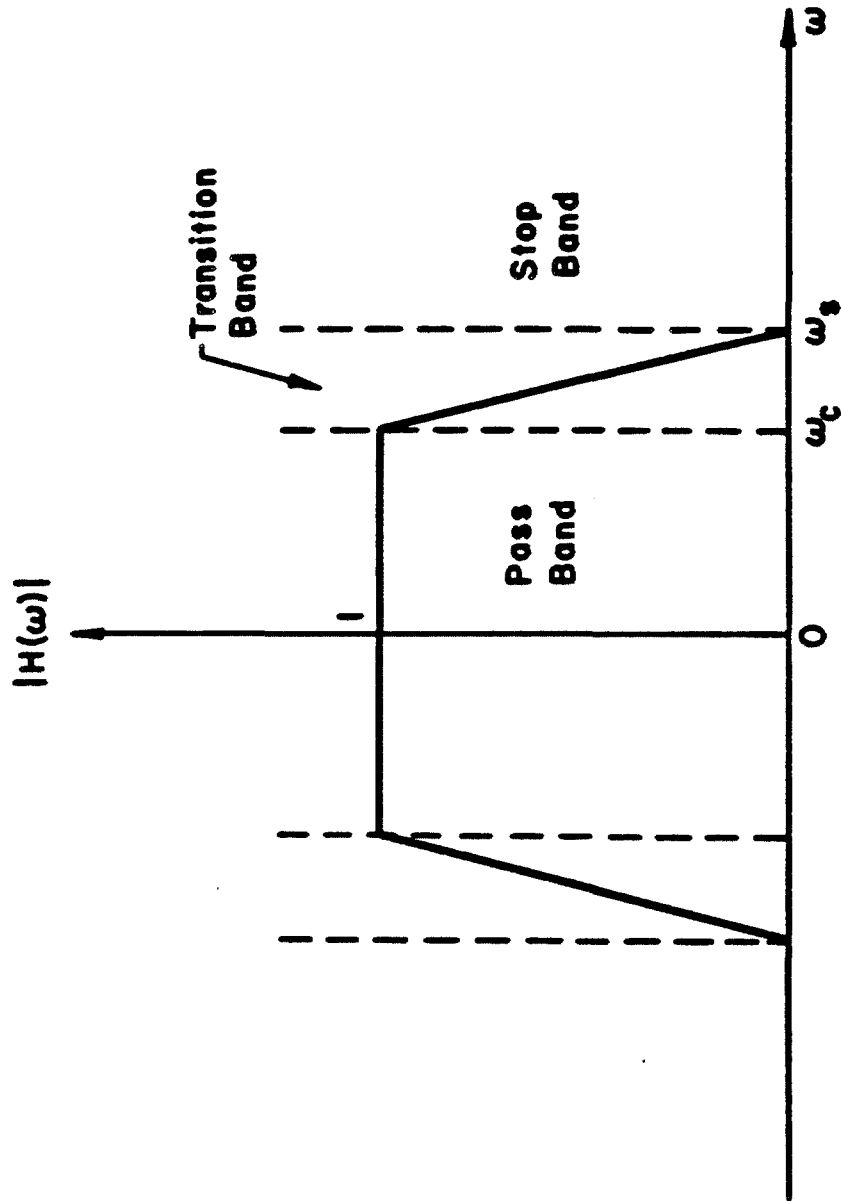


Figure 2.4 Ideal transfer function of Ormsby filter [19].

The frequency response function of the Ormsby filter, shown in Figure 2.4, is given by

$$H(\omega) = \begin{cases} 1 & |\omega| \leq \omega_c \\ 0 & |\omega| > \omega_s \\ (\omega + \omega_s)/\Delta\omega & -\omega_s \leq \omega < -\omega_c \\ (\omega_s - \omega)/\Delta\omega & \omega_c \leq \omega < \omega_s \end{cases} \quad (2.18)$$

where (ω_c, ω_s) is the transition band, $\Delta\omega = \omega_s - \omega_c$. The corresponding impulse response $h(t)$ is given by

$$h(t) = \frac{\cos \omega_c t - \cos \omega_s t}{2\pi^2 t^2 \Delta\omega}. \quad (2.19)$$

The impulse response filter weights for discrete data are obtained by quantizing $h(t)$ at equal time intervals.

As a means of sharpening the result, the estimation of the modal response is actually performed iteratively in the generalized modal identification method. The algorithm is described herein.

From previous iterations, the latest estimate of the modal response y^r is obtained and is denoted by \hat{y}^r , where $r = 1, \dots, m$. Initially, all modes are estimated by band-pass filtering. Based on equation (2.14), the model response \hat{y} is the summation of all \hat{y}^r . That is

$$\hat{y}(t) = \sum_{r=1}^m \hat{y}^r(t). \quad (2.20)$$

The difference between the actual response y^r and the model response \hat{y}^r is defined as the residual error e

$$e(t) = y^r(t) - \hat{y}^r(t). \quad (2.21)$$

The modal error $e^r(t)$ is then calculated by band-pass filtering $e(t)$ over the same frequency band chosen for the r^{th} mode. The new estimate of y^r is then determined by adding the modal error $e^r(t)$ to the latest estimate \hat{y}^r . The \dot{y}^r and \ddot{y}^r are updated in the same manner. All the new estimates of y^r , \dot{y}^r and \ddot{y}^r are used to updated the modal response employed in the subsequent estimation process.

2.6.3 Estimation of the Modal Restoring Force

Since the coupling of modes is essentially eliminated in estimation of the modal response as described in section 2.6.2. The modal equation (2.9) may be written as

$$h^r(\mathbf{y}^r, \dot{\mathbf{y}}^r) = -\beta^r \ddot{\mathbf{z}}(t) - \ddot{\mathbf{y}}^r(t) . \quad (2.22)$$

When the right hand side of equation (2.22) is specified, the identification problem is reduced to identifying the generalized restoring force h^r .

In the case of linear systems with classical normal modes [21], the generalized restoring force will be of the form

$$h^r = 2\zeta_r \omega_r \dot{\mathbf{y}}^r + \omega_r^2 \mathbf{y}^2 , \quad (2.23)$$

where ζ_r and ω_r are the modal damping ratio and frequency, respectively. Since the form is specified in terms of two parameters, ζ_r and ω_r , the identification task is to determine these two parameters for each mode. For a general nonlinear system, the analytical form of the generalized restoring force h^r is unknown and can only be estimated. Both parametric and nonparametric restoring force models can be employed to extract the nature of h^r .

Let $\hat{h}^r(\underline{\theta})$ be the estimate given by the restoring force model. The parameters $\underline{\theta}$ of the model are then selected based on an optimal matching of h^r and \hat{h}^r . That is

$$P(\underline{\theta}) = P(h^r(t) - \hat{h}^r(t; \underline{\theta})) = \text{minimum } \omega.r.t. \underline{\theta} \quad (2.24)$$

subject to (2.22), where P is the prediction error which quantifies the difference between h^r and \hat{h}^r .

At this stage of the identification process, the numerical values of the modal restoring force function and corresponding state, the modal displacement and velocity, are known at discrete time steps. It is therefore important to notice that the

parameters \underline{g}^r can be determined by minimizing $P(\underline{g}^r)$ without solving the equations of motion, which are in general nonlinear differential equations. This is in clear contrast to the traditional approach in which each new estimate of \underline{g}^r requires a new differential equation to be solved. Accordingly, the identification based on restoring force can be performed more efficiently.

Two nonlinear restoring force models are employed herein in the generalized modal identification method. The first, a nonparametric model, is used to obtain an initial estimate of the backbone relationship of the hysteretic restoring force and the second, a parametric hysteretic model, is used to obtain the final modal model. The detailed description of the identification models is presented in Chapters 3 and 4, respectively.

2.6.4 Estimation of the Modal Participation Factor

For a given effective participation factor, the modal parameters may be estimated directly according to (2.24). However, this leaves the participation factor to be determined. This simplifies the single-mode identification problem to a single-parameter optimization with respect to β^r only, namely

$$P(\beta^r) = P(y^r(t) - \hat{y}^r(t; \beta^r)) = \text{minimum } \omega.r.t. \beta^r \quad (2.25)$$

subject to (2.15), where any of y^r , \dot{y}^r and \ddot{y}^r can be substituted in (2.13) for \underline{x} depending on the application. Any one-dimensional nonlinear optimization scheme can be employed to minimize $P(\beta^r)$ in a straightforward manner [22-28]. Each numerical evaluation of $P(\beta^r)$ requires solving (2.15) once only. Note that the estimation of β^r is a loop that contains the previous estimation process for $\hat{h}^r(\underline{\theta})$.

A one-dimensional minimization method is selected in the present study which involves only evaluating the function and not the gradient of the function. Let the minimizing function be denoted by $f(\alpha)$. The method starts with an initial estimate range, $[\alpha_L, \alpha_H]$, of the minimum of $f(\alpha)$, and a step-size $\delta = (\alpha_H - \alpha_L)/N$,

where N is the total number of steps. α is incremented continually by δ , that is, $\alpha = \alpha_L, \alpha_L + \delta, \alpha_L + 2\delta, \dots$, until $\alpha = \alpha_H$. The value of f is then calculated at each step from α_L to α_H and the minimum is taken.

The key point is the choice of range $[\alpha_L, \alpha_H]$ and step-size δ . If the range $[\alpha_L, \alpha_H]$ is too small or the step-size δ is too big, the minimum of $f(\alpha)$ may be missed. On the other hand, if the range is too large or the step-size is too small, too much time may be spent in the stepping required to find the minimum of $f(\alpha)$. An approach which was found to work well is to start with a bigger range of $[\alpha_L, \alpha_H]$ and larger δ to get an approximate minimum of $f(\alpha)$. Subsequently, this minimum is refined by choosing a narrower $[\alpha_L, \alpha_H]$ and smaller δ .

2.7 Summary

A practical identification methodology has been presented that is suitable for application to multi-degree-of-freedom nonlinear structural systems. The method requires information regarding the base motion and system response at only one point.

The features of this identification methodology are:

- (1) Frequency domain information is used to estimate the "modal" response of the structure. Coupling in the generalized modal restoring force is thereby effectively eliminated.
- (2) The modal restoring force parameters are estimated by a nonparametric identification technique based on the generalized modal restoring force. This stage of the identification process requires no solution of nonlinear differential equations of motion and results in considerable computational saving.
- (3) The problem is reduced to determining an optimal estimate of the effective modal participation factor only. Any simple one-dimensional nonlinear optimization scheme can be employed for this process. The difficulties associated

with multi-variable nonlinear optimization are thereby avoided and additional computational efficiency results.

In the subsequent chapters, the generalized modal identification method, incorporating nonparametric and hysteretic restoring force models, will be described in more detail. The validation of the method and the model will be performed with simulated data. Application to real data from structures will also be presented.

References

- [1] J. L. Beck, "Determining Models of Structures from Earthquake Records," Report No. EERL 78-01, Earthquake Engineering Research Laboratory, California Institute of Technology, Pasadena, California, June 1978.
- [2] G. H. McVerry, "Frequency Domain Identification of Structural Models from Earthquake Records," Report No. EERL 79-02, Earthquake Engineering Research Laboratory, California Institute of Technology, Pasadena, California, October 1979.
- [3] B.R.I. Steel Group, "Inelastic Behavior of the Structural Members in the Phase I Test," *Proceedings of the 6th Joint Technical Coordinating Committee Meeting, U.S.-Japan Cooperative Research Program Utilizing Large-Scale Testing Facilities*, Maui, Hawaii, June 1985.
- [4] J. F. Hall, "An FFT Algorithm for Structural Dynamics," *International Journal of Earthquake Engineering and Structural Dynamics*, Vol. 10, 1982.
- [5] California Institute of Technology, "Analysis of Strong Motion Earthquake Accelerograms," Earthquake Engineering Research Laboratory Report No. EERL 74-100, California Institute of Technology, Pasadena, California, January 1974.
- [6] S. F. Masri, T. K. Caughey, "A Nonparametric Identification Technique for Nonlinear Dynamic Problems," *ASME Journal of Applied Mechanics*, Vol. 46, June 1979.
- [7] G. H. McVerry, "Structural Identification in the Frequency Domain from Earthquake Records," *International Journal of Earthquake Engineering and Structural Dynamics*, Vol. 8, 1980.
- [8] S. D. Werner, J. L. Beck, and M. B. Levine, "Seismic Response Evaluation of Meloland Road Overpass Using 1979 Imperial Valley Earthquake Records," *International Journal of Earthquake Engineering and Structural Dynamics*, Vol. 15, 1987.
- [9] P. Eykhoff, *System Identification*, John Wiley & Sons, Inc., 1974.
- [10] J. D. Raggett, "Time Domain Analysis of Structural Motions," Pre-print 2209, ASCE National Structural Engineering Meeting, Cincinnati, Ohio, 1974.
- [11] J. D. Raggett, "Estimating Damping of Real Structures," *ASCE Journal of Structural Division*, 101, ST9, September 1975.
- [12] H. Iemura and P. C. Jennings, "Hysteretic Response of a Nine-Storey Reinforced Concrete Building," *International Journal of Earthquake Engineering and Structural Dynamics*, Vol. 3, 1974.
- [13] A. M. Abdel-Ghaffar and R. F. Scott, "Experimental Investigation of the Dy-

- dynamic Response Characteristics of an Earth Dam," *Proceedings of the 2nd U.S. National Conference on Earthquake Engineering*, 1979.
- [14] A. M. Abdel-Ghaffar and R. F. Scott, "Vibration Tests of Full-Scale Earth Dam," *ASCE Journal of Geotechnical Engineering Division*, 1981.
- [15] A. O. Cifuentes, "System Identification of Hysteretic Structures," Earthquake Engineering Research Laboratory, Report No. EERL 84-04, California Institute of Technology, September 1984.
- [16] J. S. Bendat and A. G. Piersol, *Engineering Applications of Correlation and Spectral Analysis*, John Wiley & Sons Inc., 1980.
- [17] M. D. Trifunac and V. Lee, "Routine Computer Processing of Strong-Motion Accelerograms," Earthquake Engineering Research Laboratory, Report No. EERL 73-03, California Institute of Technology, Pasadena, California, October 1973.
- [18] D. E. Hudson, *Reading and Interpreting Strong Motion Accelerograms*, Earthquake Engineering Research Institute, Berkeley, California, 1979.
- [19] V. W. Lee and M. D. Trifunac, "Current Developments in Data Processing of Strong Motion Accelerograms," University of Southern California, Department of Civil Engineering, Report No. CE-84-01, Los Angeles, California, August 1984.
- [20] Blinchikoff and Zverev, *Filtering in the Time and Frequency Domains*, John Wiley & Sons Inc., 1979.
- [21] T. K. Caughey and M. E. J. O'Kelley, "Classical Normal Modes in Damped Linear Dynamic Systems," *ASME Journal of Applied Mechanics*, Vol. 32, 1965.
- [22] Lectures by Dr. L. J. Wood on Optimal Control Theory, California Institute of Technology, Pasadena, California, 1983-84.
- [23] A. E. Bryson, Jr. and Y. C. Ho, *Applied Optimal Control*, Halsted Press, 1975.
- [24] D. G. Luenberger, *Introduction to Linear and Nonlinear Programming*, Addison-Wesley, 1973.
- [25] R. P. Brent, *Algorithms for Minimization without Derivatives*, Prentice-Hall, Inc., 1973.
- [26] M. J. Box, "A Comparison of Several Current Optimization Methods and the Use of Transformations in Constrained Problems," *Comput. J.*, Vol. 9, 1966.
- [27] I. A. Dodes, *Numerical Analysis for Computer Science*, North-Holland, New York, 1978.
- [28] S. S. Kuo, *Computer Applications of Numerical Methods*, Addison-Wesley, Inc., 1972.

Chapter 3

Generalized Modal Identification Using Nonhysteretic Models

3.1 Introduction

This chapter is concerned with the generalized modal identification method incorporating nonhysteretic restoring force models. After reviewing a class of nonhysteretic models, a “nonparametric” model with only four terms is proposed based on model simplicity and computational considerations. The coefficients of these four terms are determined directly by approximating the system generalized restoring force in a least-squares sense.

The identification algorithm together with the model are verified using simulated data generated for a nonlinear (hysteretic) system. The results provide an excellent example of the use of nonparametric restoring force models and a good motivation for further studies on employing hysteretic restoring force models in the generalized modal identification method.

3.2 Nonparametric Identification Techniques

If a mathematical model of a system is known a priori, and the input and output data are used to determine the parameters of the model, then the process is known as a parametric identification. Most system identification techniques are of this type. Certain methods are termed “nonparametric” because they do not seek to determine the parameters of an assumed model. Instead, their objective is to arrive at a functional representation of the system that is capable of predicting the output for a given input.

Traditionally, nonparametric identification for a dynamic system is performed using the Volterra-series or Wiener-kernel approach [1-5]. However, these approaches

have various restrictions which limit their use in practice. For example, the nature of dynamic systems to be identified must be nonhysteretic, and only stationary and white noise can be used as the input signal. Furthermore, when dealing with systems that incorporate commonly encountered nonlinearities, such as polynomial nonlinearities, the evaluation of higher-order terms requires a prohibitive amount of computational effort, coupled with very demanding, and usually unrealistic, storage requirements.

Recent nonparametric identification development has been devoted to estimating the nonlinear restoring force in a dynamic system. This approach was first introduced by Masri, Caughey, et al. [6-8] in order to alleviate some of the aforementioned problems associated with traditional nonparametric identification techniques. This concept is extended in the present work to obtain a first estimate of the generalized modal restoring force of a hysteretic system.

3.3 Nonhysteretic Restoring Force Models

Consider the general form of the equation of motion for a single degree-of-freedom system

$$\ddot{y} + h(y, \dot{y}) = \ddot{a}(t) , \quad (3.1)$$

where y is the generalized relative displacement, $h(y, \dot{y})$ is the generalized restoring force per unit mass and $\ddot{a}(t)$ is the excitation acceleration. Equation (3.1) can be used as the basic model to represent the dynamics of a system or of a particular mode of a system. Note that the physical and modal coordinates are the same for a single degree-of-freedom system and no distinction between them is made in this section.

3.3.1 Linear Models

The system (3.1) is said to be linear if $h(y, \dot{y})$ can be expressed as

$$h(y, \dot{y}) = 2\zeta_o \omega_o \dot{y} + \omega_o^2 y , \quad (3.2)$$

where ζ_o represents the fraction of viscous damping and ω_o is the natural frequency of the system. Since the form representing the restoring force is known in terms of two parameters, ζ_o and ω_o , there is no need to identify h using nonparametric techniques. The identification of the linear system (3.2) is therefore a parameter estimation problem in which the parameters, ζ_o and ω_o , can be determined in either time or frequency domain. References [9] and [10] are examples of two fundamentally equivalent approaches in the time and frequency domains, respectively. It has been found that the response of buildings subject to earthquakes can be reproduced well by linear models only when the nonlinear behavior is not pronounced. This shows the limitation of linear models for describing nonlinear systems.

3.3.2 Nonparametric Models

In many cases, the system (3.1) is nonlinear and the analytical form of $h(y, \dot{y})$ is unknown. Determining an appropriate nonlinear model for the generalized restoring force h can be formulated as a nonparametric identification problem. Among many nonlinear models which have been used to extract the nonlinear nature of h , some nonhysteretic models will be briefly described in this section.

Masri, Caughey, Miller, et al. [6-8] have proposed a nonparametric identification technique for general nonlinear problems. The main idea behind their method is to estimate the restoring force $h(y, \dot{y})$ by an approximation function $\hat{h}(y', \dot{y}')$ expressed in terms Chebyshev orthogonal polynomials in the form

$$\hat{h}(y', \dot{y}') = \sum_{i=0}^I \sum_{j=0}^J C_{ij} T_i(y') T_j(\dot{y}'), \quad (3.3)$$

where I and J represent the order of the expansion, the functions T_i are Chebyshev polynomials and C_{ij} 's are constant coefficients. Both the generalized displacement y and velocity \dot{y} have been normalized to lie in the range -1 and 1. The normalized values y' and \dot{y}' corresponding to y and \dot{y} are defined as

$$y' = [y - (y_{\max} + y_{\min})/2] / [(y_{\max} - y_{\min})/2]$$

and (3.4)

$$\dot{y}' = [\dot{y} - (\dot{y}_{\max} + \dot{y}_{\min})/2] / [(\dot{y}_{\max} - \dot{y}_{\min})/2] .$$

The Chebyshev polynomials are defined as

$$T_n(\xi) = \cos(n \cos^{-1} \xi) ; \quad -1 < \xi < 1 . \quad (3.5)$$

They satisfy the weighted orthogonality property

$$\int_{-1}^1 w(\xi) T_n(\xi) T_m(\xi) d\xi = \begin{cases} 0 & n \neq m \\ \pi/2 & n = m \neq 0 \\ \pi & n = m = 0 , \end{cases} \quad (3.6)$$

in which the weighting function $w(\xi)$ is $(1 - \xi^2)^{1/2}$. By making use of the orthogonality of Chebyshev polynomials, the coefficients C_{ij} of equation (3.3) are given

by

$$C_{ij} = \begin{cases} (2/\pi)^2 D_{ij} & i \text{ and } j \neq 0 \\ (2/\pi^2) D_{ij} & i \text{ or } j = 0 \\ (1/\pi^2) D_{ij} & i = j = 0 , \end{cases} \quad (3.7)$$

where

$$D_{ij} = \int_{-1}^1 \int_{-1}^1 h(y', \dot{y}') T_i(y') T_j(\dot{y}') w(y') w(\dot{y}') dy' d\dot{y}' . \quad (3.8)$$

Since the orthogonal polynomials form a complete set of functions, any continuous function can be expanded in terms of the Chebyshev polynomials. This is the common basis for using orthogonal polynomials to represent or approximate functions whose exact mathematical forms are unknown. Because the form of the restoring force h is not assumed at the beginning of the identification problem, this method is referred to as a nonparametric method; yet when the function h is represented mathematically by orthogonal polynomials, the coefficients of the polynomials are the parameters of the model.

Note that in the special case when no cross-product terms are involved in any of the series terms, functions \hat{h} can be expressed as the sum of two one-dimensional

orthogonal polynomial series instead of a single two-dimensional series of the form (3.3). Note also that the Chebyshev polynomials are only a subclass of the orthogonal polynomials which satisfy the orthogonality condition

$$\int_a^b w(\xi) \phi_n(\xi) \psi_{n-1}(\xi) d\xi = 0, \quad (3.9)$$

where $w(\xi)$ is the weighting function, $\psi_{n-1}(\xi)$ is an arbitrary polynomial of degree $n-1$ or less, and $\phi_n(\xi)$ is a polynomial of degree n . Other orthogonal polynomials, such as the Legendre polynomials, the Laguerre polynomials, and the Hermite polynomials, can be defined by using different weighting functions over the domain of interest $[a, b]$ [11-12]. However, Chebyshev polynomials have the desirable feature of equal-error (equal-ripple) approximation within an interval of interest [6-8].

Udwadia and Kuo [13] extended the method of Masri, Caughey, et al to identify a chain-like nonlinear memoryless dynamic system. The problem is formulated in terms of general orthogonal polynomials rather than the specific Chebyshev polynomials. The restoring forces are assumed to be represented by two additive functions of the velocity and displacement vectors, each being represented by a sum of general orthogonal polynomials. However, a method for the general form of the restoring force is reported to be available.

Toussi and Yao [8] have used an approach similar to the method of orthogonal polynomial expansion. Instead of using orthogonal polynomials such as Chebyshev polynomials, they assumed that the restoring force can be represented as the sum of two additive functions of displacement and velocity respectively (namely, stiffness and damping functions), and that these functions are simple polynomials of their arguments, that is

$$\hat{h}(y, \dot{y}) = h_s(y) + h_d(\dot{y}), \quad (3.10)$$

where

$$h_s(y) = a_0 + a_1 y + \cdots + a_m y^m$$

and

(3.11)

$$h_d(\dot{y}) = b_0 + b_1\dot{y} + \dots + b_n\dot{y}^n .$$

This model can be viewed as a truncated form of previous nonparametric models without cross-product terms. Note that Toussi and Yao called their method a parametric method.

In principle, all the restoring force models reviewed above are nonhysteretic and are strictly only suitable for nonlinear systems with memoryless nonlinearities. The applicability of these models for nonlinear hysteretic systems is questionable. As applied to simulated data generated from a nonlinear system consisting of some hysteretic elements and some nonhysteretic elements, however, some positive results have been reported [14-15]. These positive results have indicated that nonparametric methods have a place in preliminary identification studies of hysteretic systems. That is, they may suggest forms for the parametric model which should be used and they may even provide a good initial estimate of parameters for the model which should be selected.

This important insight is exploited in this thesis to identify the hysteretic behavior of a nonlinear system in two stages. A nonparametric model is used to obtain an initial nonhysteretic estimate of the generalized restoring force for each mode. This nonparametric model suggests the parametric relationship for the backbone of the hysteretic model employed in the final stage of identification. The results of the nonparametric identification thereby can be used as an initial estimate for the backbone of the final model.

The final stage of identification is left to be discussed in Chapter 4. In this chapter, the initial stage is investigated using a simple nonparametric model.

3.4 Four-Parameter Nonparametric Model

A relatively simple nonparametric model with only four terms is herein introduced. The simplicity of the model makes it easy to illustrate the point made above regarding the role of nonparametric techniques using nonhysteretic models in the preliminary identification studies of hysteretic systems.

3.4.1 Model Considerations

A good "model" of a dynamic system is a reasonably simple mathematical description of that system which is capable of representing or extracting the essential aspects of the response in usable form. If a model is too complex, its usefulness is questionable. Simplicity is a major objective in model construction. In fact, a model is a representation of reality with complexities reduced to the extent possible.

In a nonparametric approach, the system under consideration is treated as a "black box" and the model is identified assuming no a priori knowledge. Such an approach usually results in a model which is exceedingly complex so as to make computation and interpretation difficult. The complexity is caused by attempting to describe not only the response due to important mechanisms, but also every detail resulting from unimportant mechanisms or simply from noise.

This section represents an attempt to limit the representation of a nonparametric restoring force model to the extent possible based on both computational considerations and particular aspects that are essential to select the final parametric hysteresis model.

Recall the modal equation (2.23)

$$h^r(y^r, \dot{y}^r) = -\beta^r \ddot{z}(t) - \ddot{y}^r(t) . \quad (3.12)$$

When the right hand side of equation (3.12) is measured or estimated at each time step, the modal restoring force h^r is known as a function of the modal displacement y^r and modal velocity \dot{y}^r . Thus, the numerical values of h^r , y^r and \dot{y}^r for each

time step can be stored in tabular form for later reference. This approach needs no computational effort, but usually demands unrealistic storage requirements. Also, it is difficult to interpret the tabular data, especially when they are contaminated by noise. Alternatively, for purpose of either condensing the data or extracting certain characteristics of h^r from the noise contaminated data, a function \hat{h}^r of y^r and \dot{y}^r can be introduced which gives an approximation of $h^r(y^r, \dot{y}^r)$ in some least-squares sense. The so-identified representation \hat{h}^r usually provides valuable information for interpreting the physical nature of h^r .

For a general nonlinear system, the analytical form of h^r is unknown and various nonparametric models may be employed to estimate h^r . Initially, it is assumed in this study that the generalized restoring force h^r can be expanded by a two-dimensional power series in y^r and \dot{y}^r . That is

$$\hat{h}^r(y^r, \dot{y}^r) = \sum_{i=0}^I \sum_{j=0}^J A_{ij}^r (y^r)^i (\dot{y}^r)^j, \quad (3.13)$$

where I and J represent the order of the expansion and A_{ij}^r 's are the coefficients or parameters of the model which need to be determined numerically using a least-squares method. Note that the ordinary polynomials have been used to make the physical meaning of A_{ij}^r more explicit. For example, A_{10}^r and A_{01}^r can, rather than just mathematical coefficients, be interpreted as the natural frequency and viscous damping coefficient at small amplitude oscillations, respectively.

For the nonhysteretic case, the general form (3.13) in principle yields a "best" least-squares fit of the restoring force function h^r . However, when the data are contaminated by noise and the order of expansion is allowed to be large, the results may be the identification of a function that fits not only the actual response part of the data but also the noise. It is therefore expected that nonzero coefficients will be identified for initially nonexistent terms in the system if noisy data are used. Even if the coefficients may be small compared to the predominant coefficients,

these additional coefficients have no physical significance. They also degrade the potential of using the identified parameters to extrapolate or to predict the response of the system for other than the identification signal.

In order to illustrate this point, consider a linear single degree-of-freedom system being identified by employing the general model (3.13). Because of noise in the data, nonzero coefficients, including a constant term, will be identified for initially nonexistent terms in the system. If the entire model is used to predict the response to another excitation, all these additional terms identified will degrade the predicted response. For example, the constant term will drive a motionless system to move even if there is no excitation, while the additional higher-order powers will contribute to the response unrealistically when the system is subjected to high-level loading.

It is concluded that if the general model (3.13) is used solely to compress or smooth the tabular function h^r in the approximate sense, the orders I and J can be allowed to be as large as needed for minimizing the least-square error between h^r and \hat{h}^r . On the other hand, if the model is used to extrapolate or predict the response of the system, the order should not be determined by mechanically best-fitting polynomials to the data. All a priori knowledge and physical information should be used to arrive at the best representation.

Based on the above observations, an appropriate truncated version of the non-parametric model (3.13) is sought herein. All the cross-product terms are first eliminated from (3.13) because the interpretation of coefficients A_{nm}^r , where $n \neq 0$ and $m \neq 0$, is less obvious or may require considerable effort. All the even-power terms, including the constant term, with coefficients A_{nm}^r , where n (even) ≥ 0 or m (even) ≥ 0 are also eliminated because they make the restoring force non-symmetric which is not the case of interest herein. Finally, among all the odd-power terms left, only four terms with coefficients A_{10}^r , A_{30}^r , A_{01}^r and A_{03}^r are preserved.

The reason is that, intuitively, these four coefficients alone should be sufficient to extract the main feature of nonlinearities which are commonly encountered in physical systems. It is also perceived that the nonparametric model may provide important information for constructing the final parametric model to describe the hysteretic response of a nonlinear system. The reality of the model must, of course, be justified by applying the model to both simulated and real data. This is done in the latter parts of the thesis.

From another point of view, the final truncated nonparametric model may also be considered the simplest extension of the linear model (3.2) by simply adding two cubic nonlinear terms with the coefficients A_{30}^r and A_{03}^r . It is then interesting to examine how well this simple nonhysteretic model can reproduce hysteretic response and how much information it provides in the preliminary identification studies of hysteretic systems.

3.4.2 General Description

Let a_1^r , a_2^r , a_3^r and a_4^r denote the coefficients A_{10}^r , A_{30}^r , A_{01}^r and A_{03}^r , respectively, and \hat{h}^r the estimate of the generalized modal restoring force h^r . The above truncated nonparametric model, called the four-parameter nonparametric model, can be expressed as

$$\hat{h}^r(y^r, \dot{y}^r) = a_1^r y^r + a_2^r (y^r)^3 + a_3^r \dot{y}^r + a_4^r (\dot{y}^r)^3, \quad (3.14)$$

where the coefficients a_1^r , a_2^r , a_3^r , and a_4^r are the four “parameters” of the model. The parameters can be described in two categories:

- (1) small amplitude parameters— a_1^r , a_3^r

When the system is subjected to low-level loading, the lower-power terms in (3.11) will dominate the response, i.e. the parameters a_1^r and a_3^r control the small amplitude behavior of the model. Hence, under small amplitude response, it is assumed that the model behaves like a linear oscillator.

(2) large amplitude parameters— a_2^r, a_4^r

The parameters a_1^r and a_3^r are used to describe the nonlinear behavior at large amplitude oscillations. The nonlinearity is represented by a polynomial type that is defined by cubic displacement and cubic velocity terms without cross-product terms. Depending on the sign of a_2^r , the form of (3.14) can be made to represent restoring forces with hardening or softening nonlinearities. Similarly, depending on the sign of a_4^r , the equivalent viscous damping can increase or decrease with amplitude. Thus, the nature of the system nonlinearity is reflected in both the magnitude and sign of these coefficients.

3.4.3 Parameter Estimation

The coefficients $a_i^r, i = 1, 2, 3, 4$, appearing in the four-parameter nonparametric model (3.14) may be evaluated numerically by approximating each h^r in some least-squares sense. The least-squares approximation problem is described below in general form.

Let $f(x)$ be a given real-valued function defined at discrete points $x_k, k = 1, 2, \dots, K$. Choose an approximating function $\hat{f}(x)$ of the form

$$\hat{f}(x) = \sum_{i=1}^I a_i \psi_i(x) \quad (3.15)$$

for any real set $a_i, i = 1, 2, \dots, I$ and suitable basis functions $\psi_i, i = 1, 2, \dots, I$. The coefficients a_i are to be determined so that the error between $f(x)$ and $\hat{f}(x)$ at $x_k, k = 1, 2, \dots, K$, is minimized, say in the least-squares sense. That is, the coefficients a_i are estimated based on the following criterion

$$\varepsilon = \sum_{k=1}^K \left[f(x_k) - \sum_{i=1}^I a_i \psi_i(x_k) \right]^2 = \text{minimum } \omega.r.t. \ a_i, \quad i = 1, 2, \dots, I, \quad (3.16)$$

Estimates of a_i then require the solution of the linear simultaneous equations

$$\sum_{i=1}^I C_{ij} a_i = b_j, \quad (3.17)$$

where

$$b_j = \sum_{k=1}^K f(x_k) \psi_j(x_k) \quad (3.18)$$

and

$$C_{ij} = \sum_{k=1}^K \psi_i(x_k) \psi_j(x_k) . \quad (3.19)$$

As applied to the identification of the four-parameter "nonparametric" model, the basis functions are ordinary polynomials and the discrete points are chosen at peaks only. Note that this method involves no iterative nonlinear optimization process to estimate the model parameters. This results in additional efficiency besides those points mentioned in section 2.6.

3.5 Verification with Simulated Data

The validity of the generalized modal identification method incorporating the four-parameter nonparametric model is now examined by reporting the results of identification and prediction performed with simulated data.

3.5.1 Data Generation

Verification System To test the identification approach proposed herein for hysteretic response, the verification system used is the hysteretic three-degree-of-freedom mathematical model shown schematically in Figure 3.1(a).

This planar system consists of three lumped masses m_i , $i = 1, 2, 3$. The absolute displacement of m_i is denoted by x_i , while the prescribed base acceleration is designated by $\ddot{x}_b(t)$. The relative displacement with respect to the moving base is given by $y_i = x_i - x_b(t)$, and the inter-mass relative motion is specified by $z_i = x_i - x_{i-1}$ for $i > 1$, and $z_1 = x_1 - x_b(t)$. The nonlinear restoring force of each element, denoted by g_i , is assumed to be the distributed-element hysteretic model with 15 subelements. There is no viscous damping assumed in the verification system.

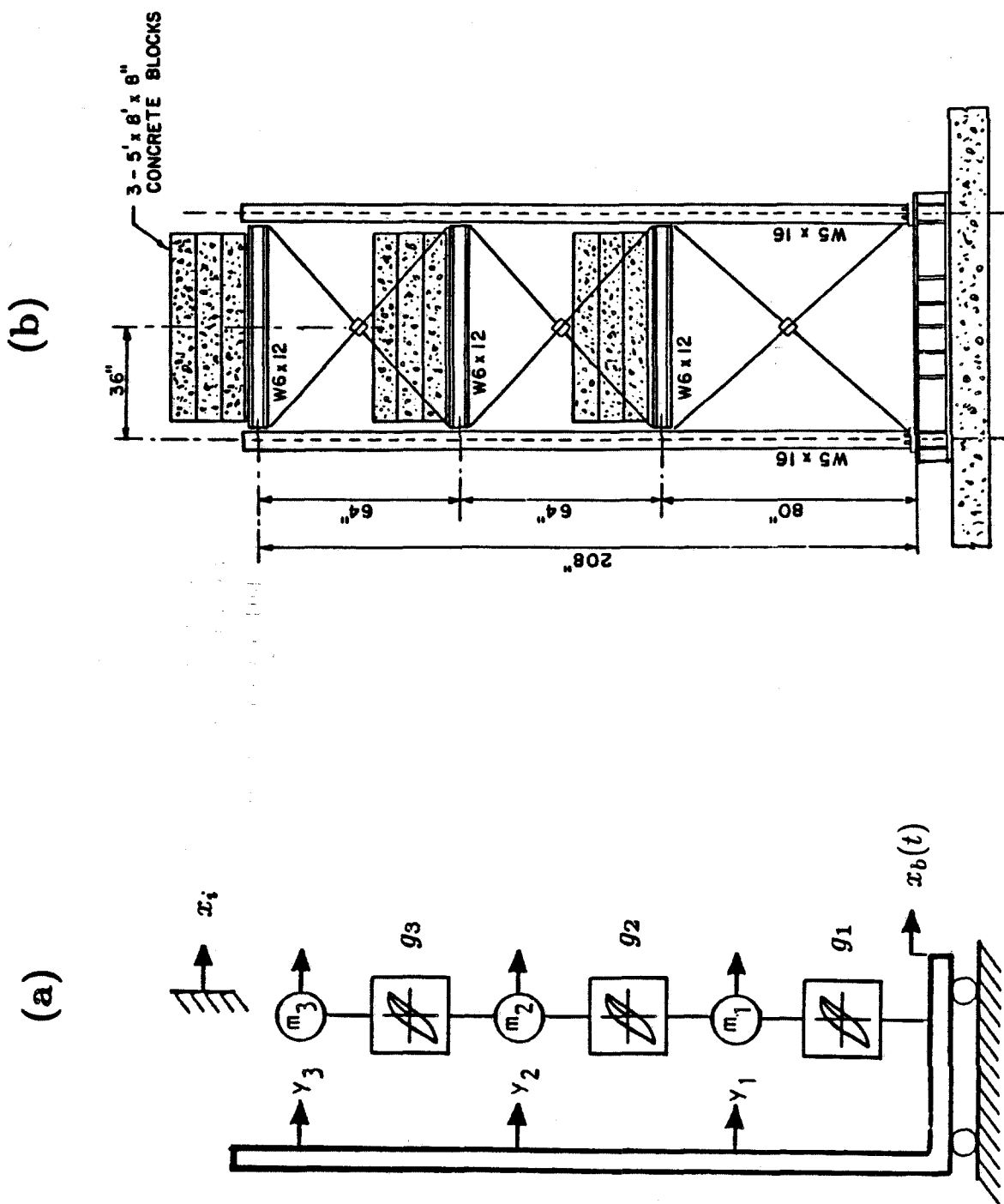


Figure 3.1 Nonlinear hysteretic verification system.

(a) Mathematical model.

(b) Test structure [16].

To represent a realistic physical system, the characteristics of the verification system are chosen to approximate those of a three-story steel frame structure tested on the shaking table at the University of California, Berkeley, Figure 3.1(b). This test structure has been extensively analyzed, both analytically and experimentally [16-17].

The values of the system masses are chosen as:

$$m_1 = 2110 \text{ kg}, m_2 = 2110 \text{ kg}, m_3 = 2110 \text{ kg} .$$

The hysteretic behavior of all elements g_i , $i = 1, 2, 3$, is illustrated by the actual inter-mass restoring force diagrams, shown in Figures 3.5, 3.6 and 3.7, for three different base excitations described below.

Probing Signals For identifying the nonlinear model of a general system, the probing signal should be rich in frequency content and should contain sufficient energy to excite the system to a response level that would bring its nonlinearities into play. For hysteretic systems, the response is nonlinear and path-dependent, i.e. dependent on the time history of the dynamic loading. It is therefore desirable to generate the simulated response with several inputs of different characteristics.

Based on the above considerations, three different earthquake accelerograms are selected as a broad-band base excitation to generate response data for the verification system. The first accelerogram, El Centro, 1940, S00E, is used to identify the system. The second accelerogram, Taft, 1952, S69E and the third, Parkfield, 1966, N65E, are used to study the prediction capability of the identified model. To assure significant nonlinear response, the amplitude of the three accelerograms are scaled to peak accelerations of 57% g, 50% g and 61% g, respectively.

The different characteristics of these three scaled accelerograms can be compared in both the time and frequency domains. Figures 3.2-4(a) show the time histories of the two accelerograms from 0 to 15 seconds which is the segment used

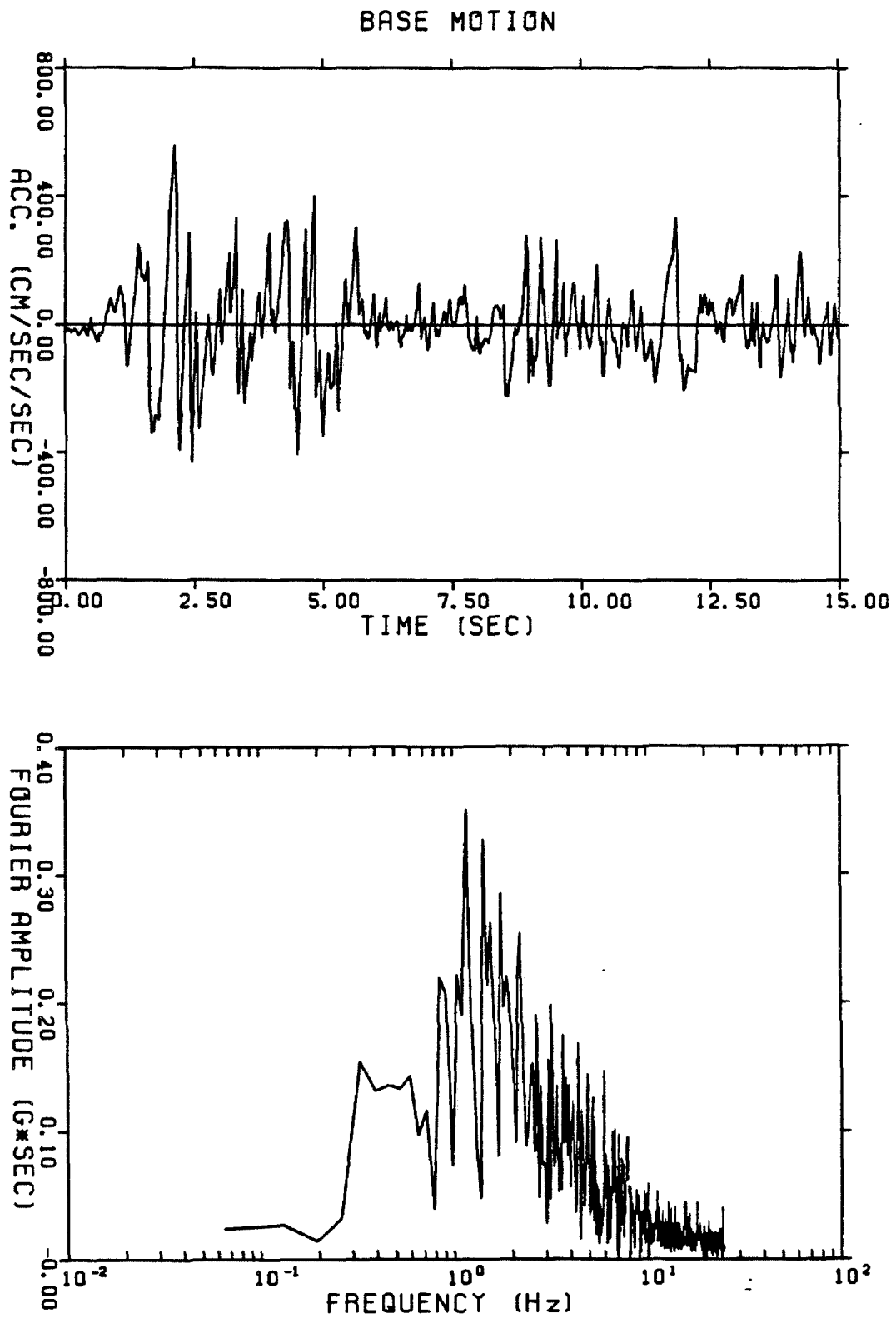


Figure 3.2 Scaled El Centro accelerogram, 1940, S00E.
(a) Time history (peak = 0.57 g).
(b) Fourier spectrum.

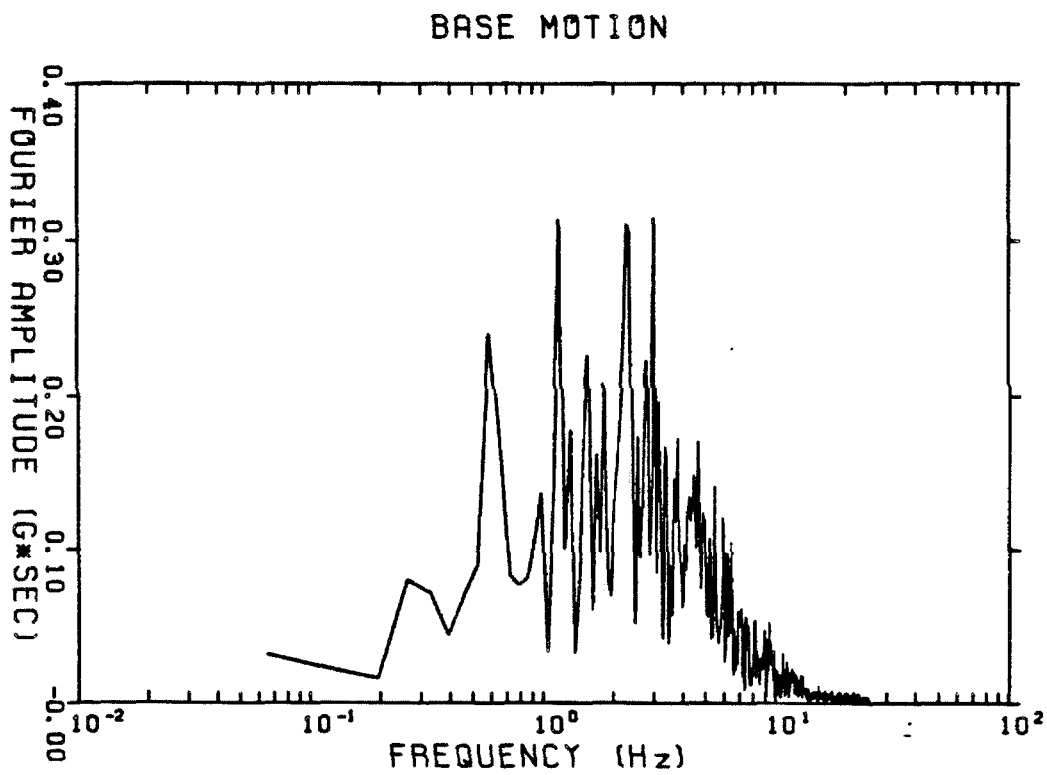
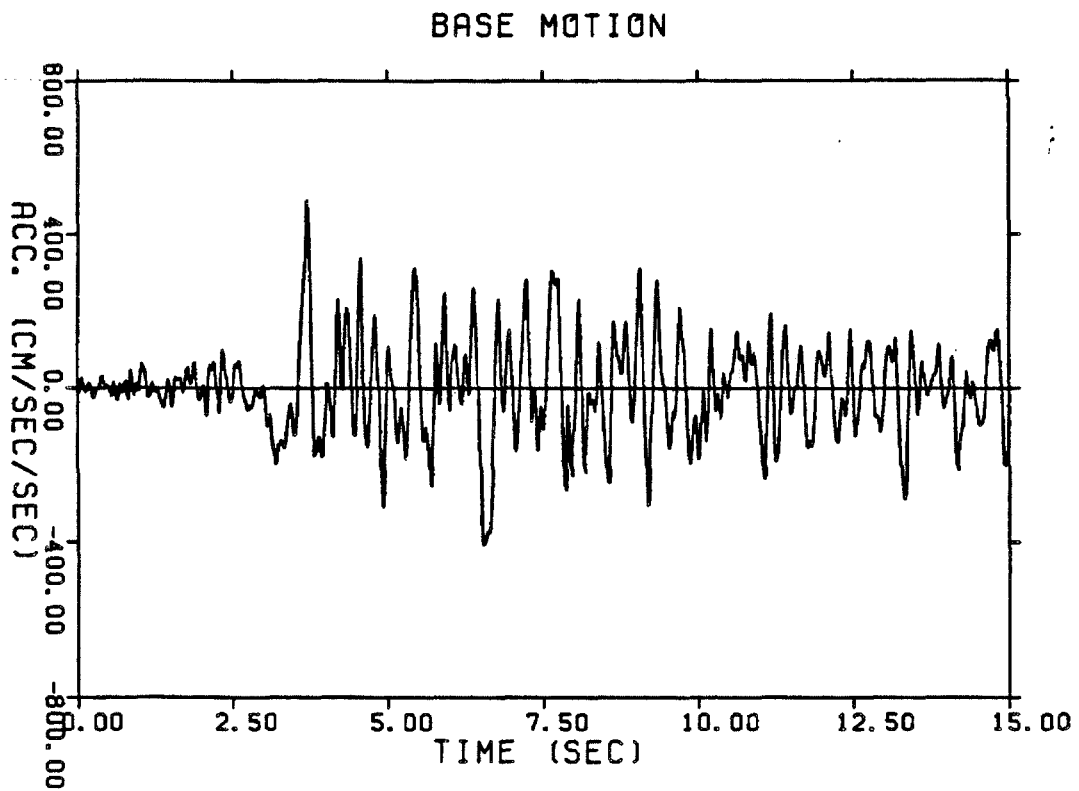


Figure 3.3 Scaled Taft accelerogram, 1952, S69E.
(a) Time history (peak = 0.50 g).
(b) Fourier spectrum.

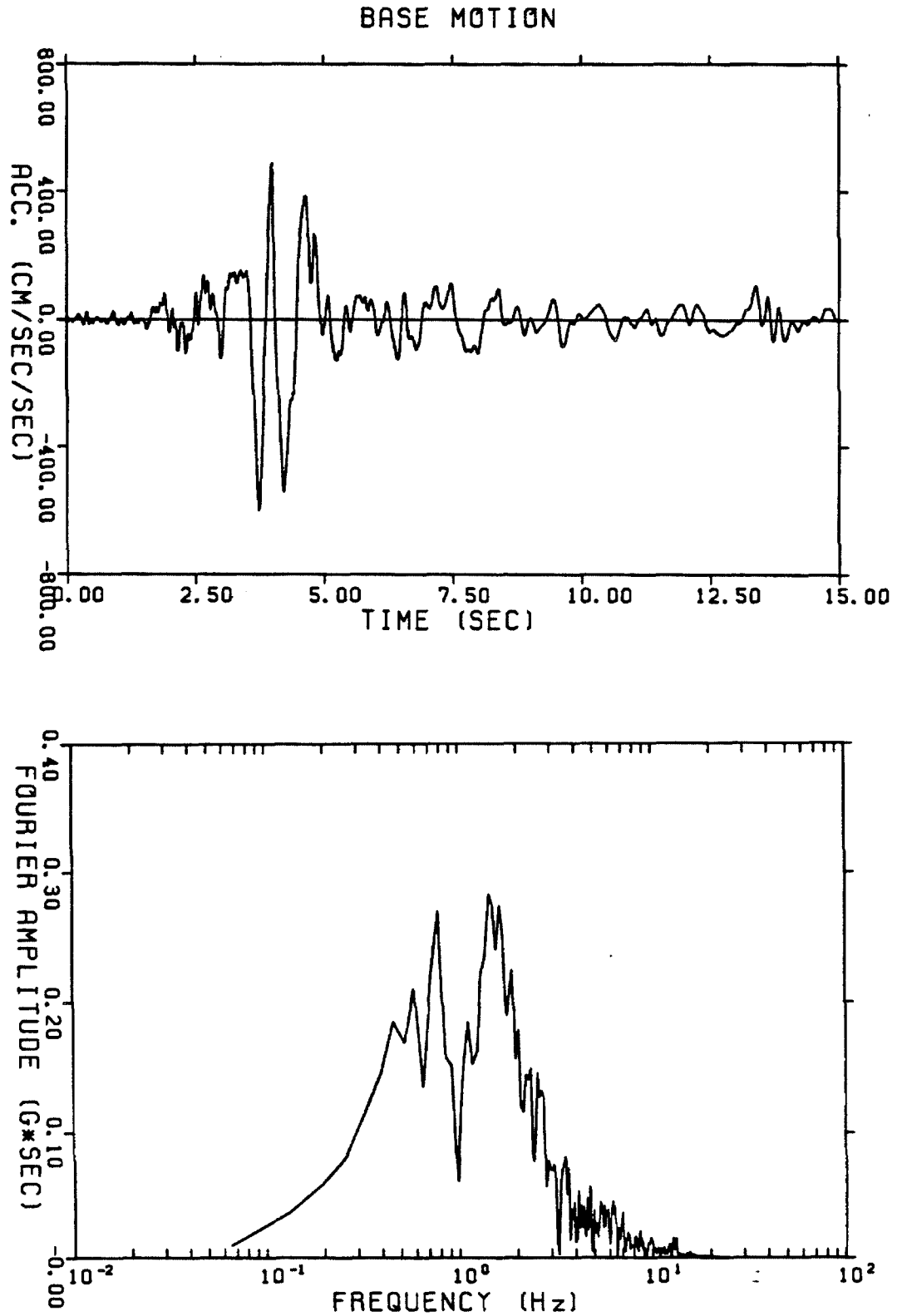
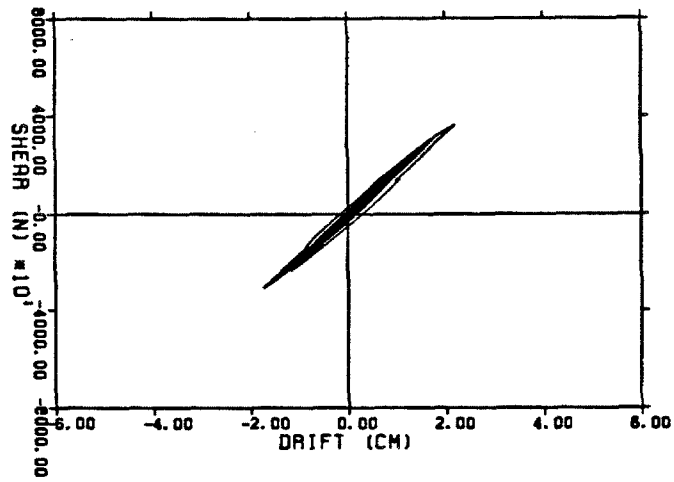
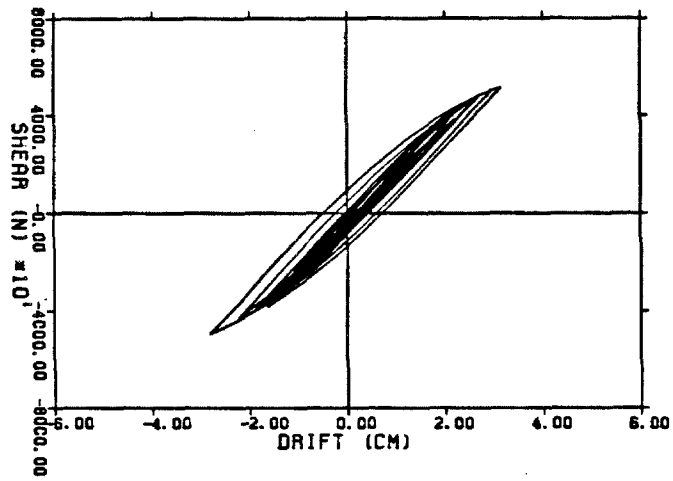


Figure 3.4 Scaled Parkfield accelerogram, 1966, N65E.
(a) Time history (peak = 0.61 g).
(b) Fourier spectrum.

ELEMENT-3



ELEMENT-2



ELEMENT-1

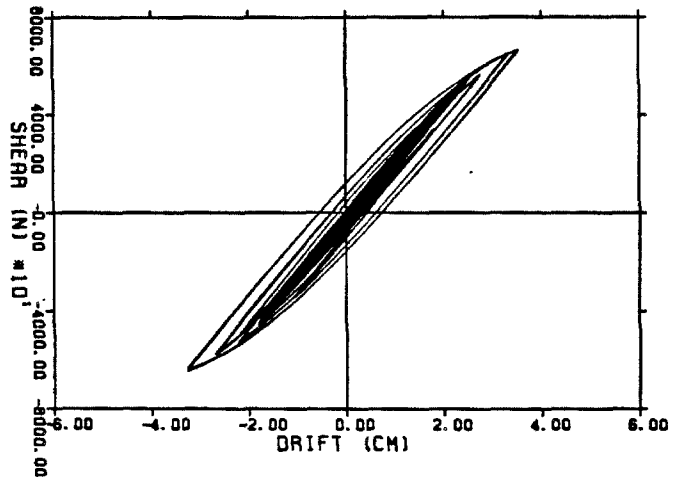
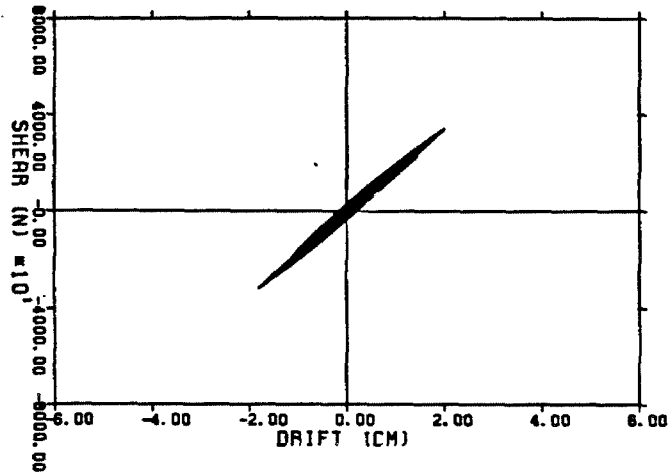
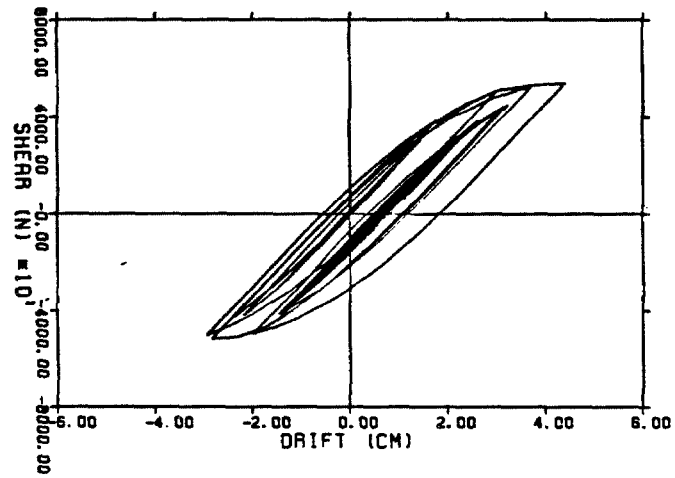


Figure 3.5 Inter-mass restoring force diagrams for verification system to scaled El Centro accelerometerogram.

ELEMENT-3



ELEMENT-2



ELEMENT-1

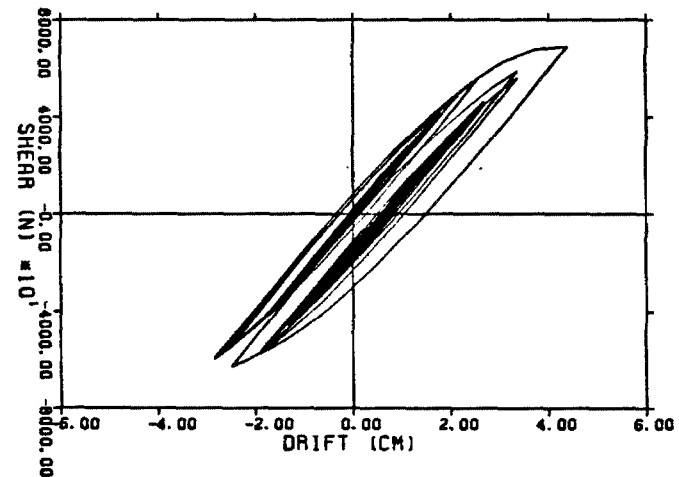
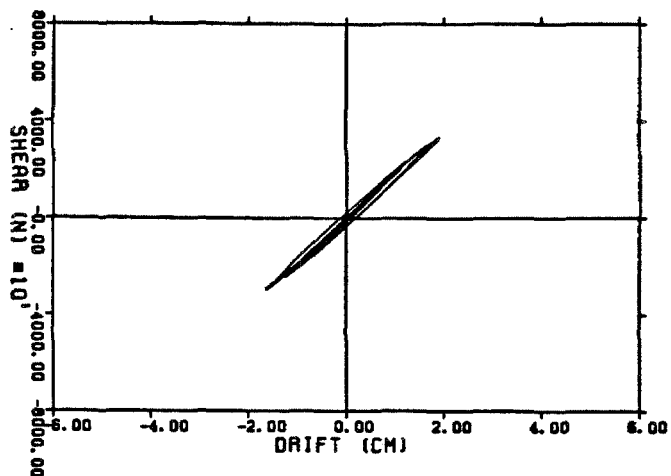
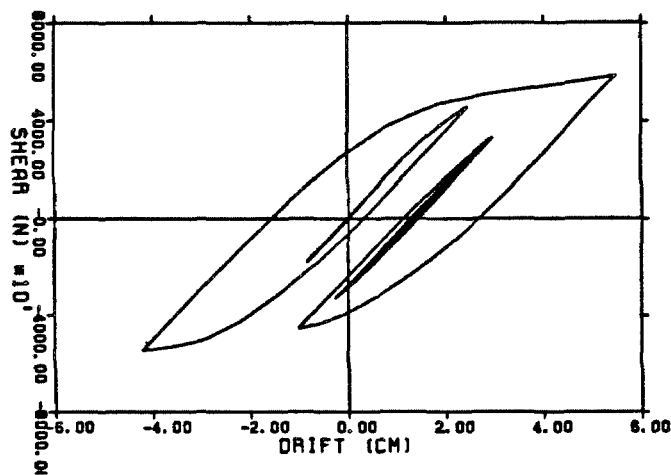


Figure 3.6 Inter-mass restoring force diagrams for verification system to scaled Taft accelerogram.

ELEMENT-3



ELEMENT-2



ELEMENT-1

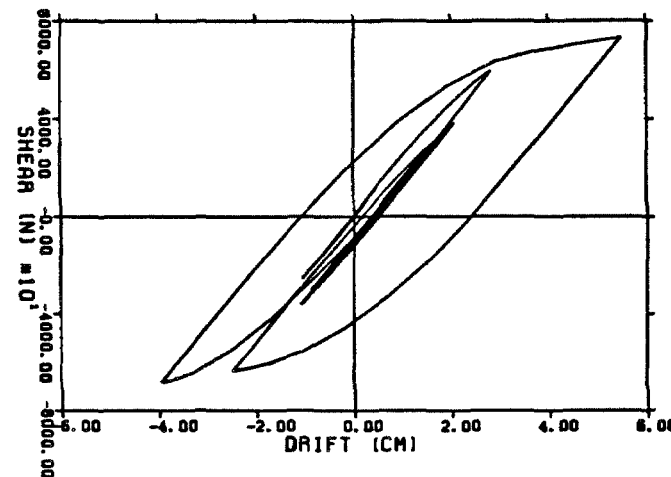


Figure 3.7 Inter-mass restoring force diagrams for verification system to scaled Parkfield accelerometer.

to generate the simulated response for the system. The frequency domain comparison is made by showing the corresponding Fourier amplitude spectra in Figures 3.2–4(b). The corresponding inter-mass restoring force diagrams are shown in Figures 3.5–3.7. Note that Figures 3.6 and 3.7 exhibit more significant hysteretic behavior than does Figure 3.5.

“Measured” Data In the present study, it will be assumed that the only “measured” data is the absolute acceleration at the roof, $\ddot{x}_3(t)$, and at the base, $\ddot{x}_b(t)$. By subtracting the base input from the absolute response, the relative response with respect to the base is obtained. The velocities and displacements are obtained by integration of the accelerations. The system is taken to be initially at rest.

3.5.2 Model Identification - Parameter Calibration

The first stage is to identify a nonlinear model for the verification system. In this stage, the model parameters are calibrated using a particular set of simulated input and response “measurements”. The data used herein are the above-mentioned scaled El Centro accelerogram and the corresponding acceleration response at the “roof”.

Observe the Fourier amplitude spectrum for the relative acceleration of the roof with respect to the base shown in Figure 3.8. Dominant frequencies are clearly visible. The somewhat erratic appearance around each dominant frequency peak is partly due to the nonlinearity of the system. However, the dominance of a number of frequencies and corresponding “modes” is quite clear. A similar phenomenon is also observed for the response frequency spectra of actual structures subjected to strong ground motions. As mentioned in Section 2.6.2, this frequency domain information can provide important guidance in choosing the frequency band of dominant modes in the response. The values of frequency bands chosen for the first two dominant modes are indicated in Table 3.1.

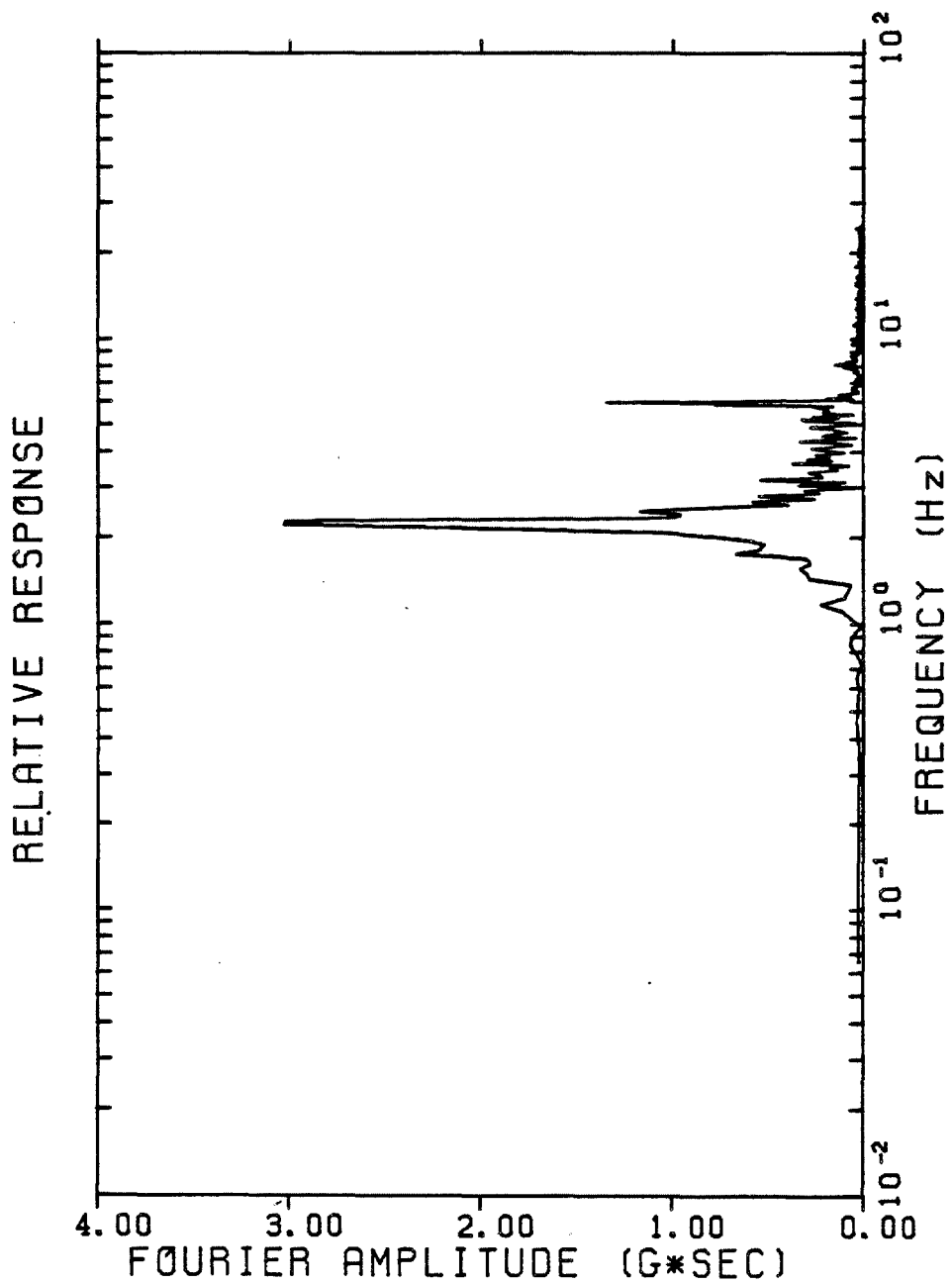


Figure 3.8 Fourier amplitude spectrum of acceleration for response at top mass of verification system.

Following the procedures described in Section 2.6, a succession of single-mode identifications is performed one mode at a time and a final modal model based on dominant modes is obtained. For each single-mode identification, initial estimates are not required because the method reduces the problem to single-parameter identification with respect to the modal effective participation factor β^r . The optimal estimate β^r is easily obtained by a simple one-dimensional nonlinear optimization scheme outlined in Section 2.6.4. For given β^r , the modal parameters for the generalized modal restoring force h^r are estimated directly by the nonparametric identification technique described in Section 3.4.3.

The only potential frequency domain problem is the determination of the appropriate frequency band for each mode from the Fourier amplitude spectra of the response. The erratic appearance around each dominant peak may sometimes make the choice difficult. However, it is found that any mistake made in choosing the frequency band will result in some parameters identified being nonphysical or the convergence of the identification algorithm being difficult. Subsequent corrections can be made if either of these two situations is encountered.

The effective participation factor β^r is determined by minimizing the difference between the model and actual system response. Recall the definition of P in Section 2.5; that is, the ratio of the r.m.s. difference of the response at peaks only to the maximum response of the system. Any response quantity can be chosen in P . The acceleration is used in this study because the signal of the high frequency modes is relatively small in both velocity and displacement and also because the acceleration time history has relatively more peaks.

The results for the optimal model determined by acceleration matching are given in Table 3.1. The prediction error P is also given. Table 3.1 shows that after the second mode has been identified, the prediction error P based on the acceleration peaks is 0.13. Softening behavior is observed from the negative sign of a_2^r

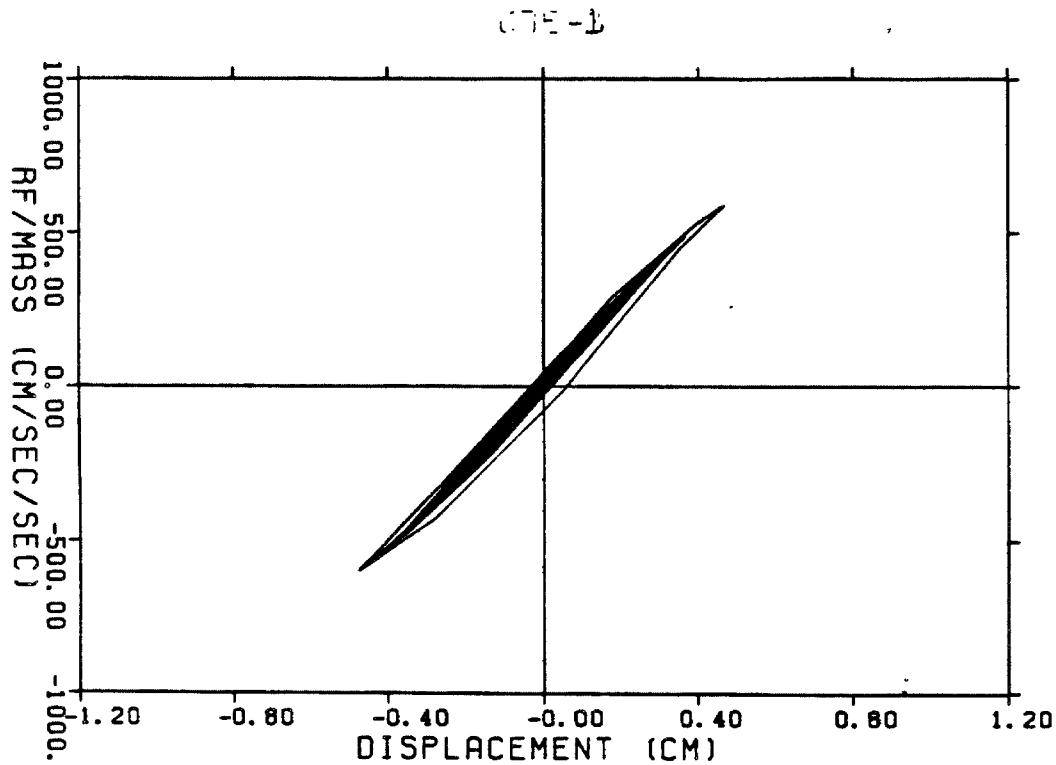
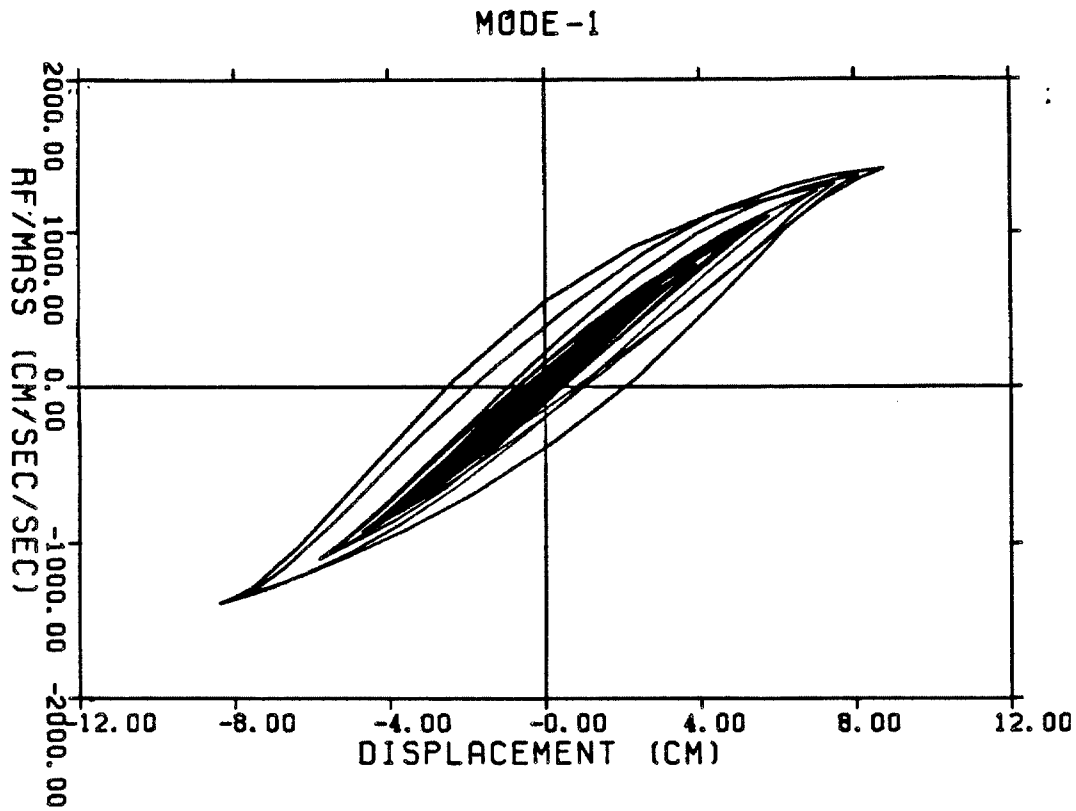


Figure 3.9 Generalized modal restoring force diagrams for identified four-parameter nonhysteretic model to scaled El Centro accelerogram.

- (a) First mode.
- (b) Second mode.

for both modes. This is also clearly seen from the generalized modal restoring force diagrams shown in Figure 3.9. Note that an attempt to identify the third mode is not successful because the third mode component of the response is relatively too small.

The fit of the response time histories using two modes is shown in Figure 3.10–3.12. The solid line is the “measured” system response and the dashed line represents the response predicted by the model. From Figure 3.10, it is seen that the two-mode model gives a very good frequency and amplitude estimate of the actual acceleration data. The identified velocity and displacement for the two-mode model are compared with the actual velocity and displacement in Figures 3.11 and 3.12, respectively. These figures show that a good frequency and amplitude match is still obtained even though the model is determined by minimizing the prediction error based on acceleration response only.

Finally, Figure 3.13(a) shows a profile of the prediction error P with respect to the effective participation factor for the first mode. The range of the effective participation factor is increased from 0 to 3 and the corresponding values of P are plotted. Observe that the profile is very smooth and that the global minimum corresponding to the effective participation factor of the first mode is apparent. The absence of other local minima is expected because other modes have been eliminated from the response by band-pass filtering. This supports the point made previously that the global minimum can be easily obtained by any one-dimensional optimization method and no initial estimates of the modal parameters are necessary. A similar plot is shown for the second mode identification in Figure 3.13(b). The global minimum corresponding to the effective participation factor of the second mode is also apparent.

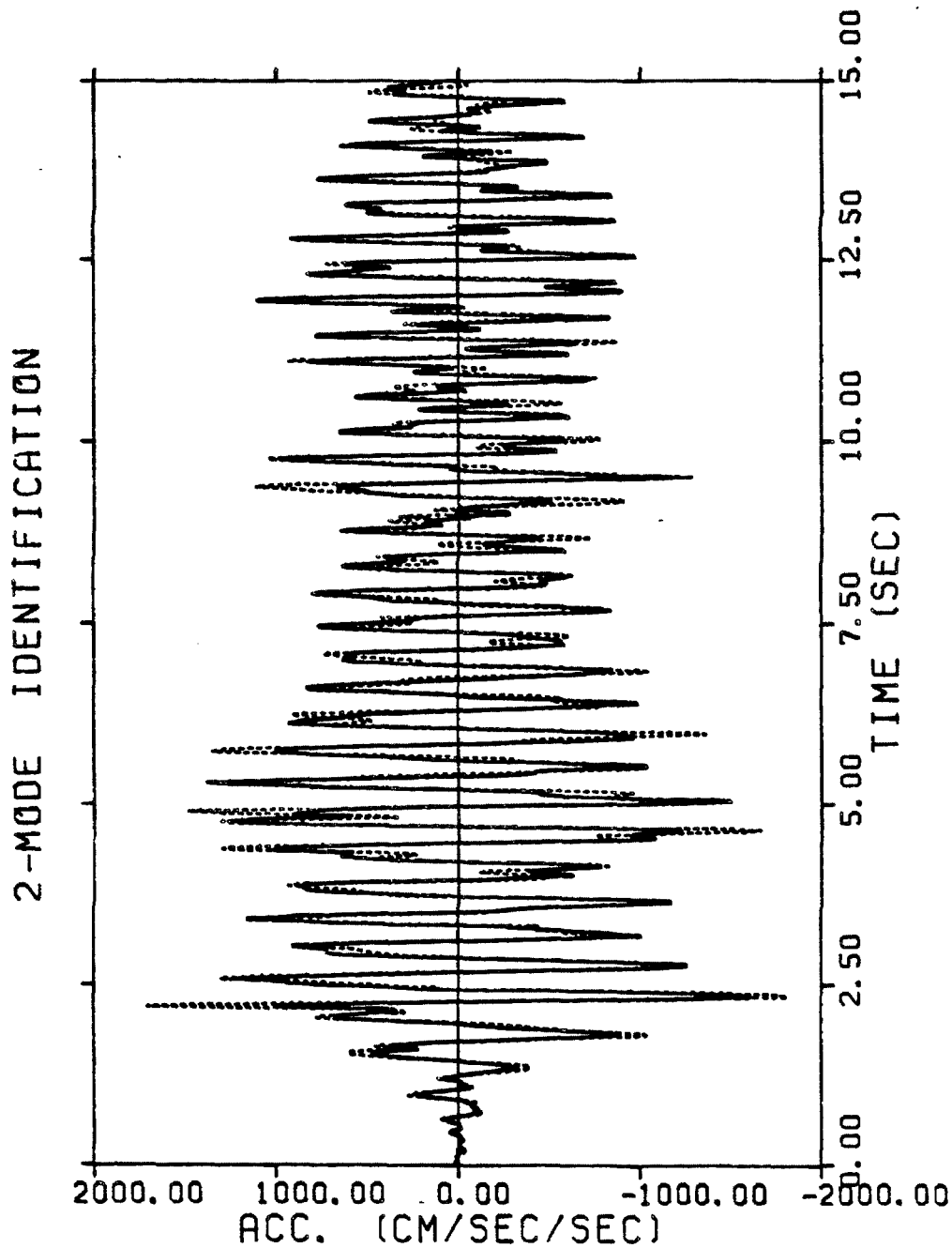


Figure 3.10 Identification of relative acceleration at top mass of verification system to scaled El Centro accelerogram. Actual response (—), optimal four-parameter nonhysteretic model with two modes (- - -).

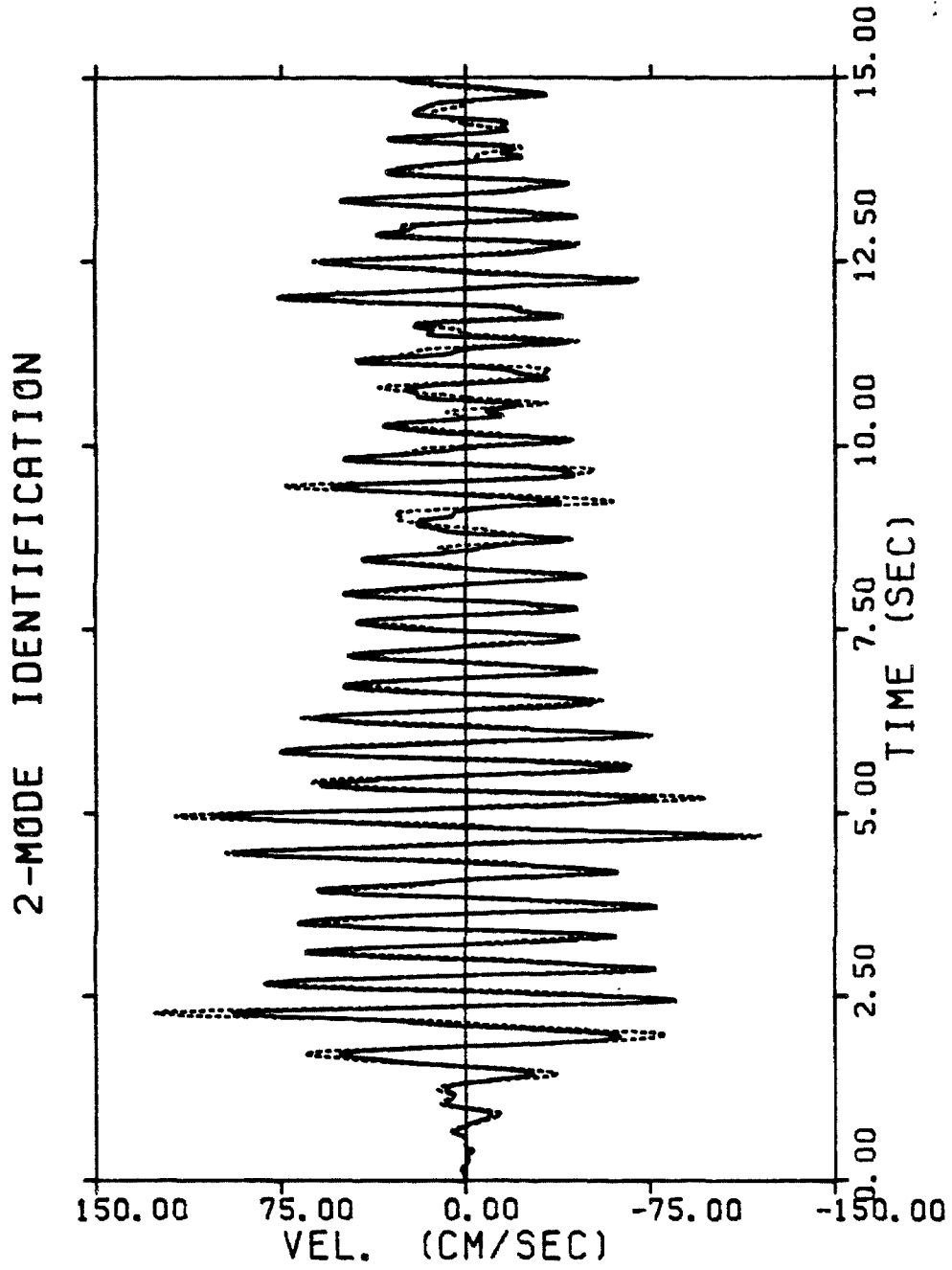


Figure 3.11 Identification of relative velocity at top mass of verification system to scaled El Centro accelerogram. Actual response (—), optimal four-parameter nonhysteretic model with two modes (---).

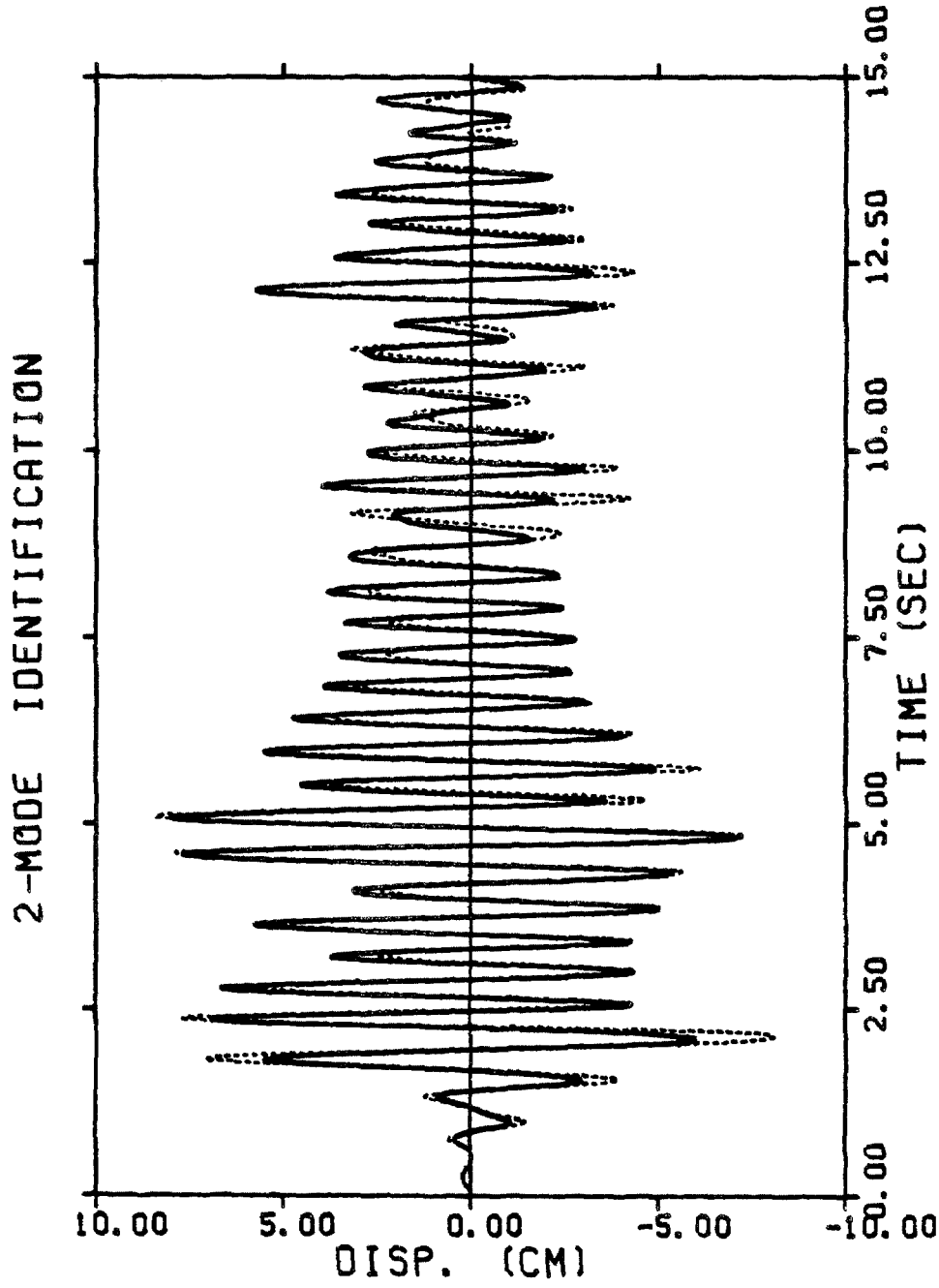


Figure 3.12 Identification of relative displacement at top mass of verification system to scaled El Centro accelerogram. Actual response (—), optimal four-parameter nonhysteretic model with two modes (- - -).

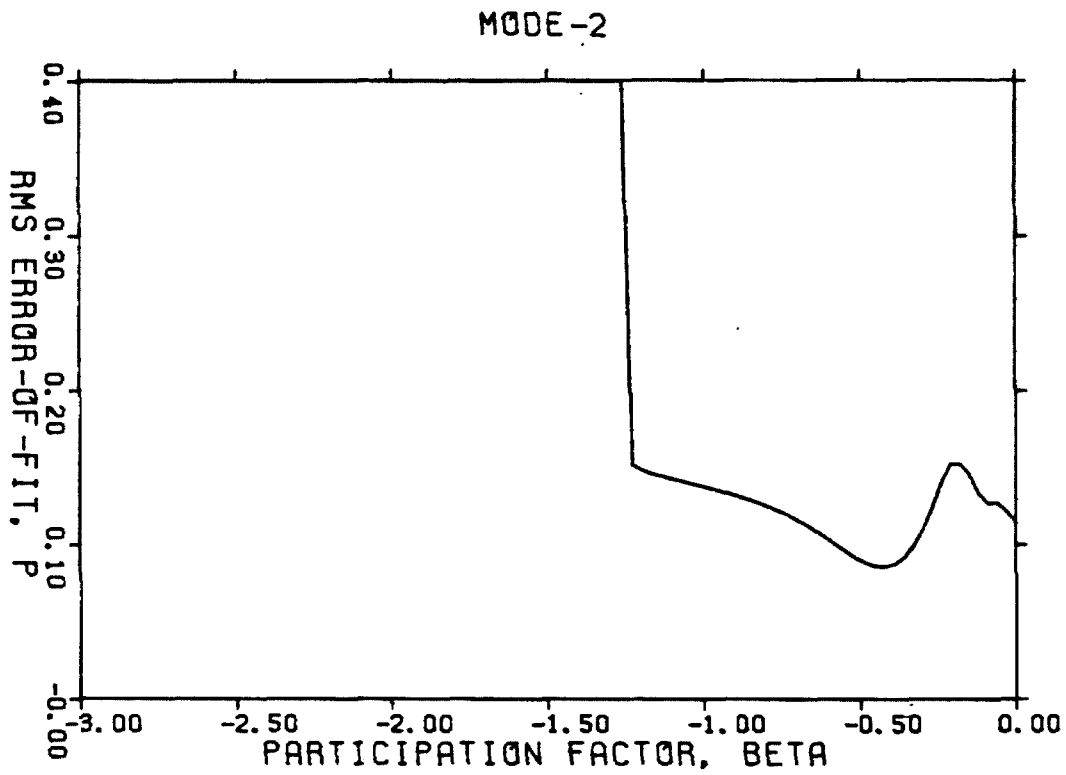
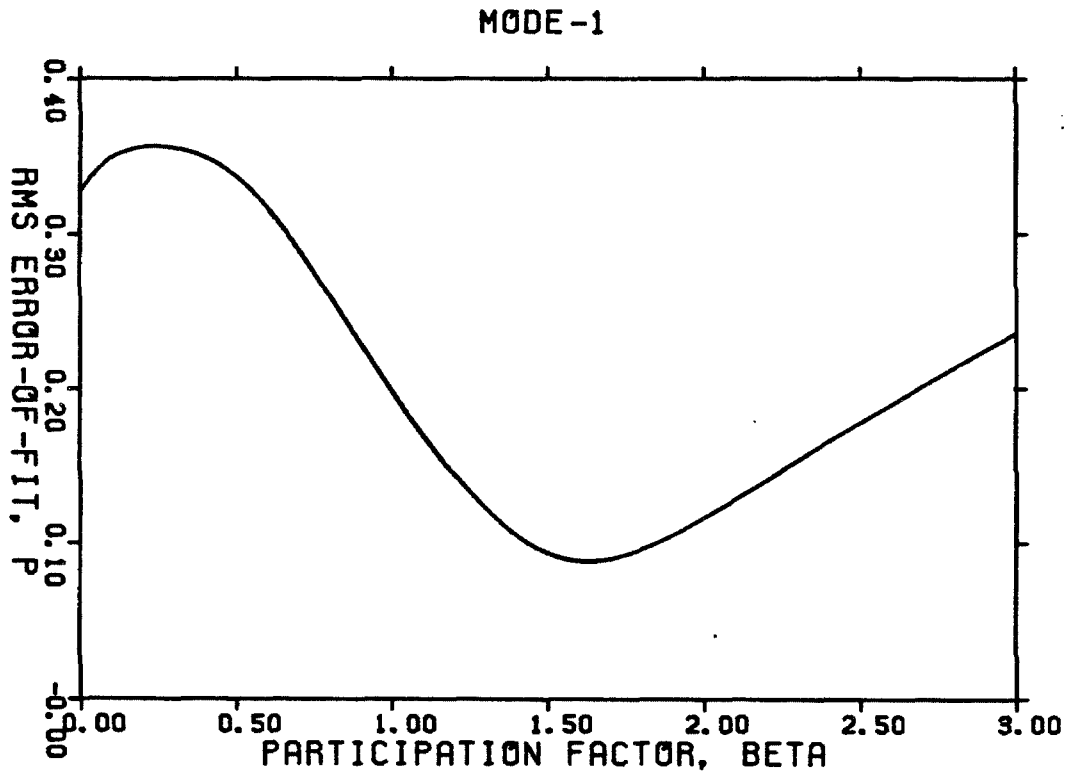


Figure 3.13 Profiles of prediction error P for determining effective modal participation factors based on peaks of relative acceleration of verification system to El Centro accelerogram.
(a) First mode
(b) Second mode.

3.5.3 Model Validation - Response Prediction

As the second stage of verification, the previously identified nonlinear model is used to predict the roof response to two different base excitations consisting of the scaled Taft and Parkfield earthquakes mentioned above.

Figures 3.14–3.16 show the response time histories of the system to the scaled Taft earthquake as obtained from the model identified using the scaled El Centro earthquake. The prediction error P based on acceleration peaks is summarized in Table 3.1. In general, the agreement between the actual response (solid) and that predicted by the model (dashed) is seen to be quite good. This shows that the nonlinear stiffness and energy dissipation behavior of the system can be fairly well predicted in this case by the equivalent nonhysteretic model identified previously. However, some details of the response time histories, especially the permanent or drift displacement, are not reproduced by the model. This illustrates the fundamental problem of all nonhysteretic models that they have no mechanism with which the hysteretic behavior of a nonlinear system can be identified.

In order to support this point, the previously identified model is used to predict the response to the scaled Parkfield accelerogram. The characteristics of the excitation and response in this case are quite different from those in the identification case. The prediction error P based on acceleration peaks is summarized in the last column of Table 3.1. The fit of the time histories is shown in Figures 17–19. From the results, it is clearly seen that the model does not predict the response as well as before, especially the prediction of the displacement time history. This is due to the limitation of nonhysteretic models for identifying and predicting the nonlinear response behavior of hysteretic systems.

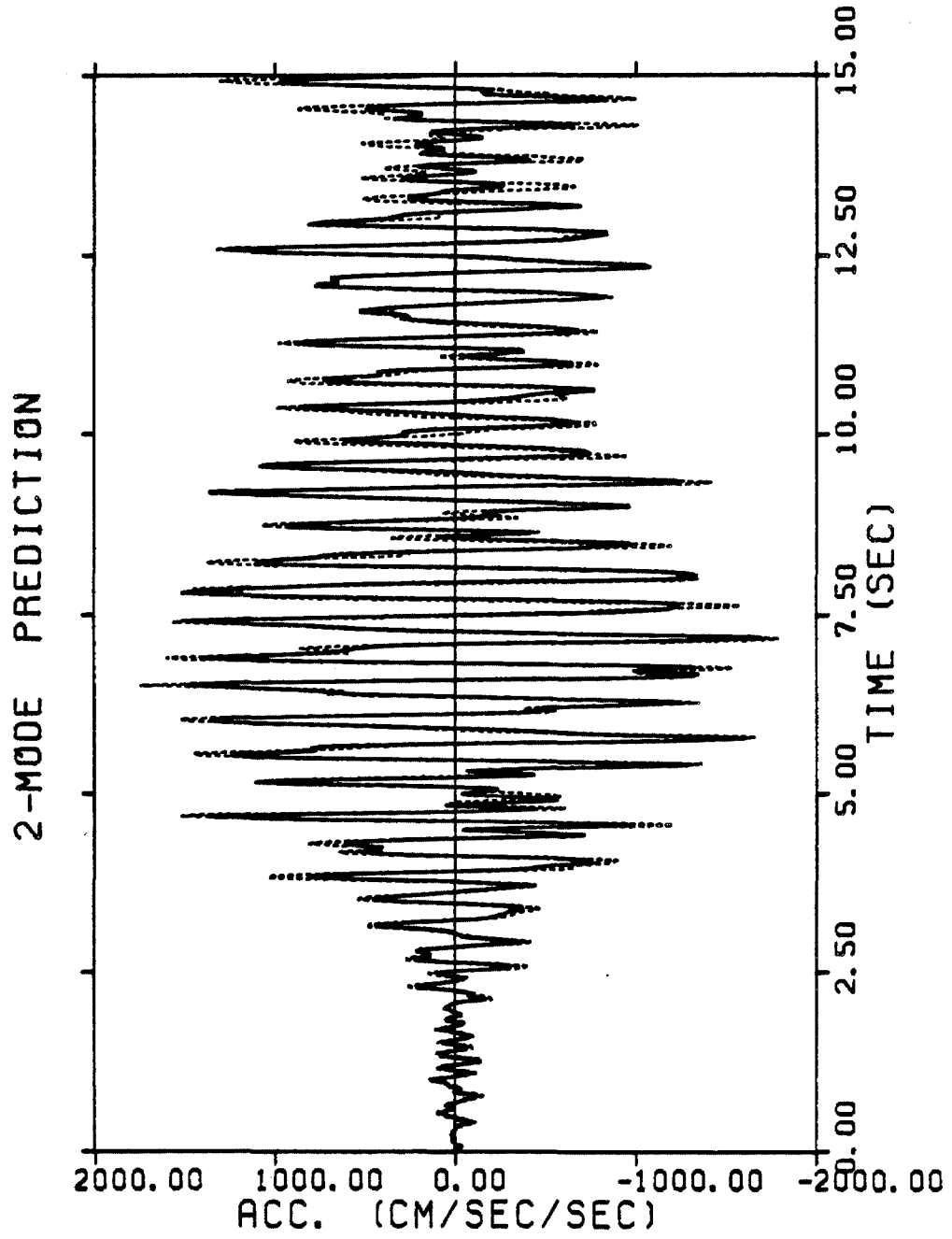


Figure 3.14 Prediction of relative acceleration at top mass of verification system to scaled Taft accelerogram. Actual response (—), optimal four-parameter nonhysteretic model with two modes (- - -).

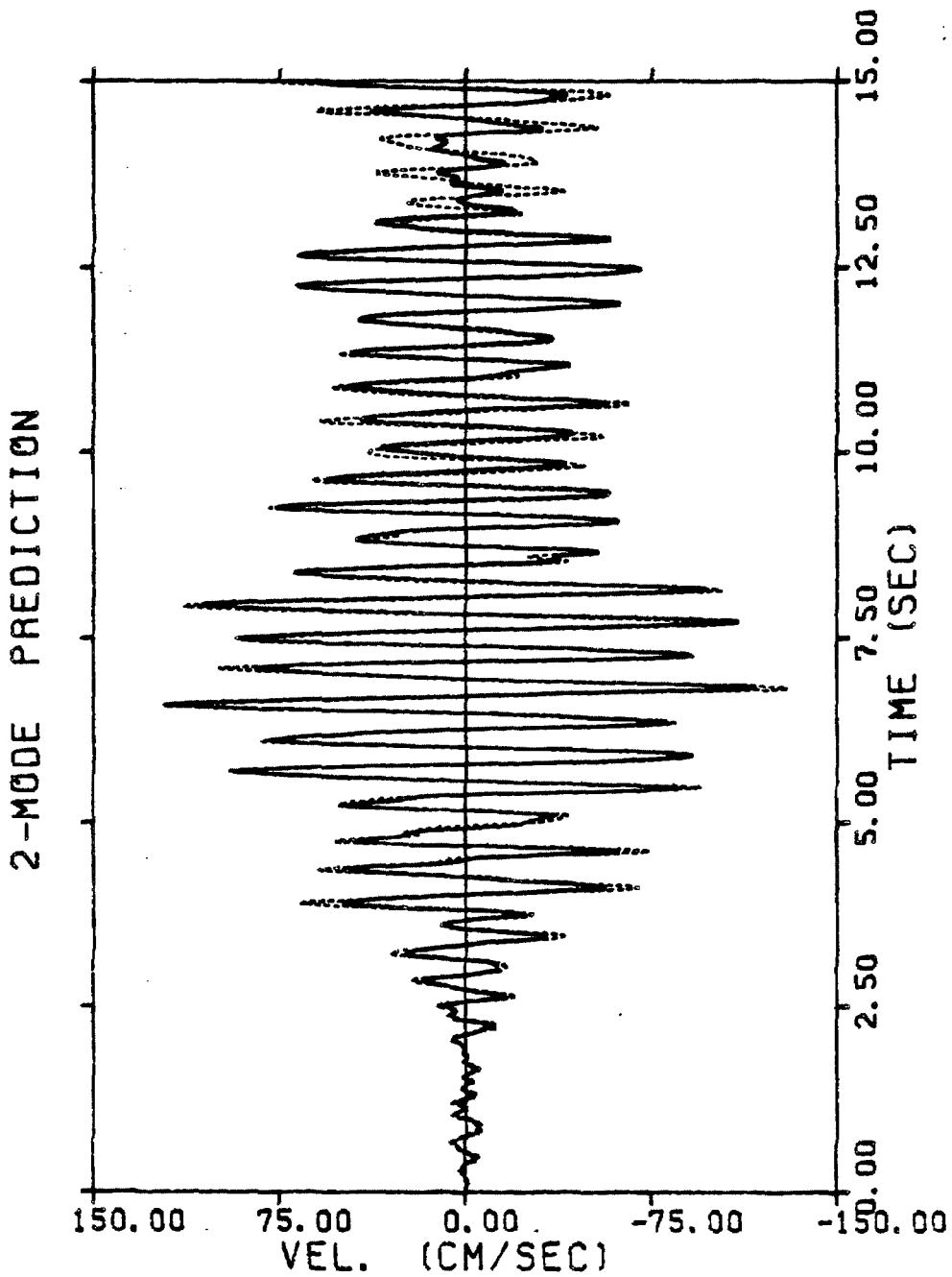


Figure 3.15 Prediction of relative velocity at top mass of verification system to scaled Taft accelerogram. Actual response (—), optimal four-parameter nonhysteretic model with two modes (- - -).

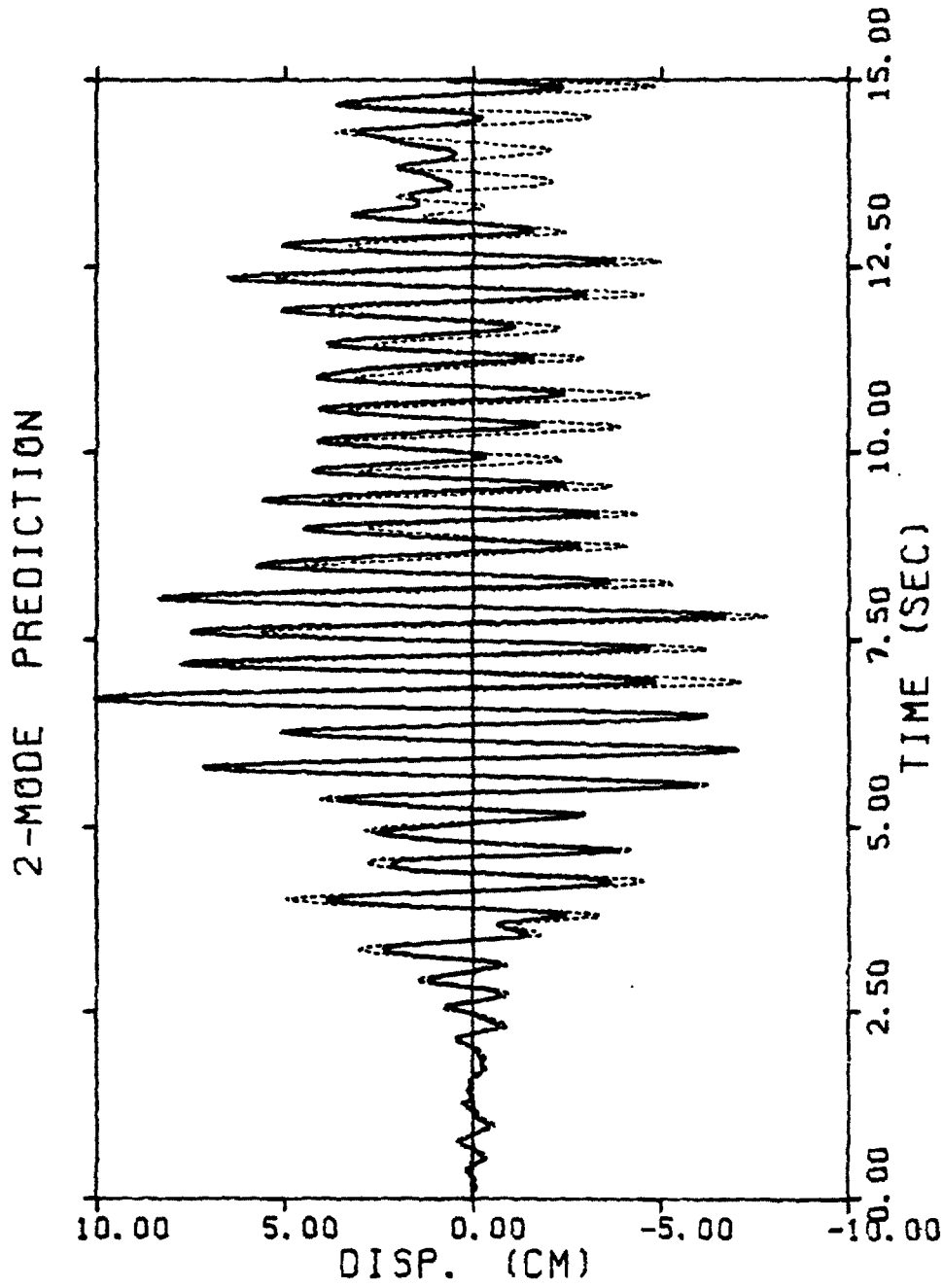


Figure 3.16 Prediction of relative displacement at top mass of verification system to scaled Taft accelerogram. Actual response (—), optimal four-parameter nonhysteretic model with two modes (- - -).

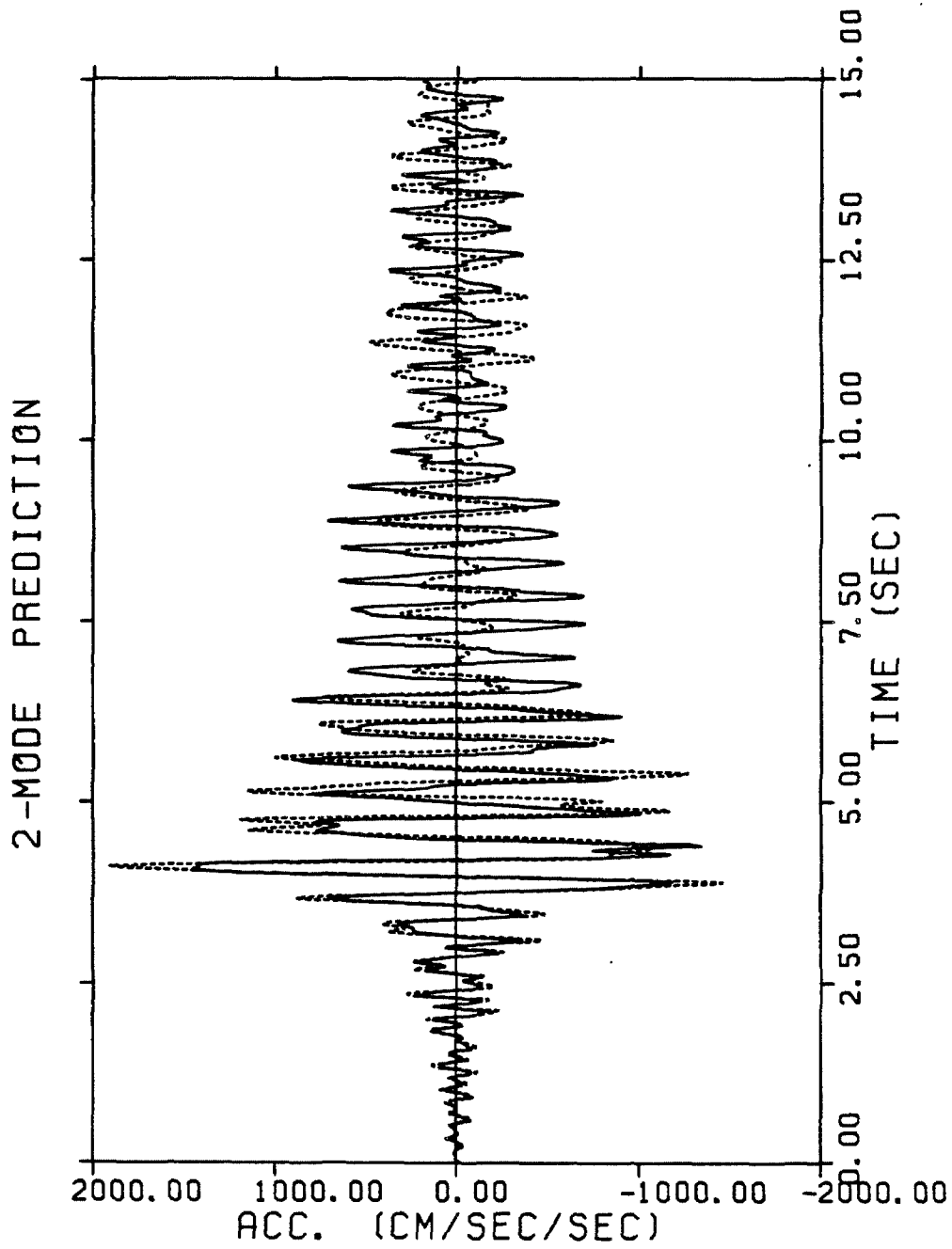


Figure 3.17 Prediction of relative acceleration at top mass of verification system to scaled Park-field accelerogram. Actual response (—), optimal four-parameter nonhysteretic model with two modes (- - -).

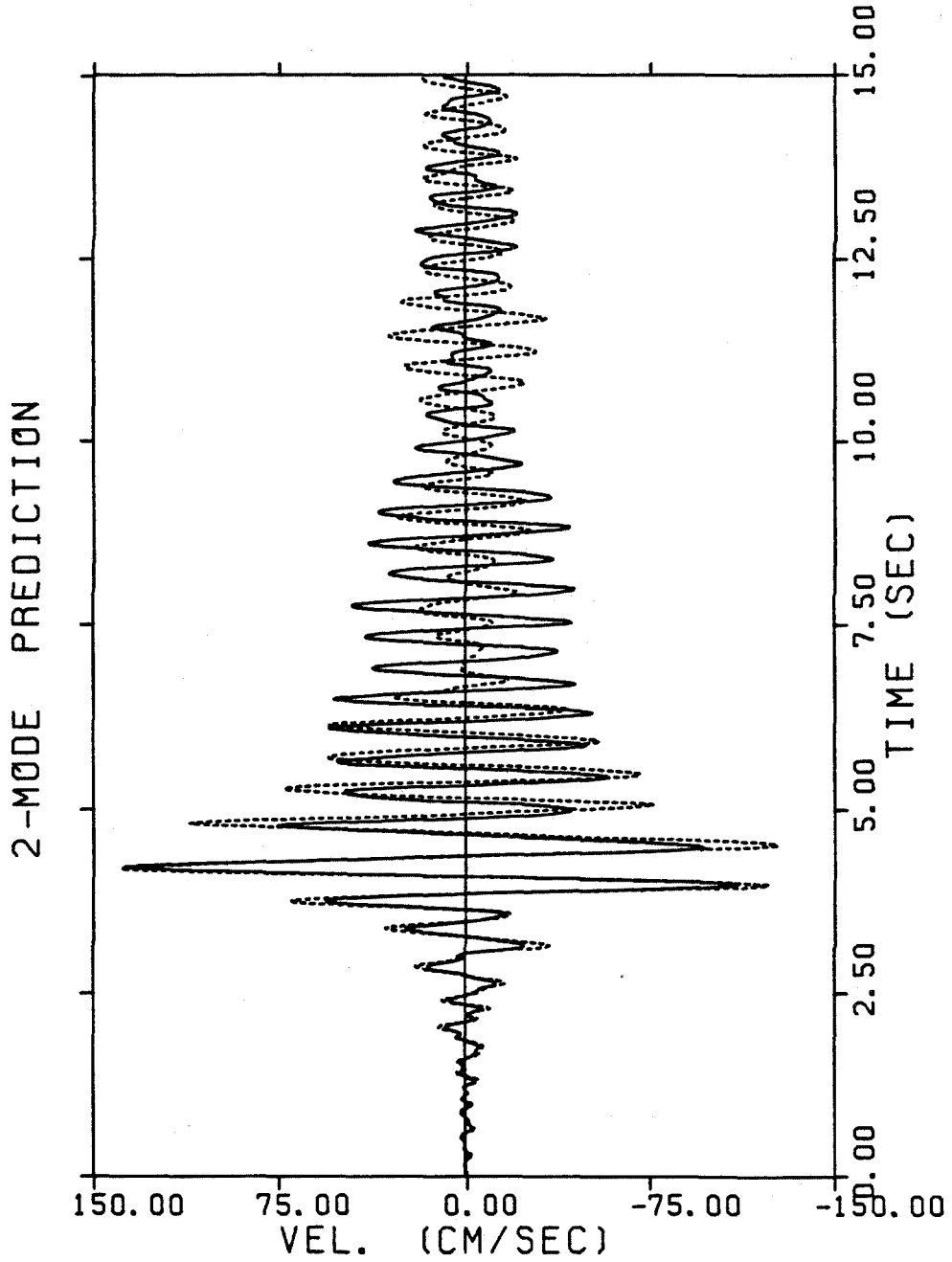


Figure 3.18 Prediction of relative velocity at top mass of verification system to scaled Parkfield accelerogram. Actual response (—), optimal four-parameter nonhysteretic model with two modes (- - -).

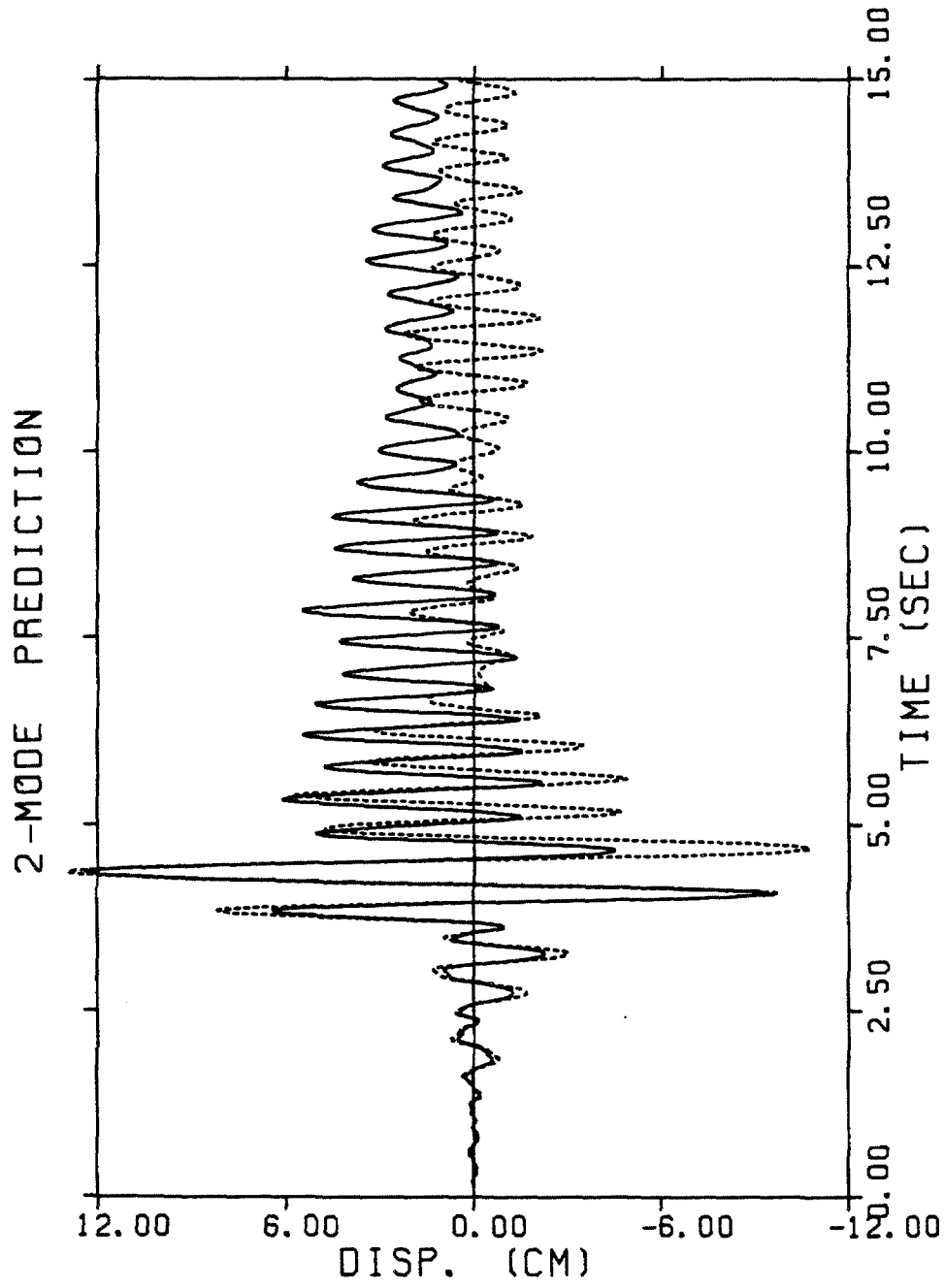


Figure 3.19 Prediction of relative displacement at top mass of verification system to scaled Park-field accelerogram. Actual response (—), optimal four-parameter nonhysteretic model with two modes (- -).

Identification										Prediction		
El Centro ⁽¹⁾										Taft ⁽²⁾	Parkfield ⁽³⁾	
Mode	Frequency Band (Hz)	α_1^f (1/sec ²)	α_2^f 1/(cm · sec) ²	α_3^f (1/sec)	α_4^f (sec/cm ²)	β^r	α_5^f (1/sec)	α_6^f (sec/cm ²)	β^r	P	. P	P
1	0.0-4.0	2.13×10^2	-6.74×10^{-1}	8.48×10^{-2}	3.25×10^{-4}	1.610	1.11×10^{-1}	1.60×10^{-2}	1.67×10^{-1}	1.30×10^{-1}	1.21×10^{-1}	1.89×10^{-1}
2	4.0-7.5	1.44×10^3	-8.29×10^2	1.11×10^{-1}	1.60×10^{-2}	-0.442	1.11×10^{-1}	1.60×10^{-2}	1.30×10^{-1}	1.30×10^{-1}	8.63×10^{-2}	1.90×10^{-1}

- (1) Simulated response with the El Centro, 1940, S00E, scaled to a peak of 57% g
(2) Simulated response with the Taft, 1952, S69E, scaled to a peak of 50% g
(3) Simulated response with the Parkfield, 1966, N65E, scaled to a peak of 61% g

Table 3.1 Identification and Prediction Results of the Four-Parameter Nonhysteretic Model Using Simulated Data

3.6 Summary

It is concluded that the identification process presented in this chapter yields a nonparametric nonhysteretic model for an equivalent memoryless nonlinear system [18-24]. The energy dissipated per cycle of motion by the hysteretic elements in the system is approximately equal to that dissipated by the equivalent nonparametric model identified. It should be noted that the identification does not find any characteristics of the hysteretic response. Rather, it produces the “best” coefficients of a model whose response matches the measured system response in a least-square sense for the given excitation.

An important objective of this dissertation is to identify and to characterize the hysteretic behavior for a nonlinearly responding system from a single measured response and base input. Once a model for the system has been identified, it is intended to use this model to predict its response to other excitations. It is clear from the above prediction studies that the four-parameter nonparametric model identified cannot serve this purpose and a parametric hysteresis model must ultimately be employed. However, some preliminary results estimated from the nonparametric identification can be exploited in the further identification studies of hysteretic systems. This point will be illustrated in the remaining parts of the thesis.

References

- [1] V. Volterra, *Theory of Functionals and of Integral and Integro-Differential Equations*, Dover, New York, 1959.
- [2] N. Wiener, *Nonlinear Problems in Random Theory*, M.I.T. Press, Cambridge, Massachusetts, 1958.
- [3] T. K. Caughey, "Nonlinear Analysis, Synthesis and Identification Theory," *Proceedings of the Symposium on Testing and Identification of Nonlinear Systems*, California Institute of Technology, March 1975.
- [4] F. E. Udvia and P. Z. Marmarelis, "The Identification of Building Systems. I The Linear Case," *Bulletin of Seismology Society of America*, Vol. 66, 1976.
- [5] F. E. Udvia and P. Z. Marmarelis, "The Identification of Building Systems. II The Nonlinear Case," *Bulletin of Seismology Society of America*, Vol. 66, 1976.
- [6] S. F. Masri, T. K. Caughey, "A Nonparametric Identification Technique for Nonlinear Dynamic Problems," *ASME Journal of Applied Mechanics*, Vol. 46, June 1979.
- [7] S. F. Masri, H. Sassi, and T. K. Caughey, "Nonparametric Identification of Nearly Arbitrary Nonlinear Systems," *ASME Journal of Applied Mechanics*, Vol. 11, January 1981.
- [8] S. F. Masri, G. A. Bekey, H. Sassi, and T. K. Caughey, "Nonparametric Identification of a Class of Nonlinear Multidegree Dynamic Systems," *International Journal of Earthquake Engineering and Structural Dynamics*, Vol. 10, 1982.
- [9] J. L. Beck, "Determining Models of Structures from Earthquake Records," Report No. EERL 78-01, Earthquake Engineering Research Laboratory, California Institute of Technology, Pasadena, California, June 1978.
- [10] G. H. McVerry, "Frequency Domain Identification of Structural Models from Earthquake Records," Report No. EERL 79-02, Earthquake Engineering Research Laboratory, California Institute of Technology, Pasadena, California, October 1979.
- [11] F. B. Hilderbrand, *Introduction to Numerical Analysis*, McGraw-Hill Book Company, 1974.
- [12] P. J. Davis, *Interpolation and Approximation*, Dover Publications, Inc. 1975.
- [13] F. E. Udvia and C-P Kuo, "Nonparametric Identification of a Class of Nonlinear Close-Coupled Dynamic Systems," *International Journal of Earthquake Engineering and Structural Dynamics*, Vol. 9, 1981.

- [14] S. Toussi and J. Yao, "Identification of Hysteretic Behavior for Existing Structures," Report No. CE-STR-80-19, School of Civil Engineering, Purdue University, December 1980.
- [15] S. Toussi and J. Yao, "Hysteretic Identification of Multi-Story Buildings," Report No. CE-STR-81-15, School of Civil Engineering, Purdue University, May 1981.
- [16] R. W. Clough and D. T. Tang, "Earthquake Simulated Study of a Steel Frame Structure, Vol. I: Experimental Results," Earthquake Engineering Research Center, Report No. UCB/EERC 75/06, University of California, Berkeley, California, April 1975.
- [17] D. T. Tang, "Earthquake Simulated Study of a Steel Frame Structure, Vol. II: Analytical Results," Earthquake Engineering Research Center, Report No. UCB/EERC 75/36, University of California, Berkeley, California, October 1975.
- [18] D. E. Hudson, "Equivalent Viscous Friction for Hysteretic Systems with Earthquake-Like Excitation," *Proceedings of 3rd World Conference on Earthquake Engineering*, New Zealand, 1965.
- [19] P. C. Jennings, "Equivalent Viscous Damping for Yielding Structures," *ASCE Journal of Engineering Mechanics Division*, February, 1968.
- [20] W. D. Iwan, "Application of an Equivalent System Approach to Dissipative Dynamical Systems," *ASME Journal of Applied Mechanics*, Vol. 36, No. 3, September 1969.
- [21] W. D. Iwan, "On the Steady-State Response of a One-Dimensional Yielding Continuum," *ASME Journal of Applied Mechanics*, September 1970.
- [22] W. D. Iwan, "Response of Multi-Degree-of-Freedom Yielding Systems," *ASCE Journal of Engineering Mechanics Division*, Vol. 94, No. EM2, April 1968.
- [23] W. D. Iwan, "Steady-State Response of Yielding Shear Structure," *ASCE Journal of Engineering Mechanics Division*, Vol. 96, No. EM6, December 1970.
- [24] W. D. Iwan and N. C. Gate, "The Effective Period and Damping of a Class of Hysteretic Structures," *Earthquake Engineering and Structural Dynamics*, Vol. 7, 1979.

Chapter 4

Generalized Modal Identification Using Hysteretic Models

4.1 Introduction

The objective of this chapter is to improve the modeling of the hysteretic behavior of a nonlinear structural system by employing a hysteretic restoring force model in the generalized modal identification method. This is done against the backdrop of the observations made in Chapter 3 regarding nonhysteretic nonlinear models.

First, a number of hysteretic models are reviewed with emphasis on the mathematical form of the backbone curves. A physically motivated model with the backbone characterized by only two parameters, called the two-parameter distributed-element model, is then introduced. This model employs the results of the nonparametric identification as an initial estimate for the model parameters. This approach greatly improves the convergence and efficiency of the subsequent parameter optimization process.

The validity of the identification method presented is verified with the same simulated data used in Chapter 3. Improved results are obtained including the prediction of the permanent drift of the response.

4.2 The Backbone Curve

Figure 4.1 [1] shows a typical force-deformation behavior commonly encountered in the systems composed of nonlinear constitutive materials. Observe that the behavior is not elastic even at relatively small force and is hysteretic for forces far below the ultimate strength. Observe also that all the hysteresis loops are smooth except at the turning points.

Many one-dimensional force-deformation relationships have been proposed to model actual hysteretic behavior as observed above. In most of these models, the basic concept is that the hysteretic loops can be characterized by the “skeleton” or “backbone” curve, which has features similar to the force-deformation curve for initial monotonic loading. Hysteretic behavior for these models is usually described using the criterion suggested by Masing in 1926 [2]. The Masing criterion stipulates that the unloading and reloading portions of a hysteresis loop have the same shape as the backbone curve but with the scale expanded by a factor of two and with the origin translated to the point of force reversal. The family of cyclic loading/reloading curves resulting from this assumption is shown in Figure 4.2. Note that Masing’s hypothesis is the one-dimensional equivalent of the kinematic hardening law for an elasto-plastic material.

The use of the backbone curve for nonlinear analysis of structures subjected to earthquake excitations was initiated in the early 1960s [3-4]. A variety of mathematical forms have since been suggested for the backbone curve, including the bilinear, multilinear, hyperbolic and Ramberg-Osgood formulations. In most cases, the construction of hysteresis loops for steady-state cyclic loading is performed by means of the Masing criterion as described above, while for transient cyclic loading, rules such as those proposed by Jennings (1965) or Iwan (1967) are utilized. The latter has been shown to be consistent with test results [5,10-13].

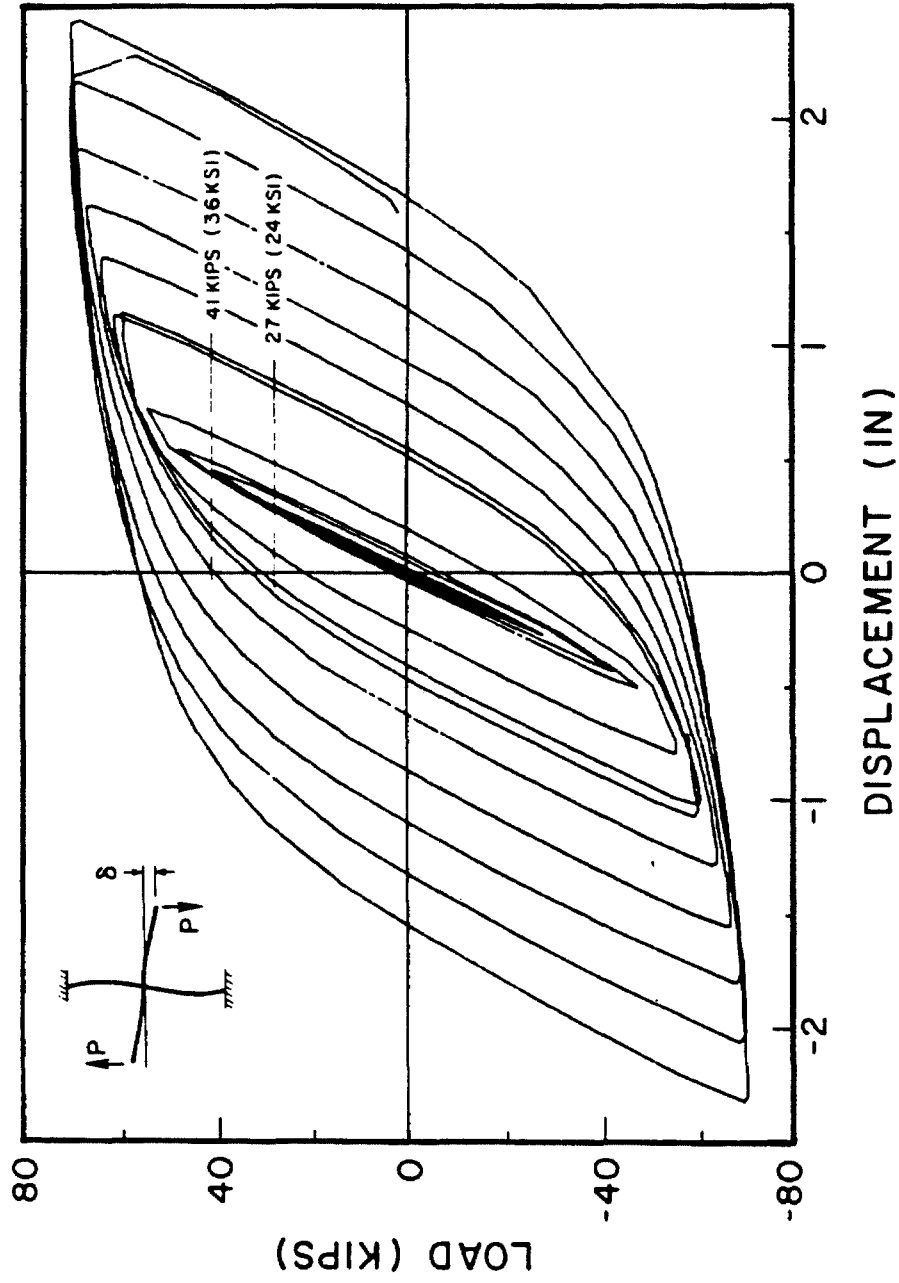


Figure 4.1 Hysteresis loops for beam-column assembly experiment [1].

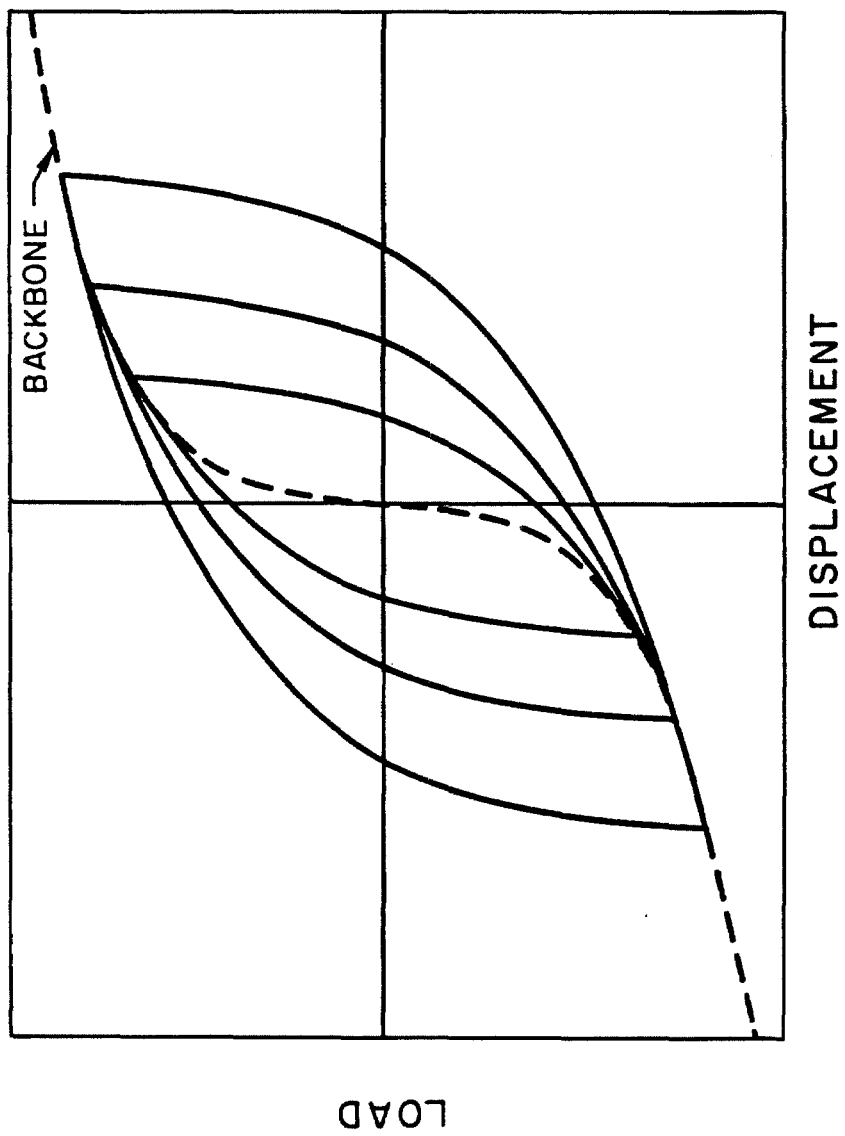


Figure 4.2 Hysteresis loops obtained from backbone curve based on Masing's hypothesis.

4.3 Hysteretic Restoring Force Models

Consider the equation of motion of the system or a particular mode of the system which can be written in the form

$$\ddot{y} + h(y, \dot{y}) = \ddot{a}(t), \quad (4.1)$$

where y and \dot{y} are the generalized relative displacement and velocity, respectively. $h(y, \dot{y})$ is the generalized restoring force per unit of mass and $\ddot{a}(t)$ represents the excitation acceleration.

Hysteretic behavior of $h(y, \dot{y})$ is commonly observed in many nonlinear systems. These range from systems composed of a single structural component to structures consisting of a number of separate elements. In order to identify the hysteretic behavior of real systems, it is desirable to have a model which is mathematically tractable and physically meaningful. Many analytical models have been proposed to describe the hysteresis in nonlinearly restoring systems. It is of interest to review some of these models. This is done below with an emphasis on the initial loading curve, or the backbone curve.

4.3.1 The Elasto-Plastic Model

The elasto-plastic model may be considered a "building block" for more sophisticated hysteretic models. This model has the simplest backbone curve, shown in Figure 4.3(a), that is

$$\begin{aligned} h &= ky; & \dot{y} > 0, 0 \leq y \leq y^* \\ &= ky^*; & \dot{y} > 0, y \geq y^* \end{aligned} \quad (4.2)$$

A physical idealization of such behavior is illustrated in Figure 4.3(b) which consists of a linear spring with stiffness k in series with a Coulomb or slip damper with a maximum allowable force ky^* , where y^* denotes the yielding level.

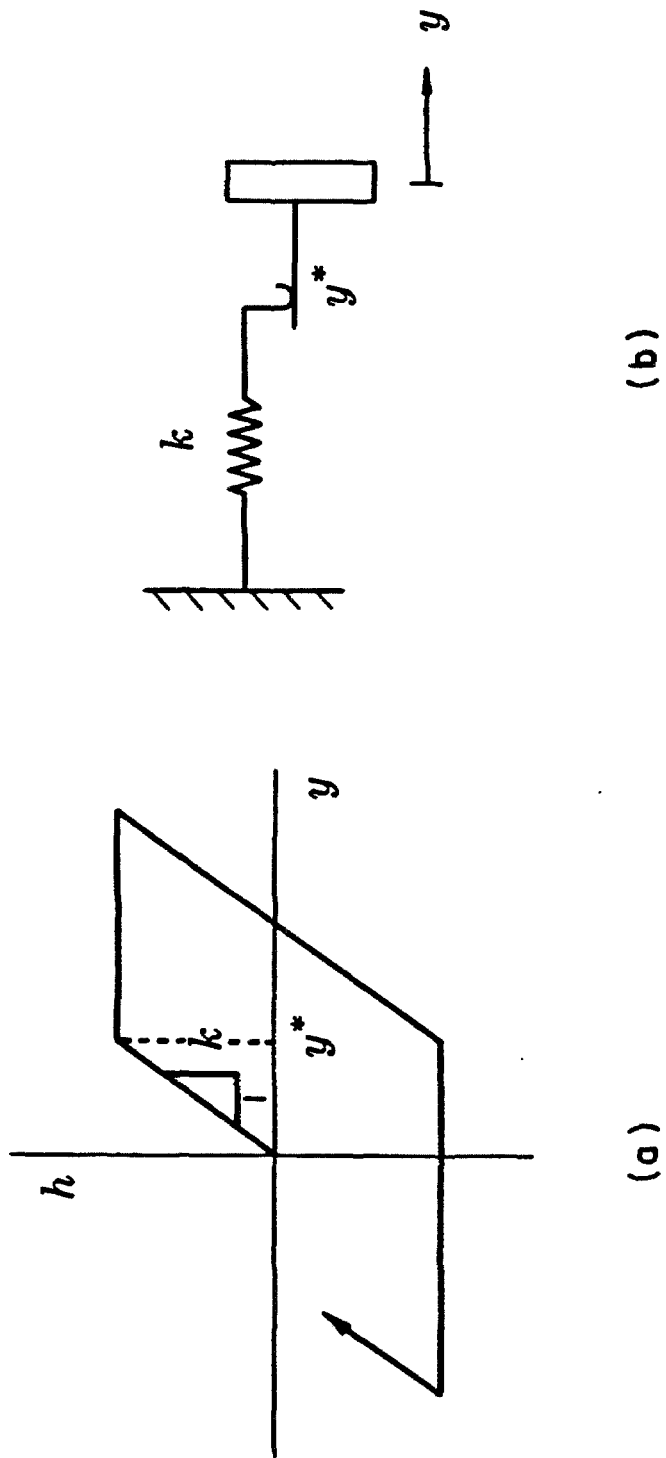


Figure 4.3 Elasto-plastic hysteretic model.
(a) Restoring force diagram.
(b) Physical representation of model.

Due to its simplicity, this model has been used by many analysts. However, for many hysteretic systems, it is too idealized to represent the actual hysteretic characteristics of restoring force such as the post-yield hardening behavior [14].

4.3.2 The Bilinear Model

The bilinear model is the simplest model proposed so far for the study of hysteretic systems with post-yield hardening behavior. As shown in Figure 4.4(a), this model approximates the backbone curve by line segments with two different slopes, $(k_1 + k_2)$ and k_2 , which can be expressed as

$$\begin{aligned} h &= (k_1 + k_2)y; & \dot{y} > 0, 0 \leq y \leq y^* \\ &= k_2y; & \dot{y} > 0, y \geq y^* \end{aligned} \tag{4.3}$$

where $(k_1 + k_2)$ represents the initial stiffness, and the post-yield hardening behavior is modeled by the second slope k_2 . An idealized system that behaves consistently with the model is shown in Figure 4.4(b). This system is made by adding the second linear spring to the elasto-plastic system shown in Figure 4.3(b). The bilinear model is, therefore, a physically motivated model.

Considerable research has been done using the bilinear model [3,4,7-9,15-16]. In general, the results have been satisfactory. This is because the model captures the most important features of hysteretic behavior. However, in system modeling and identification, it is difficult to describe the detailed hysteretic behavior of real systems using this simplified model, especially, when the transient response is important. For example, Iemura and Jennings [17] showed that it was not possible to model the E-W response of Millikan Library during the San Fernando earthquake using a single time invariant bilinear model.

4.3.3 Smooth Backbone Models

Both elasto-plastic and bilinear models are too simplified to describe the actual hysteretic behavior observed in Figure 4.1. In an effort to overcome this difficulty,

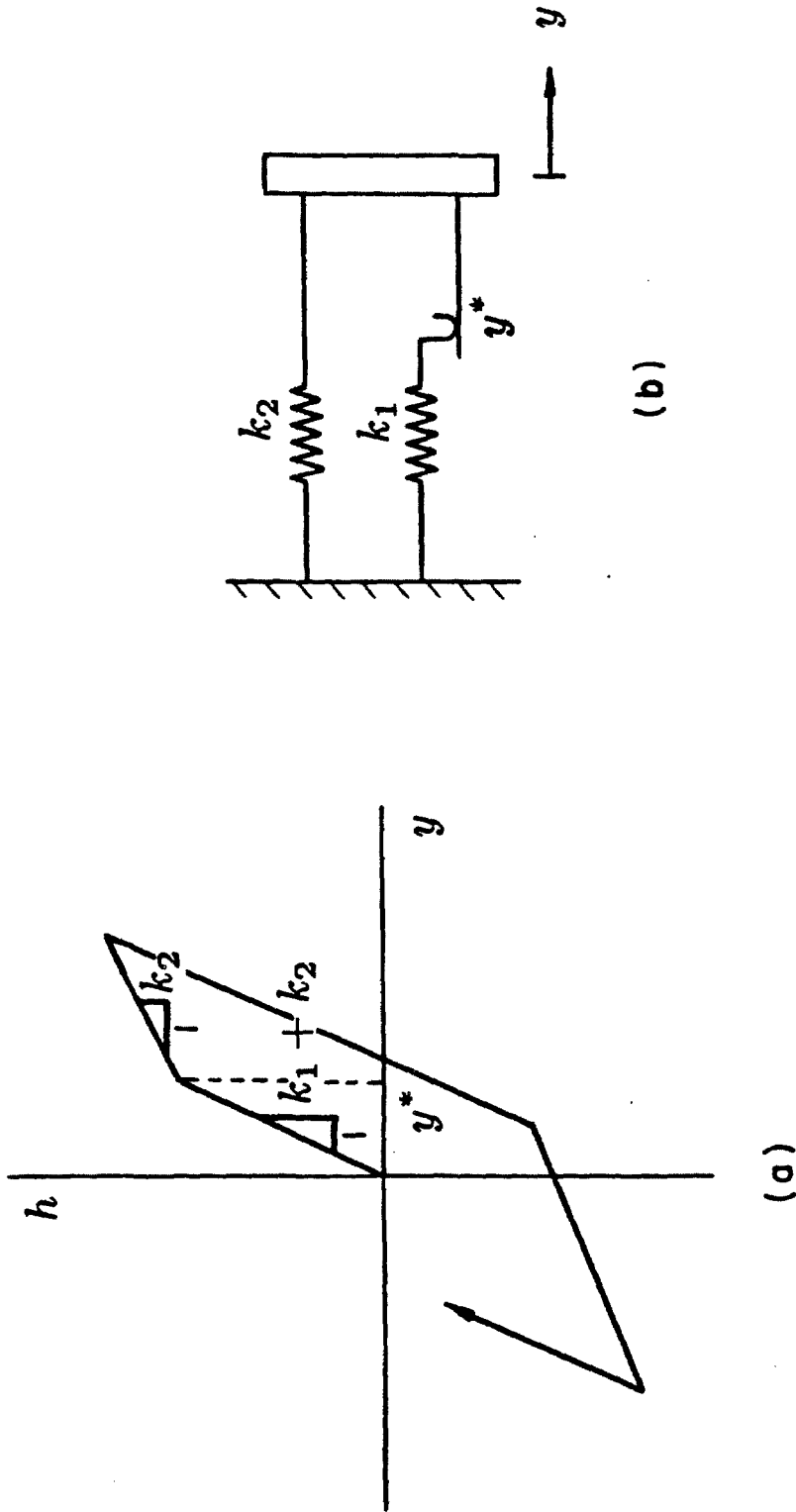


Figure 4.4 Bilinear hysteretic model.
(a) Restoring force diagram
(b) Physical representation of model.

several hysteretic models giving smooth backbone of hysteresis curves have been proposed [18-21]. They are motivated either mathematically or physically. Two illustrative examples are given below based on these two approaches, respectively.

Bouc and Wen [22-23] modeled the hysteretic component of the restoring force mathematically by defining an additional variable $z(t)$, where

$$h(y, \dot{y}) = z(t) , \quad (4.4)$$

$z(t)$ is then defined by the auxiliary equations

$$\dot{z} = -\alpha|\dot{y}|z^n - \beta\dot{y}|z^n| + \gamma\dot{y} \quad \text{for } n \text{ odd}, \quad (4.5)$$

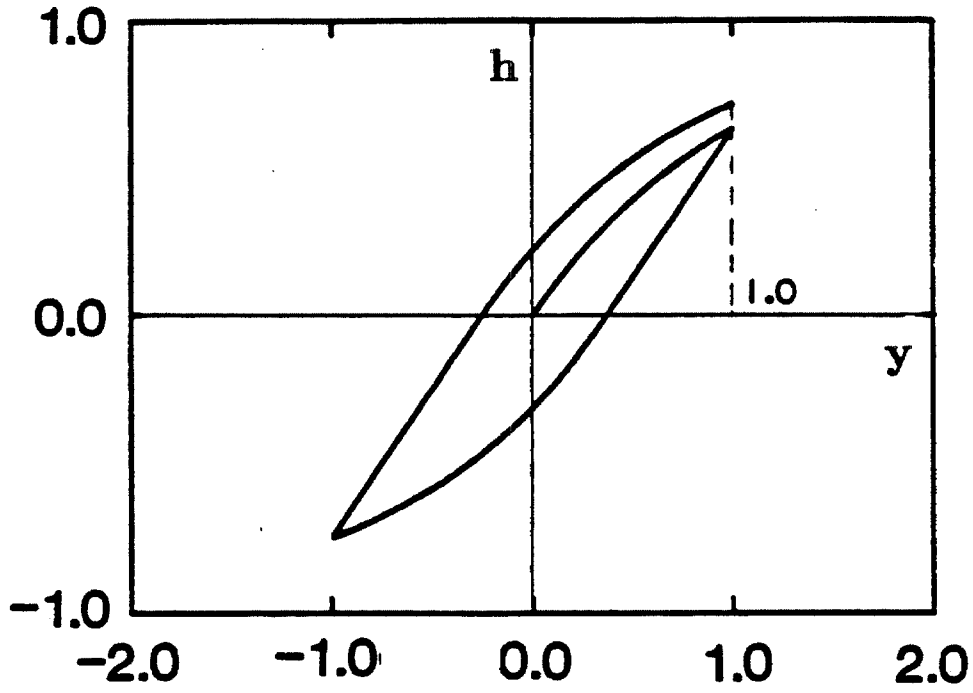
or,

$$\dot{z} = -\alpha|\dot{y}|z^{n-1}|z| - \beta\dot{y}z^n + \gamma\dot{y} \quad \text{for } n \text{ even}. \quad (4.6)$$

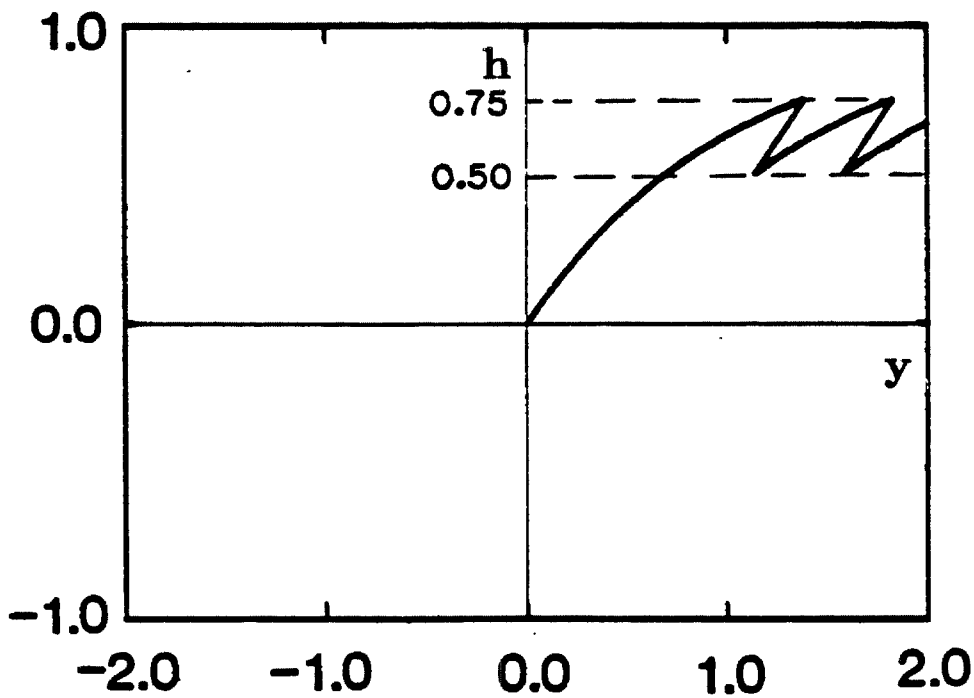
α , β , γ and n are the model parameters. This model has been generalized to exhibit different types of hysteretic behavior. A detailed review of all these models is available in a recent paper by Wen [24].

By defining an additional state variable $z(t)$, these models allow analytical treatment and have been applied to system identification problems. It has been found recently [13,25] that these models behave inconsistently in certain situations. As shown in Figure 4.5, the hysteresis loops generated by the model are not always closed under cyclic displacement loading and the loops drift continuously under certain types of cyclic force loading. This is due to the fact that the hysteresis loops are constructed mathematically and may not be physical under some circumstances.

For most hysteretic models which are mathematically motivated, the drawback lies in the areas of transient loading and cycling between variable limits where additional mathematical assumptions must be made. Also, it is sometimes difficult to relate the mathematical model parameters to the physical parameters of a system.



(a)



(b)

Figure 4.5 Inconsistent behavior of Wen's model in certain loading situations [25].
(a) Open hysteresis loop under symmetric cyclic loading.
(b) Drifting characteristic under certain cyclic loading.

However, all these problems can be alleviated by developing a physically based hysteretic model.

Iwan [26] introduced a physically motivated model, called the distributed-element model. Based on the general approach suggested by S. P. Timoshenko in 1930, this model assumes that a general hysteretic system may be represented by a series of so-called Jenkin's elements. Each Jenkin's element is actually an elasto-plastic unit consisting of a linear spring with stiffness K/N in series with a Coulomb or slip damper that has a maximum allowable force f_i^*/N . N is the total number of elements. The backbone curve of the entire system is given by

$$h = \sum_{i=1}^N f_i^*/N + Ky(N - n)/N; \quad \dot{y} > 0 \quad (4.7)$$

where the first term represents the contribution from n yielded elements and the second from the $(N - n)$ elements which have not as yet yielded. If the total number of elements N becomes very large, the backbone curve expressed by (4.7) can be very smooth.

Since the hysteretic behavior of the model is based on the physics of a particular mechanical system, no mathematical rules are needed to assure physical hysteresis loops under complicated loading histories.

4.4 Two-Parameter Distributed-Element Model

There are two attractive features of the distributed-element model:

- (1) The relationship between the backbone and hysteresis loops are determined by the physical nature of the model. Thus, no mathematical rules are necessary to assure physical behavior of hysteresis under complicated loading histories.
- (2) It is relatively easy to estimate the model parameters by fitting the backbone of the model to a variety of initial loading or backbone curves.

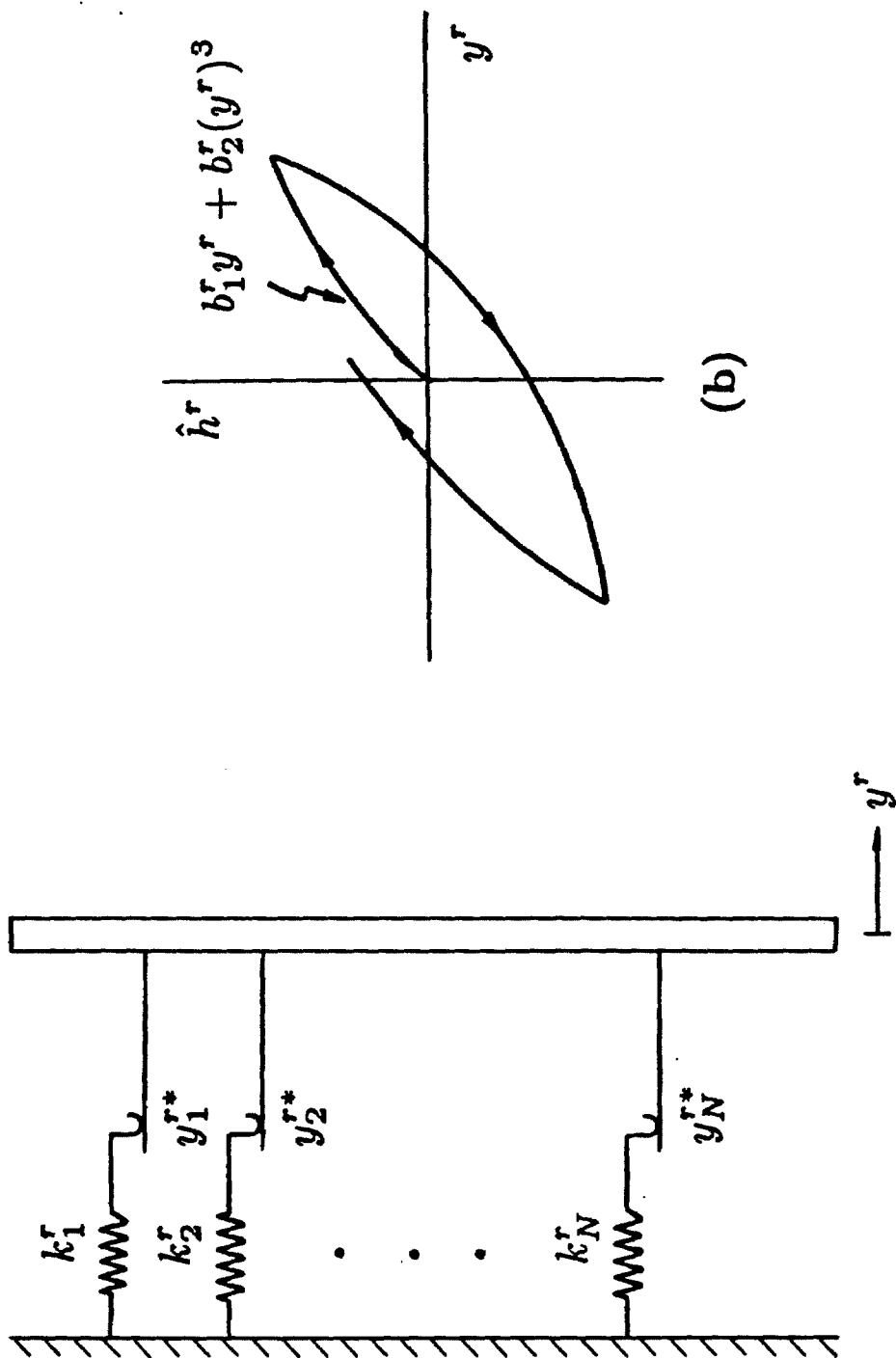
The first feature has been explained in the last section and the second is explored in this section to develop a simple hysteretic model with only two parameters, called the two-parameter distributed element model.

4.4.1 Model Considerations

Figure 4.6(a) illustrates a general distributed element model, which is a collection of elasto-plastic elements arranged in a parallel configuration. Each elasto-plastic sub-element is completely defined in terms of two parameters: the spring stiffness k_i^r and the yielding displacement y_i^{r*} . Therefore, for a model consisting of N elements, there will be $2N$ parameters, k_i^r and y_i^{r*} , $i = 1, 2, \dots, N$, to be determined in an identification problem.

In order to make such a model attractive for use in system identification, the number of parameters to be identified must be reduced. One approach presented herein is to prescribe the form of the backbone in terms of M parameters and then establish a relationship between the $2N$ model parameters and the M backbone parameters. Using this approach, the number of parameters which need to be identified is reduced from $2N$ to M . In general, M is much less than $2N$. A relationship is derived in the section 4.4.3 which can be used to determine the model parameters from any prescribed backbone curve.

The problem now is the choice of the mathematical form of the backbone curve.



(a)

Figure 4.6 Two-parameter distributed-element hysteretic model.

(a) Physical representation of model.

(b) Typical restoring force diagram for case in which N becomes large, indicating backbone equation.

In this study, the form is assumed to be

$$\begin{aligned}\hat{h}^r &= b_1^r y^r + b_2^r (y^r)^3; & y^r \leq y^{r*} & \text{ and } \dot{y}^r > 0 \\ &= b_1^r y^{r*} + b_2^r (y^{r*})^3; & y^r \geq y^{r*} & \text{ and } \dot{y}^r > 0\end{aligned}\quad (4.8)$$

\hat{h}^r is the estimate of the generalized modal restoring force h^r given by the two-parameter distributed element model. b_1^r and b_2^r are two parameters used to specify the backbone curve of the model. The numerical values of b_1^r and b_2^r need to be estimated to capture the essential features of the hysteretic behavior being modeled.

This simple parametric backbone relationship is proposed based on the results of the nonparametric identification studies in Chapter 3. It is observed that the four-parameter “nonparametric” model provides a good nonhysteretic estimate of the nonlinear stiffness behavior of the system. However, the hysteretic nature of the response is not identifiable by the nonparametric model. The failure to identify the hysteretic component of the response is due to the nonhysteretic nature of the model and motivates the present study of using hysteretic models. The fairly good match of time history response data indicates that the backbone identified by the form $a_1^r y^r + a_2^r (y^r)^3$ can be used as an initial estimate of the backbone relationship (4.8) of the distributed-element model. By doing this, the subsequent optimization process for refining the backbone parameters b_1^r and b_2^r becomes very straightforward and efficient. A simple parameter estimation algorithm is described in section 4.4.4. Note that the power series expansion of hysteretic relations with damping has been used by Jennings for a simple yielding structure [32].

4.3.2 General Description

The initial stiffness of the model is denoted by b_1^r and the ultimate strength of the system is given by $b_1^r y^{r*} + b_2^r (y^{r*})^3$, where $y^{r*} = \sqrt{-b_1^r / 3b_2^r}$ representing the yielding displacement of the system. The smoothness of the transition from elastic to plastic response of the force-deformation curve is controlled by the cubic relationship (4.8).

The force-deformation relation of the model for any hysteresis loop other than the backbone curve is determined by the elasto-plastic behavior of each sub-element and no mathematical hysteresis rules are needed. For cyclic loading, the hysteresis loops generated by the model are consistent with Masing's criterion. For transient response, it has been shown that the hysteresis loops generated by the model are consistent with the testing behavior of some actual systems [13]. Figure 4.6(b) shows the typical restoring force diagram of the model for the case in which the total number of elements, N , becomes very large.

4.4.3 Specification of k_i^r and y_i^{r*}

Consider the distributed-element model shown in Figure 4.5(a) with the backbone curve prescribed by

$$\hat{h}^r = f^r(y^r), \quad (4.9)$$

where $f^r(y^r)$ is any mathematical form which approximates the backbone curve of h^r .

If the model has N elasto-plastic elements, the parameters needing to be specified are k_i^r and y_i^{r*} , $i = 1, 2, \dots, N$.

When the total number of elements, i.e., N , is sufficiently large, the choice of the yielding displacement of each element, $y_1^{r*}, y_2^{r*}, \dots, y_N^{r*}$, becomes immaterial. For simplicity, it is convenient to take the values $y_1^{r*}, y_2^{r*}, \dots, y_N^{r*}$ equally spaced and let y_N^{r*} be the yielding displacement of the system, y^{r*} . This simplification leads to

$$y_i^{r*} = \frac{i}{N} y^{r*} \quad i = 1, 2, \dots, N. \quad (4.10)$$

Therefore, the parameters remaining to be specified are k_i^r , $i = 1, 2, \dots, N$.

By fitting the backbone of the model to the expression $f^r(y^r)$, one may obtain

$$k_i^r = f^{r'}(y_i^{r*}) - f^{r'}(0) \quad \text{for } i = 1 \quad (4.11)$$

or

$$= f^{r'}(y_i^{r*}) - f^{r'}(y_{i-1}^{r*}) \quad \text{for } i = 2, 3, \dots, N. \quad (4.12)$$

This relationship allows k_i^r to be determined from the y_i^* and $f^r(y^r)$.

In this study, $f^r(y^r)$ is chosen to be of the form (4.8) which has two parameters, b_1^r and b_2^r . The above procedure reduces the number of parameters associated with the distributed-element model consisting of N elements, initially equal to $2N$, to only two. It will be seen later, this two-parameter distributed-element model is able to capture the essential features of the hysteretic behavior under consideration.

4.4.4 Parameter Estimation

Let \hat{h}^r be the estimate of the restoring force h^r by the two-parameter distributed element model. The coefficients b_1^r and b_2^r appearing in the backbone relationship (4.8) of the model are determined by minimizing the prediction error P . In this study, P is defined as the r.m.s. value of the difference between the the peaks of the system and model response in acceleration.

Noting that the prediction error P is a function of b_1^r and b_2^r , the optimal estimate of these two parameters can be obtained as

$$P = P(b_1^r, b_2^r) = \text{minimum w.r.t. } b_1^r \text{ and } b_2^r. \quad (4.13)$$

This is a standard nonlinear optimization problem, in which the optimum must be found by means of numerical techniques. Many approaches are available to solve such a problem [27-30]. In this investigation, a series of one-dimensional minimizations are performed by minimizing P alternately with respect to b_1^r and with respect to b_2^r . Each one-dimensional minimization process is performed using the same algorithm described in Section 2.6.4 for optimizing β^r .

Two features of the method for finding the minimum of the function $P(b_1^r, b_2^r)$ are:

- (1) The method is equivalent to the steepest descent method because there are only two parameters being optimized [31]. In the latter approach, the gradient of P

needs to be evaluated to determine the direction of steepest descent and then a one-dimensional minimization would be performed in this direction. However, the present approach needs no such evaluations.

- (2) The initial estimates of b_1^r and b_2^r may be taken from the a_1^r and a_2^r identified by the four-parameter “nonparametric” model which are generally very close to the optimal parameters of the model. This saves considerable computational effort in finding appropriate initial estimates for b_1^r and b_2^r .

4.5 Verification with Simulated Data

The validity of the generalized modal identification method incorporating the two-parameter distributed-element model is now tested with simulated data for a verification system. The excitation and response data used in the present study are the same as those in Chapter 3. The results of identification and prediction are reported herein.

4.5.1 Model Identification - Parameter Calibration

To initiate the verification study, a nonlinear model for the verification system is identified first from the “measured” response and base input. The simulated input and output data used to calibrate the model parameters are the scaled El Centro accelerogram and the corresponding absolute acceleration response of the top mass. By processing these data, the relative response with respect to the moving base is readily obtained.

By observing the Fourier amplitude spectrum for the relative acceleration of the top mass, the frequency band of the dominant modes can be determined. The same values of the frequency band for the first two dominant modes are chosen as in Chapter 3. The values are listed in Table 4.1 and are used to estimate the uncoupled modal response following the band-pass filtering procedures explained in Section 2.6.2.

As described in Section 2.6, the dominant modes are identified one at a time by performing a succession of single-mode identifications. The optimal estimate β^r is determined by a simple and direct one-dimensional minimization scheme as outlined in Section 2.6.4. For given β^r , the backbone parameters b_1^r and b_2^r of the generalized restoring force h^r are estimated by a parametric identification technique described in Section 4.4.4. Note that the initial estimates of the modal parameters b_1^r , b_2^r and β^r are taken from the optimal values of a_1^r , a_2^r and β^r obtained in previous identification using the the four-parameter “nonparametric” model. Since the initial values of parameters estimated in this way are generally very close to the final optimal values, the optimization process used to refine the parameters is performed very efficiently. No convergence problems have been encountered.

Determined by minimizing the prediction error based on the acceleration peaks of the system response, the results for the optimal models are given in Table 4.1. Only a two-mode model is identified for the same reason as in previous nonparametric study. Comparing Table 4.1 with Table 3.1, it is clear that the model parameters b_1^r , b_2^r and β^r are indeed close to their counterparts, a_1^r , a_2^r and β^r , $r = 1, 2$, obtained in Chapter 3. This supports the point made above regarding the closeness of the values of these parameters.

The negative sign of b_2^1 and b_2^2 indicated the softening stiffness behavior of the hysteretic system. This is also illustrated by the identified generalized modal restoring force diagrams depicted in Figure 4.7.

The quality of the response match using two modes is shown in Figures 8-10. In general, the model fits the actual time history response better than does the four-parameter nonparametric model. This improvement is considered the consequence that the hysteretic component of the response has been identified by employing the two-parameter distributed element model.

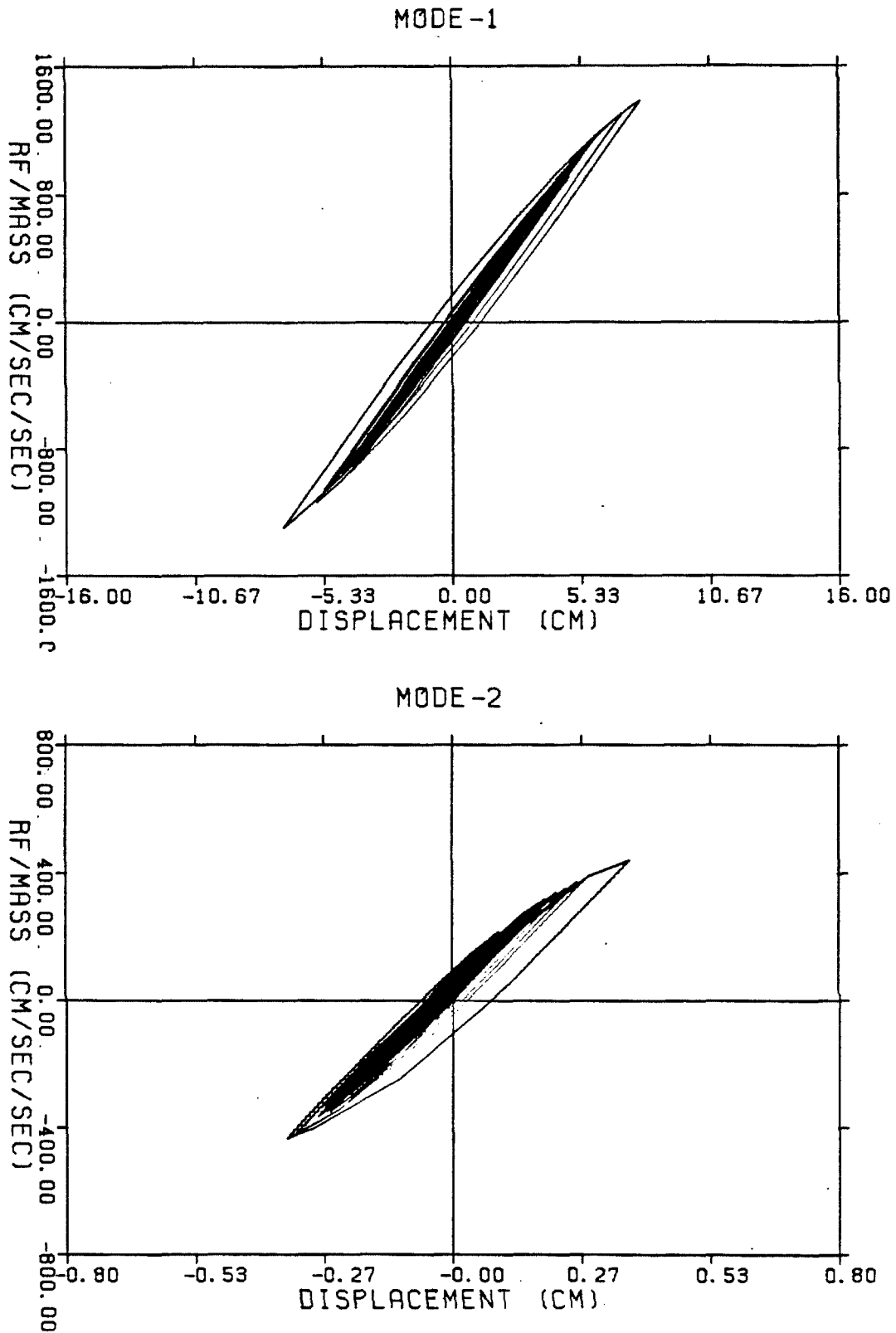


Figure 4.7 Generalized modal restoring force diagrams for identified two-parameter distributed-element hysteretic model to scaled El Centro accelerogram.
(a) First mode.
(b) Second mode.

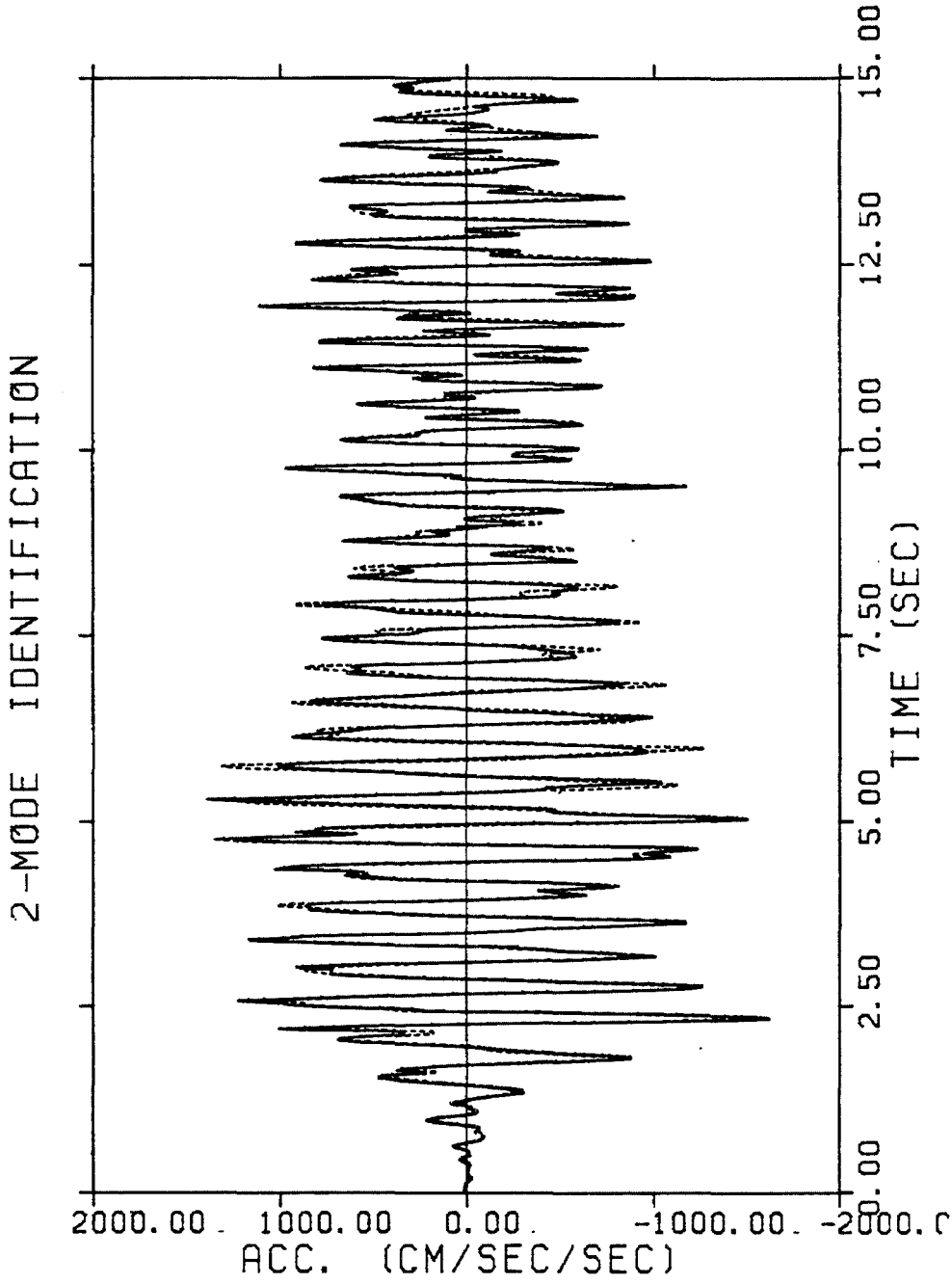


Figure 4.8 Identification of relative acceleration at top mass of verification system to scaled El Centro accelerogram. Actual response (—), optimal two-parameter distributed-element hysteretic model with two modes (- - -).

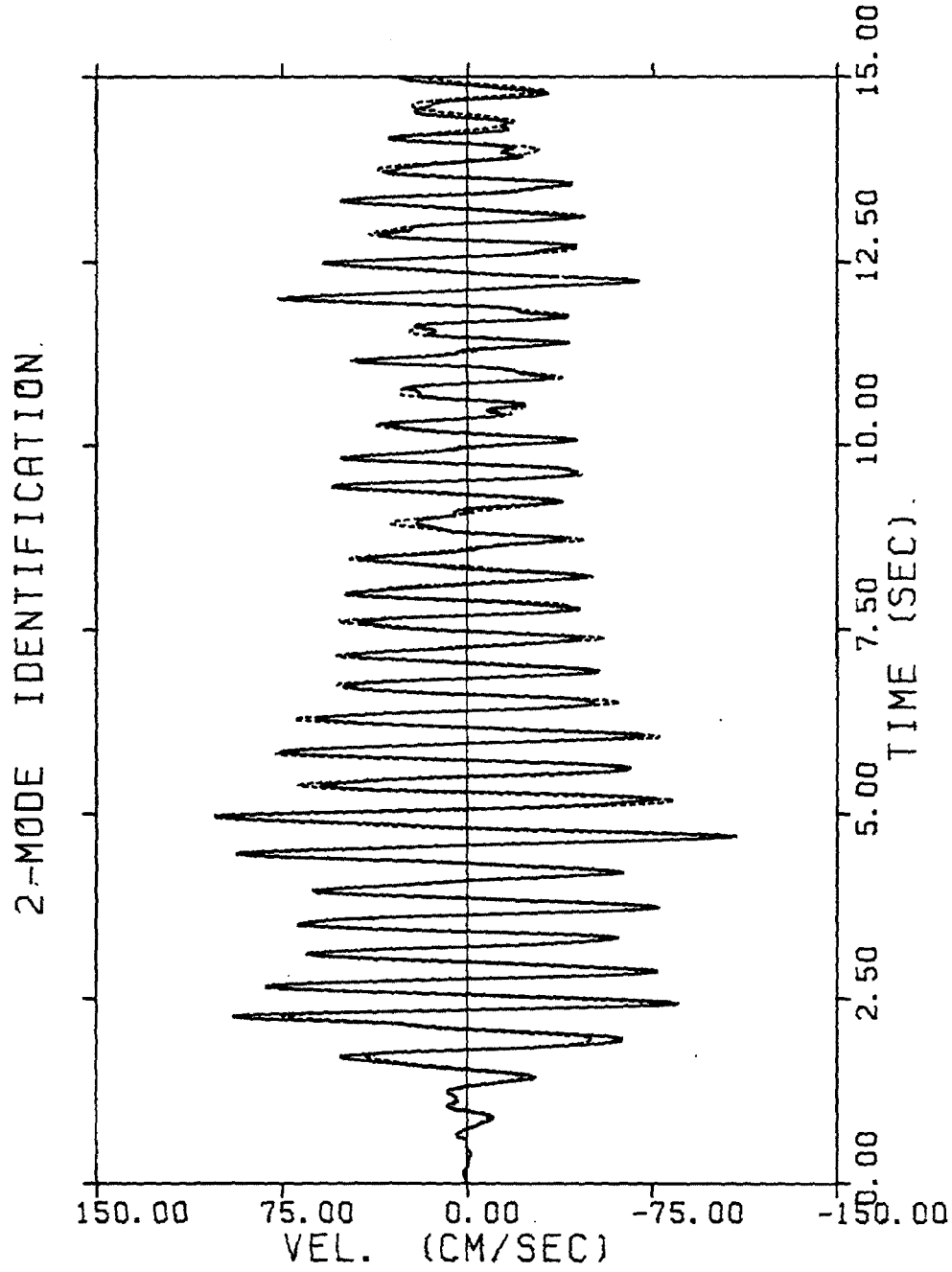


Figure 4.9 Identification of relative velocity at top mass of verification system to scaled El Centro accelerogram. Actual response (—), optimal two-parameter distributed-element hysteretic model with two modes (- - -).

2-MODE IDENTIFICATION

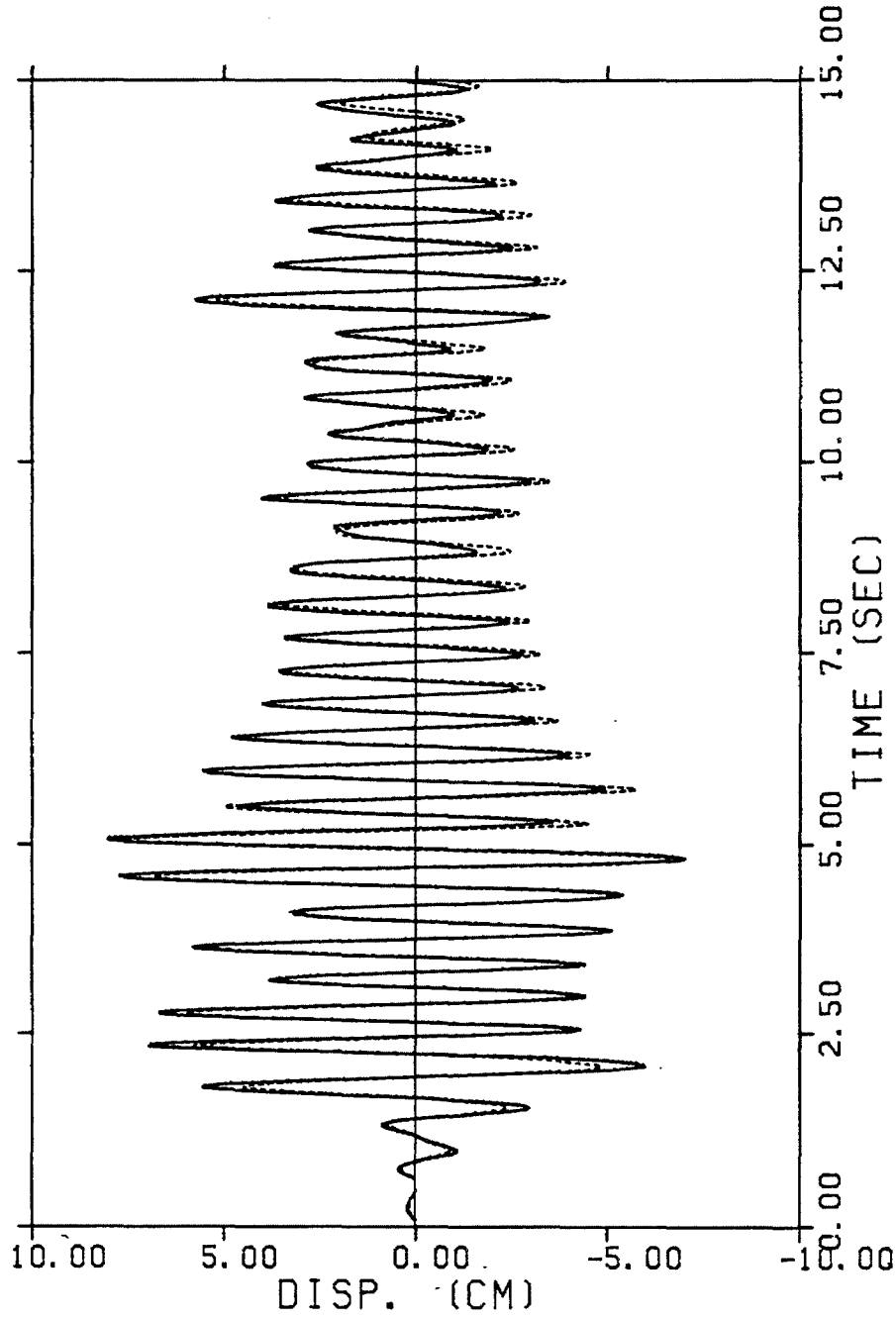


Figure 4.10 Identification of relative displacement at top mass of verification system to scaled El Centro accelerogram. Actual response (—), optimal two-parameter distributed-element hysteretic model with two modes (- - -).

It is next desirable to examine how well the identified model can predict the hysteretic response to other excitations and how much it improves the results predicted by the four-parameter nonparametric model.

4.5.2 Model Validation - Response Prediction

To continue the verification study, the nonlinear model identified in section 4.4.2 is used to predict the roof response of the same system when subjected to other base excitations. The same scaled Taft and Parkfield earthquakes and corresponding response of the top mass are employed as in Chapter 3 and the prediction results are compared.

Figures 11-13 show the time histories predicted by the model and "measured" from the system to the scaled Taft earthquake. A similar comparison for the response to the scaled Parkfield earthquake is presented in Figures 14-16. The prediction error P based on acceleration peaks is summarized in the last two columns of Table 4.1 for both cases. By comparing all these results with their counterparts in Chapter 3, it is clearly seen that the prediction of the time history of the response made by the optimal two-parameter distributed-element model is superior to that obtained using the four-parameter nonhysteretic model. Especially significant are the better reproduction of the hysteretic features of the response such as the drift displacement shown in Figures 10 and 13.

It is concluded that the two-parameter distributed-element model with a small number of modes is capable of predicting the hysteretic response, including the permanent displacement, under different base excitations. Noting that the hysteretic behavior is more pronounced in the response used for prediction than for identification, this example emphasizes the importance of employing an appropriate hysteretic model in the identification study of a hysteretic system so that the

2-MODE PREDICTION.

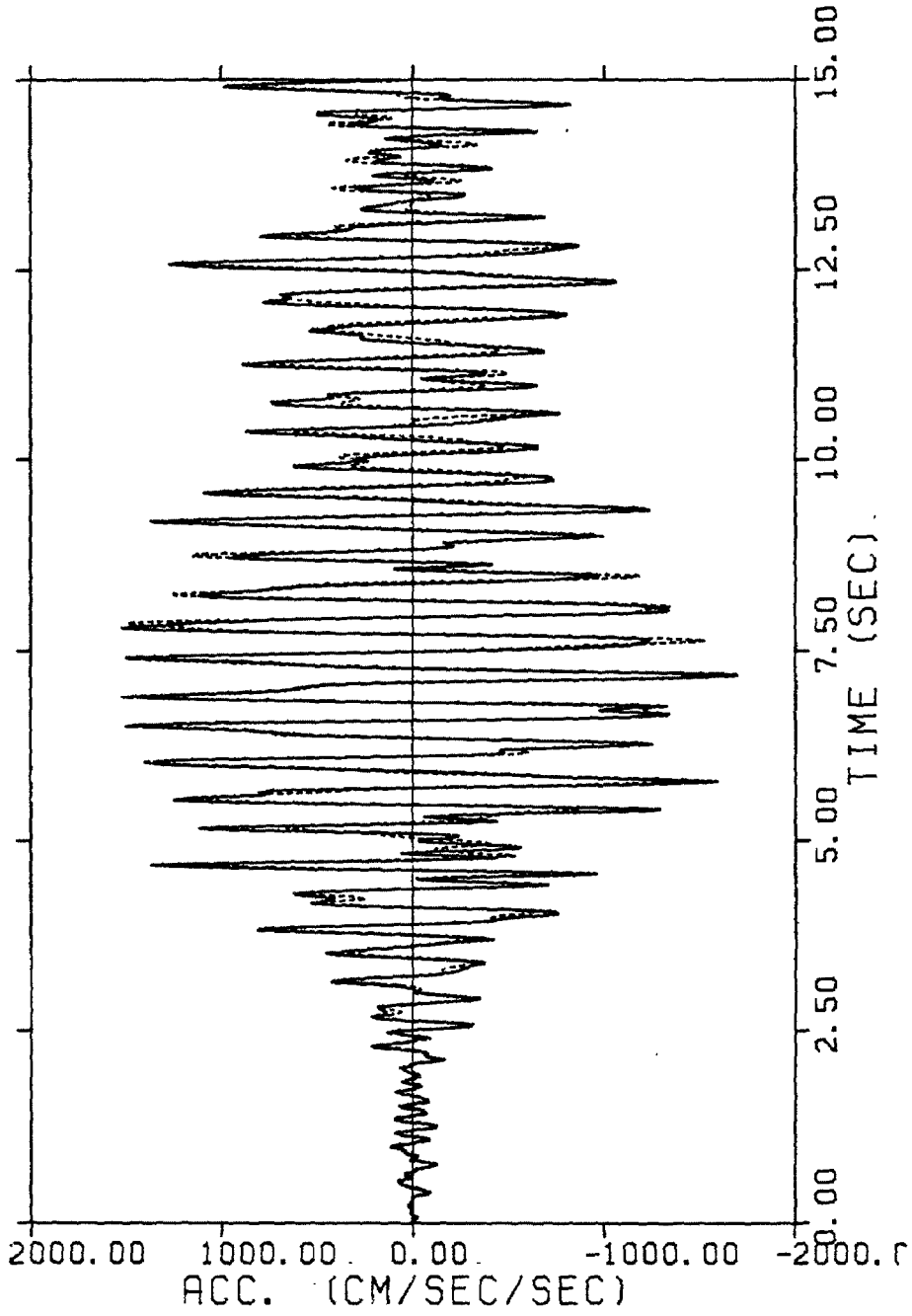


Figure 4.11 Prediction of relative acceleration at top mass of verification system to scaled Taft accelerogram. Actual response (—), optimal two-parameter distributed-element hysteretic model with two modes (---).

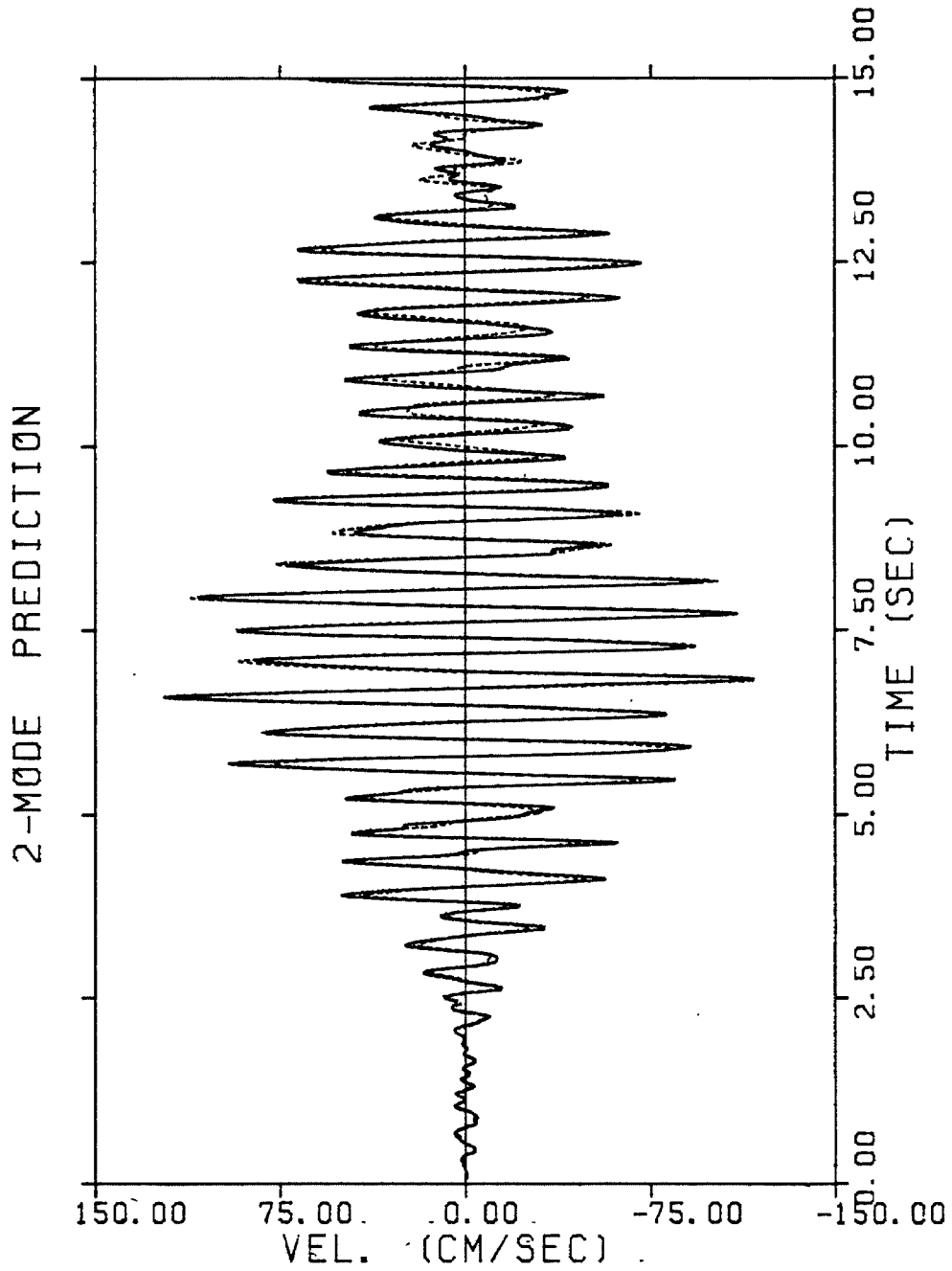


Figure 4.12 Prediction of relative velocity at top mass of verification system to scaled Taft accelerogram. Actual response (—), optimal two-parameter distributed-element hysteretic model with two modes (- - -).

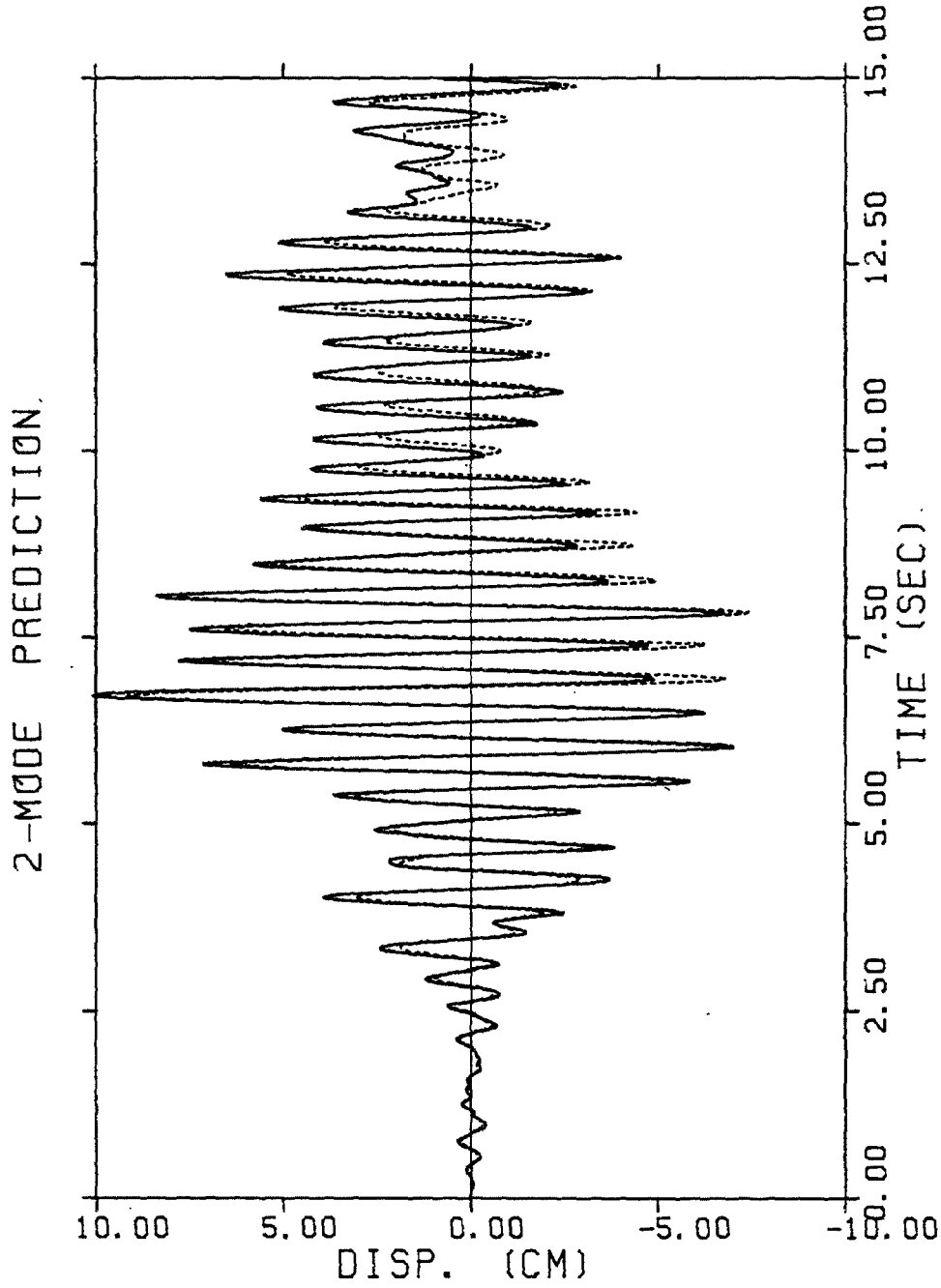


Figure 4.13 Prediction of relative displacement at top mass of verification system to scaled Taft accelerogram. Actual response (—), optimal two-parameter distributed-element hysteretic model with two modes (---).

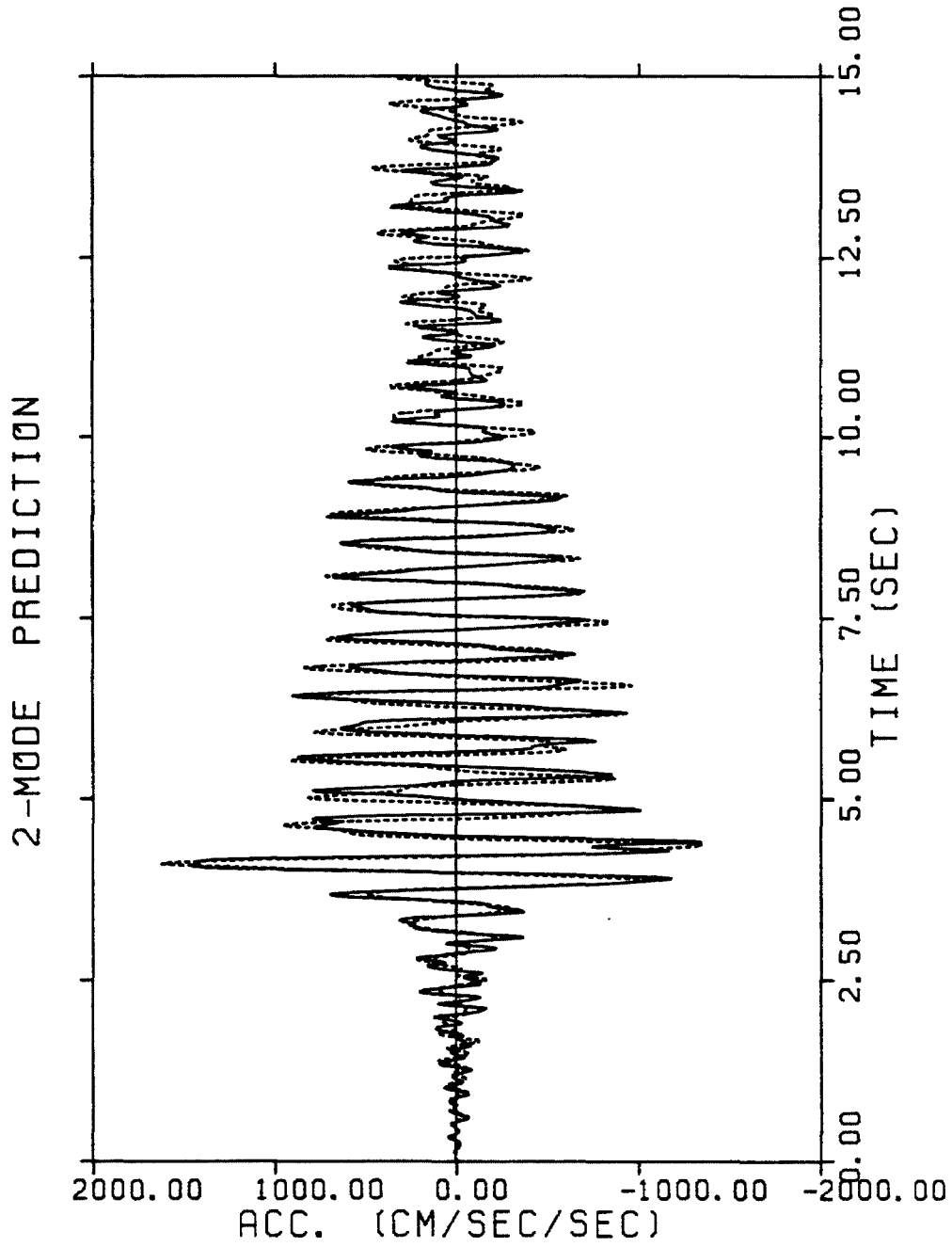


Figure 4.14 Prediction of relative acceleration at top mass of verification system to scaled Park-field accelerogram. Actual response (—), optimal two-parameter distributed-element hysteretic model with two modes (- - -).

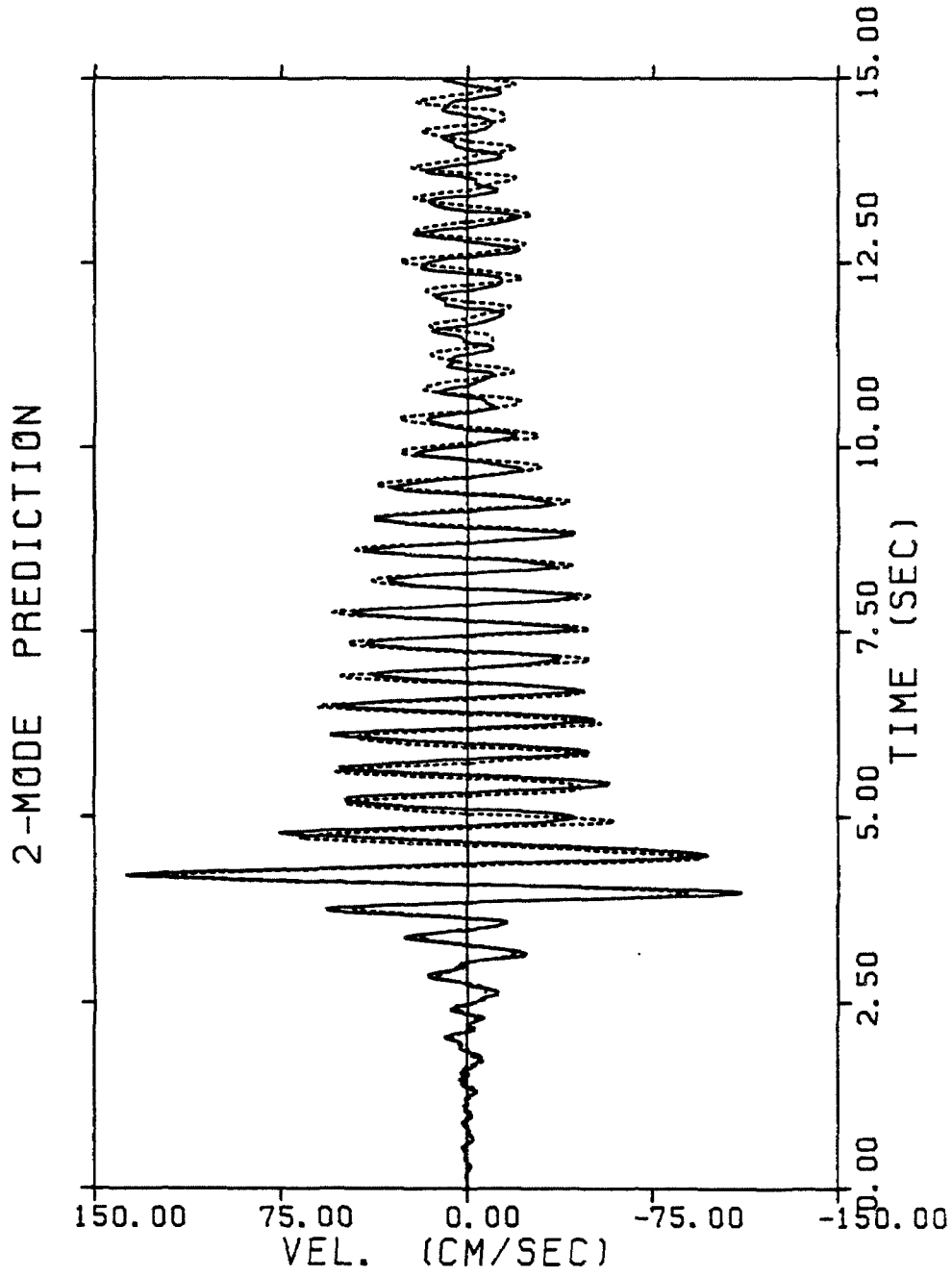


Figure 4.15 Prediction of relative velocity at top mass of verification system to scaled Parkfield accelerogram. Actual response (—), optimal two-parameter distributed-element hysteretic model with two modes (- - -).

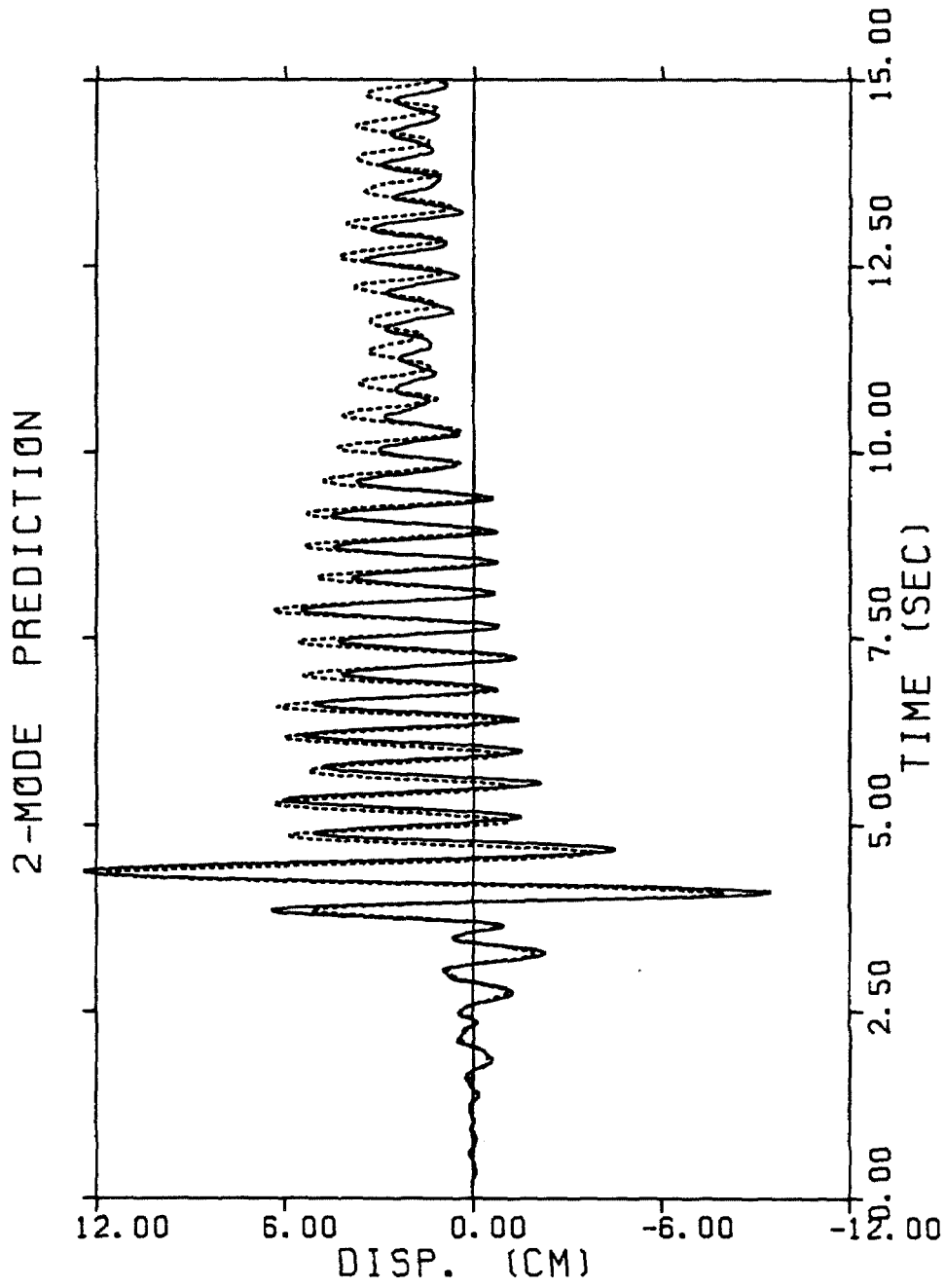


Figure 4.16 Prediction of relative displacement at top mass of verification system to scaled Parkfield accelerogram. Actual response (—), optimal two-parameter distributed element hysteretic model with two modes (- - -).

Identification										Prediction			
El Centro ⁽¹⁾										Taft ⁽²⁾		Parkfield ⁽³⁾	
Mode	Frequency Band (Hz)	b_1 (1/sec ²)		b_2 1/(cm · sec) ²		β^r		P	P	P	P	P	
		Initial	Optimal	Initial	Optimal	Initial	Optimal						
1	0.0-4.0	2.13 × 10 ²	2.15 × 10 ²	-6.74 × 10 ⁻¹	-6.69 × 10 ⁻¹	1.610	0.992	1.38 × 10 ⁻¹	1.22 × 10 ⁻¹				
2	4.0-7.5	1.44 × 10 ³	1.62 × 10 ³	-8.29 × 10 ²	-3.25 × 10 ³	-0.442	-0.383	8.66 × 10 ⁻²	9.24 × 10 ⁻²	9.24 × 10 ⁻²	9.24 × 10 ⁻²	1.29 × 10 ⁻¹	

- (1) Simulated response with the El Centro, 1940, S00E, scaled to a peak of 57% g
- (2) Simulated response with the Taft, 1952, S69E, scaled to a peak of 50% g
- (3) Simulated response with the Parkfield, 1966, N65E, scaled to a peak of 61% g

Table 4.1 Identification and Prediction Results of the Two-Parameter Distributed-Element Hysteretic Model Using Simulated Data

identified model is capable of predicting the response to the input motions other than the identification signal.

4.6 Summary

An efficient algorithm has been developed for the generalized modal identification method using a special form of the distributed element hysteresis model. The backbone relationship of the model is characterized by only two parameters which is based on insight obtained from previous nonparametric studies in Chapter 3 and an understanding of the physical nature of the distributed-element model. As applied to identifying the generalized modal restoring force of a hysteretic system, it is totally unnecessary to specify any additional mathematical rules for generating physical hysteresis loops. Furthermore, since the initial estimate of the backbone parameters obtained from the nonparametric technique using the four-parameter model is generally very close to the optimal estimate, the subsequent optimization process is very straightforward and efficient and no convergence problems have been encountered.

The identification method together with the model is verified with simulated data generated for a hysteretic system. The results illustrate the excellent ability of the present approach to identify and also predict the nonlinear response for a hysteretic verification system including the permanent displacement. The improvement of identification/prediction is due to the hysteretic response being modeled appropriately by the two-parameter distributed-element model.

Encouraged by the results of applying the generalized modal identification method to simulated data, the method is applied to the pseudo-dynamic test data from a full scale steel structure in the next chapter.

References

- [1] E. P. Popov, et al., "Cyclic Behavior of Large Beam-Column Assemblies," *Earthquake Spectra*, Vol. 1, February 1985.
- [2] G. Masing, "Eigenspannungen und Verfestigung beim Messing (Self Stretching and Hardening for Brass)," *Proceedings of the 2nd International Congress of Applied Mechanics*, Zurich, Switzerland, 1926. (German)
- [3] T. K. Caughey, "Random Excitation of a System with Bilinear Hysteresis," *ASME Journal of Applied Mechanics*, Vol. 27, December 1960.
- [4] W. D. Iwan, "The Dynamic Response of Bilinear Hysteretic Systems," Ph.D. Thesis, California Institute of Technology, Pasadena, California, June 1961.
- [5] P. C. Jennings, "Response of Simple Yielding Structures to Earthquake Excitation," Ph.D. Thesis, California Institute of Technology, Pasadena, California, 1963.
- [6] P. C. Jennings, "Periodic Response of a General Yielding Structure," *ASCE Journal of Engineering Mechanics Division*, Vol. 90(2), April 1964.
- [7] W. D. Iwan, "The Dynamic Response of the One-Degree-of-Freedom Bilinear Hysteretic System," *Proceedings of the Third World Conference on Earthquake Engineering*, 1965.
- [8] W. D. Iwan, "The Steady-State Response of a Two-Degree-of-Freedom Bilinear Hysteretic System," *ASME Journal of Applied Mechanics*, Vol. 32, No. 1, March 1965.
- [9] W. D. Iwan, "The Steady-State Response of the Double Bilinear Hysteretic System," *ASME Journal of Applied Mechanics*, Vol. 32, No. 4, December 1965.
- [10] P. C. Jennings, "Earthquake Response of a Yielding Structure," *ASCE Journal of Engineering Mechanics Division*, Vol. 91, No. 4, August, 1965.
- [11] W. D. Iwan, "On a Class of Models for the Yielding Behavior of Continuous and Composite Systems," *ASME Journal of Applied Mechanics*, Vol. 34, No. 3, September 1967.
- [12] W. D. Iwan, "The Distributed-Element Concept of Hysteretic Modeling and Its Application to Transient Response Problems," *Proceeding of the 4th World Conference on Earthquake Engineering*, Vol. II, A-4, Santiago, Chile, January 1969.
- [13] P. Jayakumar, "Modeling and Identification in Structural Dynamics," Report No. EERL 87-01, Earthquake Engineering Research Laboratory, California Institute of Technology, Pasadena, California, May 1987.

- [14] J. Casey and P. M. Naghdi, "On the Characterization of Strain-Hardening in Plasticity," *ASME Journal of Applied Mechanics*, Vol. 48, June 1981.
- [15] W. D. Iwan and L. D. Lutes, "Response of the Bilinear Hysteretic System to Stationary Random Excitation," *Journal of the Acoustical Society of America*, Vol. 43, No. 3, March 1968.
- [16] K. Asano and W. D. Iwan, "An Alternative Approach to the Random Response of Bilinear Systems," *Earthquake Engineering and Structural Dynamics*, Vol. 12, 1984.
- [17] H. Iemura and P. C. Jennings, "Hysteretic Response of a Nine-Story Reinforced Concrete Building," *International Journal of Earthquake Engineering and Structural Dynamics*, Vol. 3, 1974.
- [18] W. Ramberg and W. R. Osgood, "Description of Stress-Strain Curves by Three Parameters," Technical Note No. 902, National Advisory Committee on Aeronautics, July 1973.
- [19] R. Dobry and D. Athanasiou-Grivas, "Stress-Strain Relation for Soils under Earthquake Loading," Rensselaer Polytechnic Institute, Department of Civil Engineering, Report No. 78-02, Troy, New York, July 1978.
- [20] E. Kavazanjian, Jr. and T. Hadj-Hamou, "Determination of the Dynamic Material Properties of Soils from the Results of Static Shear Tests," The John A. Blume Earthquake Engineering Center, Stanford University, Report No. 45, California, June 1980.
- [21] R. Dobry, "Damping in Soils: Its Hysteretic Nature and the Linear Approximation," Research Report R70-14, Soils Publication No. 253, Department of Civil Engineering, School of Engineering, Massachusetts Institute of Technology, Cambridge, Massachusetts, January 1970.
- [22] R. Bouc, "Forced Vibration of Mechanical Systems with Hysteresis," *Proceedings of the 4th Conference on Nonlinear Oscillation*, Prague, Czechoslovakia, 1967.
- [23] Y-K Wen, "Method for Random Vibration of Hysteretic Systems," *ASCE Journal of Engineering Mechanics Division*, Vol. 102, April 1976.
- [24] Y-K Wen, "Stochastic Response and Damage Analysis of Inelastic Structures," *Probabilistic Engineering Mechanics*, Vol. 1, No. 1, 1986.
- [25] L. G. Papanizos, "Some Observations on the Random Response of Hysteretic Systems," Report No. EERL 86-02, Earthquake Engineering Research Laboratory, California Institute of Technology, Pasadena, California, 1986.
- [26] W. D. Iwan, "A Distributed-Element Model for Hysteresis and Its Steady-State Dynamic Response," *ASME Journal of Applied Mechanics*, Vol. 33, No. 4, December 1966.

- [27] J. B. Rosen (Editor), *Nonlinear Programming*, Academic Press, 1970.
- [28] Lectures by Dr. L. J. Wood on Optimal Control Theory, California Institute of Technology, Pasadena, California, 1983-84.
- [29] R. Fletcher, *Practical Methods of Optimization*, John Wiley & Sons, 1980.
- [30] D. G. Luenberger, *Introduction to Linear and Nonlinear Programming*, Addison Wesley, 1973.
- [31] J. L. Beck, "Determining Models of Structures from Earthquake Records," Report No. EERL 78-01, Earthquake Engineering Research Laboratory, California Institute of Technology, Pasadena, California, June 1978.
- [32] P. C. Jennings, "Force-Deflection Relations from Dynamic Tests," *ASCE Journal of Engineering Mechanics Division*, April 1967.

Chapter 5

Application to Pseudo-Dynamic Test Data

5.1 Introduction

The objective of this chapter is to apply the method of generalized modal identification to the analysis of response data obtained from an actual structure. The structure selected is a full-scale six-story steel-frame structure which was excited into the nonlinear range in the U.S.-Japan cooperative pseudo-dynamic test. It is intended to use this example to illustrate that the method proposed in this dissertation is capable of providing an accurate representation of the hysteretic response of a real structure.

Generalized modal identification is performed with the two simple nonlinear models introduced previously. In the preliminary investigation, the test structure is identified by employing a four-parameter nonparametric model. This model provides a nonhysteretic estimate of the nonlinear stiffness and energy dissipation behavior. Subsequently, a two-parameter distributed-element model is used to obtain a hysteretic estimate of the nonlinear behavior. This model employs the results of the nonparametric identification as the prior estimates of the model parameters. The final result is a fully hysteretic structural model which characterizes the nonlinear behavior of the test structure.

5.2 Pseudo-Dynamic Testing Method

This section contains an overview of the pseudo-dynamic testing method for simulating or estimating seismic effects on buildings and similar structures.

5.2.1 General Features

The pseudo-dynamic method is an on-line computer-controlled, experimental technique which can be used to evaluate the inelastic seismic behavior of full-scale structural systems. This relatively new technique was initiated in 1975 by Takanashi, et al. [1-5] at the University of Tokyo, Japan. In this method the usual pseudo-static test procedures are combined with an on-line computer control system. The on-line computer is used to control the simulated earthquake force applied by hydraulic actuators so as to model the inertial properties of the structure.

In contrast to the usual pseudo-static test procedures, the restoring force-displacement relationship of a test specimen is not prescribed prior to the test. Instead, the actual restoring force characteristics measured by the displacement and force transducers are used to compute the movement that must be enforced at each degree-of-freedom. The process is performed interactively at each time step as the experiment proceeds. Hence, the pseudo-dynamic method makes it possible to simulate the dynamic behavior of a structure subjected to strong ground motions in a step-by-step procedure while taking into account the continuously changing structural stiffness.

The physical equipment used in the pseudo-static experiments is largely applicable for pseudo-dynamic testing. However, very precise displacement control systems must be implemented. This requires the use of some very sensitive servovalves, as well as a suitable on-line computer and a rapid data-acquisition system [6-7]. The test results in many respects are comparable to those achieved on more costly shaking tables. Moreover the testing structure can be of large size limited

mainly by the capacity of conventional test equipment. Studies of subassemblages can also be made with relative ease. This emerging technology offers a means for seismic testing of full-size structures into the inelastic region.

5.2.2 Test Procedure

In a pseudo-dynamic test, the equilibrium of a multi-degree-of-freedom structural system is enforced only at discrete time steps. For such a step-by-step procedure, the basic equation is

$$M\ddot{\underline{y}}^{(i)} + C\dot{\underline{y}}^{(i)} + \underline{f}^{(i)} = \underline{p}^{(i)} = -M\underline{1}\ddot{\underline{z}}^{(i)} \quad (5.1)$$

where M and C are the mass and viscous-damping matrices; $\ddot{\underline{y}}^{(i)}$, $\dot{\underline{y}}^{(i)}$, and $\underline{f}^{(i)}$ are the acceleration, velocity, and restoring force vectors at time $i\Delta t$; and $\underline{p}^{(i)}$ is the external excitation force vector due to earthquake acceleration $\ddot{\underline{z}}^{(i)}$. All the components of $\underline{1}$ are unity.

Using the central-difference method, velocity and accelerations can be approximated as

$$\dot{\underline{y}}^{(i)} = \frac{\underline{y}^{(i+1)} - \underline{y}^{(i-1)}}{2\Delta t} \quad (5.2)$$

and

$$\ddot{\underline{y}}^{(i)} = \frac{\underline{y}^{(i+1)} - 2\underline{y}^{(i)} + \underline{y}^{(i-1)})}{\Delta t^2} \quad (5.3)$$

in which $\underline{y}^{(i-1)}$, $\underline{y}^{(i)}$, and $\underline{y}^{(i+1)}$ are displacement vectors at consecutive loading steps. On combining equations (5.1), (5.2) and (5.3), one obtains an explicit expression for $\underline{y}^{(i+1)}$ [7] as

$$\underline{y}^{(i+1)} = \left[M + \frac{\Delta t}{2} C \right]^{-1} \left[\Delta t^2 \left(\underline{p}^{(i)} - \underline{f}^{(i)} \right) + \left(\frac{\Delta t}{2} C - M \right) \underline{y}^{(i-1)} + 2M\underline{y}^{(i)} \right] \quad (5.4)$$

Based on the known mass distribution of the test structure and the assumption of the mass being lumped at each degree-of-freedom, the mass matrix M is

obtained. The viscous-damping matrix C is estimated from the preliminary tests at low amplitudes assuming Rayleigh damping. For a given earthquake $\underline{p}^{(i)}$ or $\underline{\ddot{z}}^{(i)}$ is prescribed. Thus, once $\underline{f}^{(i)}$ is experimentally measured, equation (5.4) can be solved by an on-line computer, and the increments in displacements at nodal points can be determined. The calculated nodal displacements are then imposed on the structure using hydraulic actuators. This process is illustrated schematically in Figure 5.1.

Since in a pseudo-dynamic test the displacements to be imposed on a test structure are computed based on the structural restoring forces directly measured from the deformed structure, experimental errors associated with displacement control and force measurement are inevitably introduced into the computational procedure. Because of the large number of loading steps generally involved, cumulative errors in the numerical results can be significant even though the experimental feedback errors introduced in each step are small. The studies of Shing and Mahin [8-12] showed that the rate of cumulative error growth with respect to the loading step increases rapidly with the natural frequency of the test structure and the integration time interval used. Hence, the higher frequency response is more sensitive to experimental errors and the cumulative growth of errors can be minimized by reducing the integration time interval Δt .

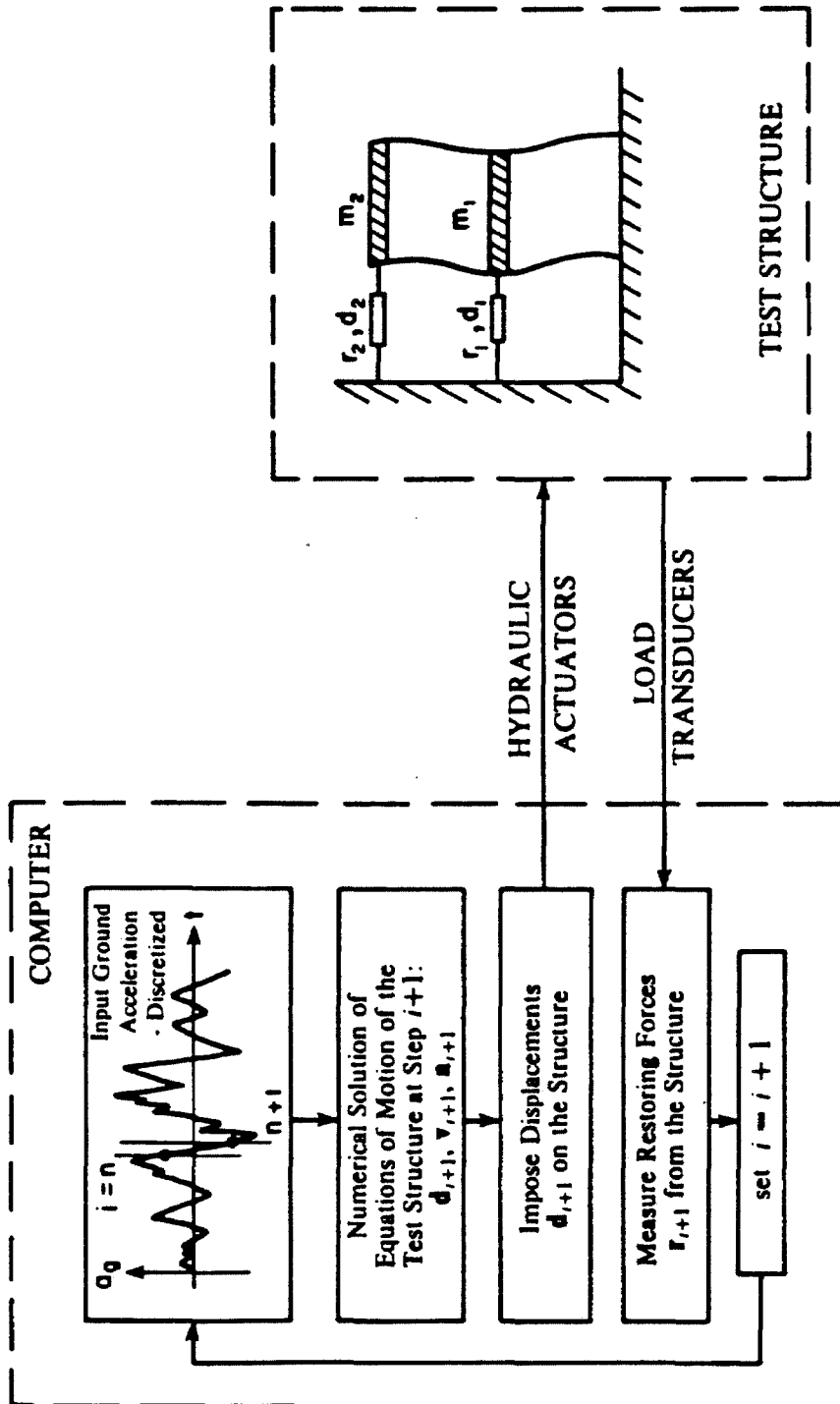


Figure 5.1 Basic experimental scheme for pseudo-dynamic method [1].

5.3 BRI Testing Program

Although the pseudo-dynamic testing method is still in a developmental stage, very significant seismic research has already been completed using this approach. The recent work on building systems at the Building Research Institute (BRI) in Tsukuba, Japan, under the U.S.-Japan Cooperative Research Program Utilizing Large-Scale Testing facilities is particularly noteworthy [13-14]. Figure 5.2 shows the pseudo-dynamic testing facility of the Building Research Institute [15]. The facility permits the test specimen to be anchored to the floor and lateral forces are applied by hydraulic actuators attached to a cellular strong-wall. Large programmed actuators were used to apply lateral forces from one side at each floor level. The test under the U.S.-Japan Cooperative Research Program for steel structures is briefly described below.

A six-story, two-bay, full-scale steel-frame structure was tested at the pseudo-dynamic testing facility at BRI during November, 1983 - March, 1984. The plan and cross-section of the test structure are shown in Figure 5.3. This structure was designed to satisfy the requirements of both the 1979 U.S. Uniform Building Code (UBC) and the 1981 Architectural Institute of Japan code [16]. The dimension was 15 m \times 15 m in plan and 21.5 m high. In the direction of loading, the structure consisted of three moment resistant frames. The two exterior frames A and C were unbraced. The north bay of the interior frame B was braced with eccentric K-bracing. All the girder-to-column connections were designed as moment connections in the loading direction and shear connections in the transverse direction. The floor was built compositely with the girders and floor beams with a formed metal decking and cast-in-place light-weight concrete. No nonstructural components were attached to the frame system.

The pseudo-dynamic tests were performed at low amplitudes to give nominally elastic response and at larger amplitude to excite the structure into the inelastic

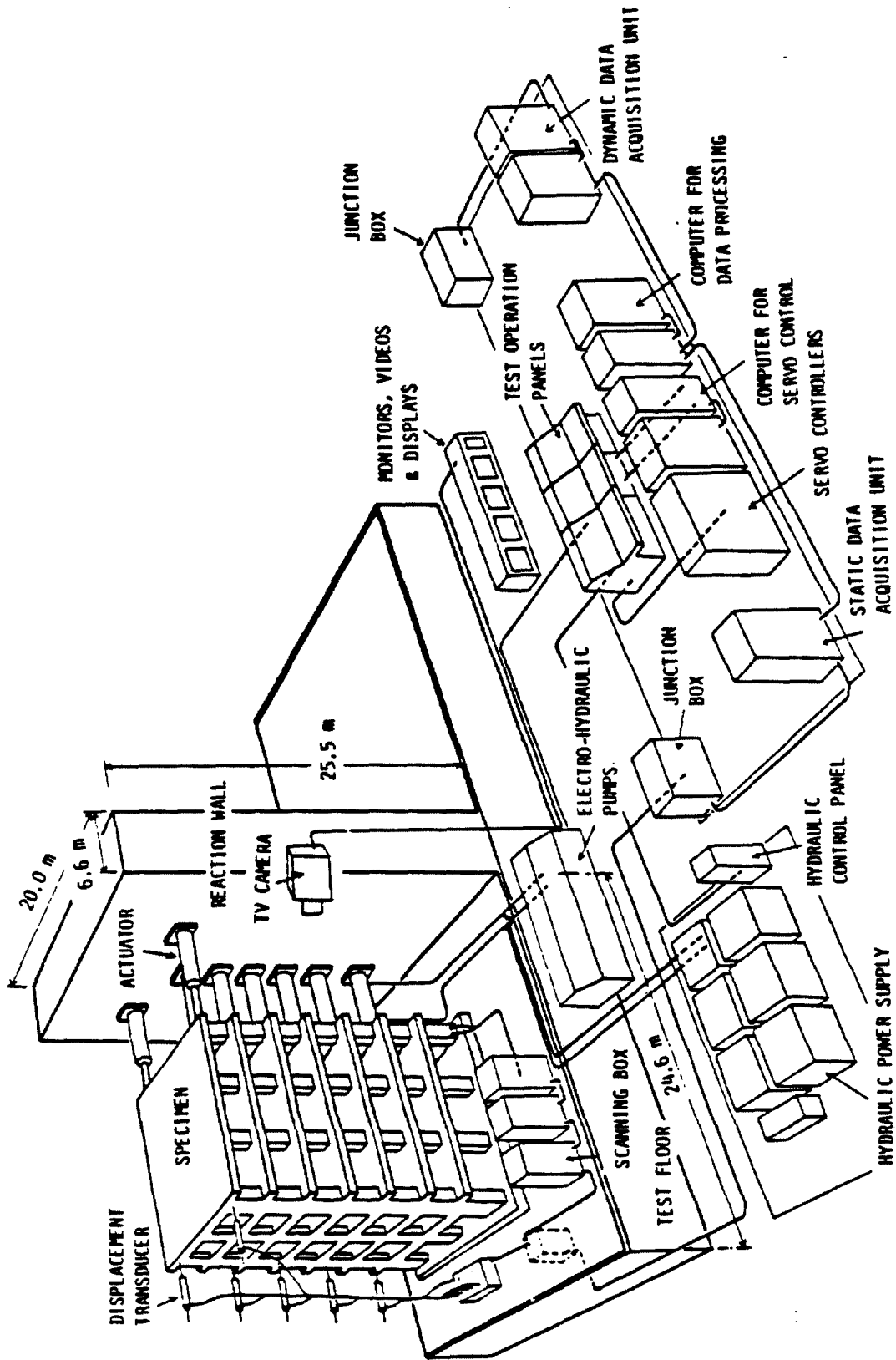
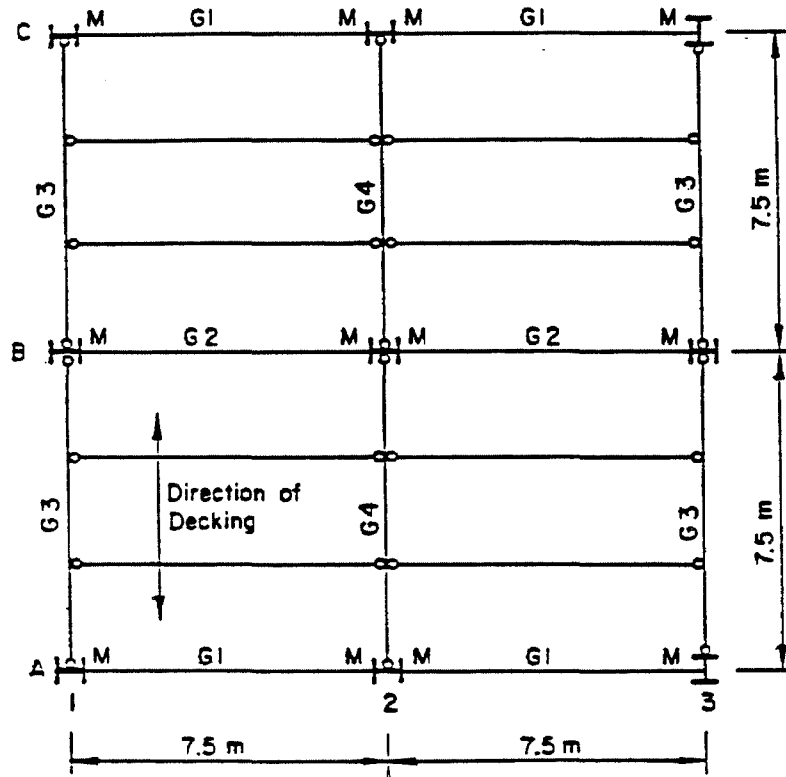


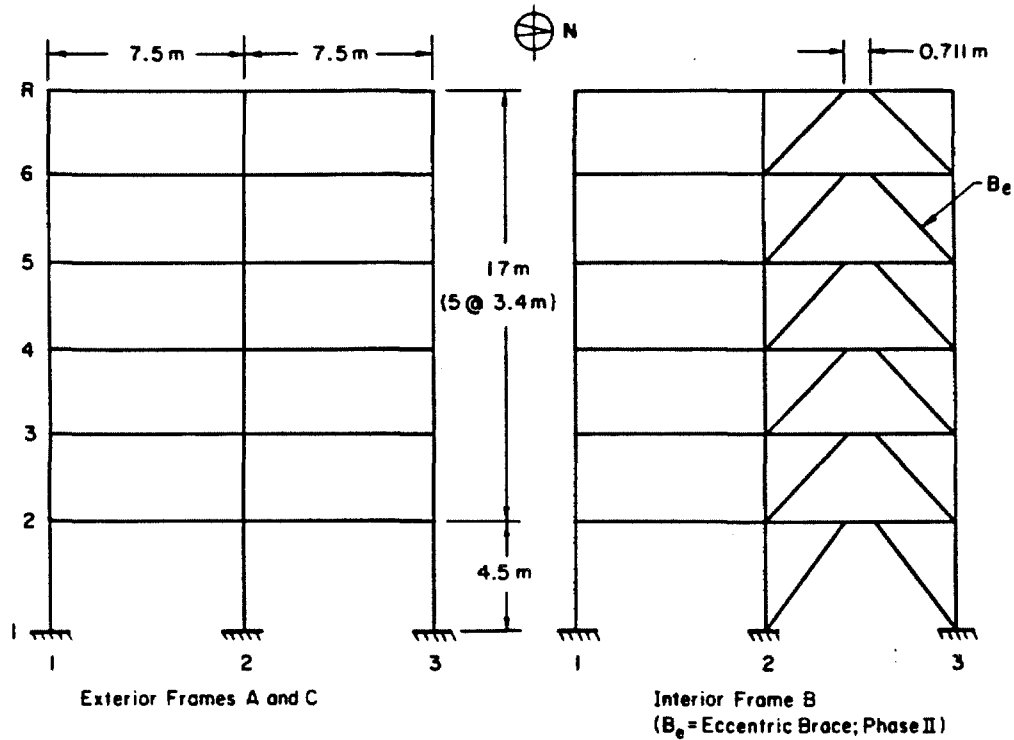
Figure 5.2 Pseudo-dynamic testing facility at Building Research Institute, Tsukuba, Japan [15].

Direction of Loading

S \longleftrightarrow N



M — Moment Connection
 ○ — Shear Connection



Exterior Frames A and C

Interior Frame B
 (B_e = Eccentric Brace; Phase II)

Figure 5.3 Plan (top) and cross-section (bottom) of test structure [16].

range. In the elastic and inelastic tests, the test structure was subjected to the S21W component of the Taft record from the 1952 Kern County, California, earthquake scaled to a peak acceleration of 6.5% and 50%.

The study of the elastic response data using system identification techniques performed by Jayakumar and Beck revealed the cumulative effect of experimental errors inherent in the test [17-20]. They observed that a negative damping present in the third mode and the accelerations calculated from system identification did not agree well with the test accelerations. The inelastic data have also been analyzed using the response data of all six floors [17,21] based on a shear building idealization with a three-parameter hysteretic model relating the story shear and story drift of each inter-story structure. The algorithm developed involved continual alternating between the steepest descent and the modified Gauss-Newton methods for the simultaneous identification of the optimal parameter values in a $(3N + 1)$ -dimensional space where N is the number of floors. Therefore, the final results were a shear building model with 18 model parameters.

In the next two sections, an analysis of the inelastic test data is performed using the generalized modal identification method. Both nonlinear nonhysteretic and hysteretic models are employed. In marked contrast to most nonlinear system identification approaches, the input and roof response data only are used in the analysis.

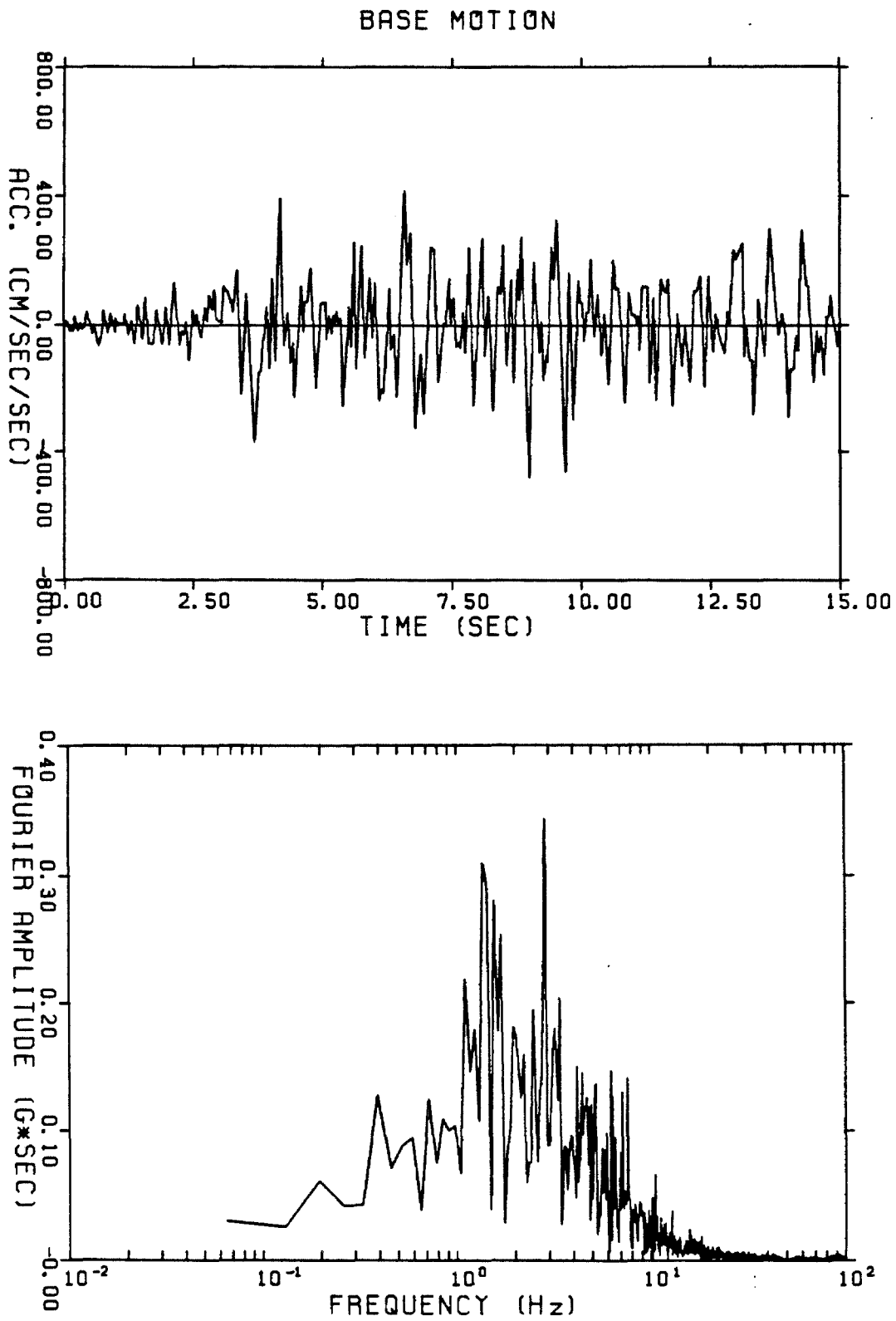


Figure 5.4 Taft S21W accelerogram, 1952 Kern County, California.
(a) Time history (peak = 0.50 g).
(b) Fourier spectrum.

5.4 Four-Parameter Nonhysteretic Model

In the preliminary investigation into the nonlinear behavior of the test structure, the pseudo-dynamic data are analyzed by employing the four-parameter nonparametric model (3.14). The purpose of doing this is to obtain an initial nonhysteretic estimate of the nonlinear behavior.

The test input to the structure is used as the base excitation to the models. The time history and Fourier amplitude spectra are shown in Figure 5.4. The relative acceleration of the roof with respect to the base is used as the response data in the analysis. The length of the pseudo-dynamic test records is 17.1 seconds. The model parameters are estimated for the segment from 0 to 15 seconds.

Observe the Fourier amplitude spectrum of the relative acceleration of the roof in Figure 5.5. The erratic appearance around each dominant frequency peak is typical of the frequency spectra for nonlinear system. However, the dominance of three "modal" frequencies is clearly observed and can be used to estimate the frequency band of each dominant mode. The values of frequency band chosen for the first two dominant modes are summarized in Table 5.1. These values are used to obtain the uncoupled modal response by band-pass filtering as described in Section 2.6.2.

Following the general procedure described in section 2.6, the modal parameters are estimated one mode at a time by a succession of single-mode identifications until a final modal model based on dominant modes is obtained. For each single-mode identification, initial estimates for parameters are not required because the method reduces the problem to single-parameter identification with respect to the effective participation factor β^r . The optimal value for the effective participation factor β^r is determined by a simple one-dimensional nonlinear optimization scheme outlined in Section 2.6.4. For given β^r , the parameters a_i^r , $i = 1, 2, 3, 4$ of the generalized

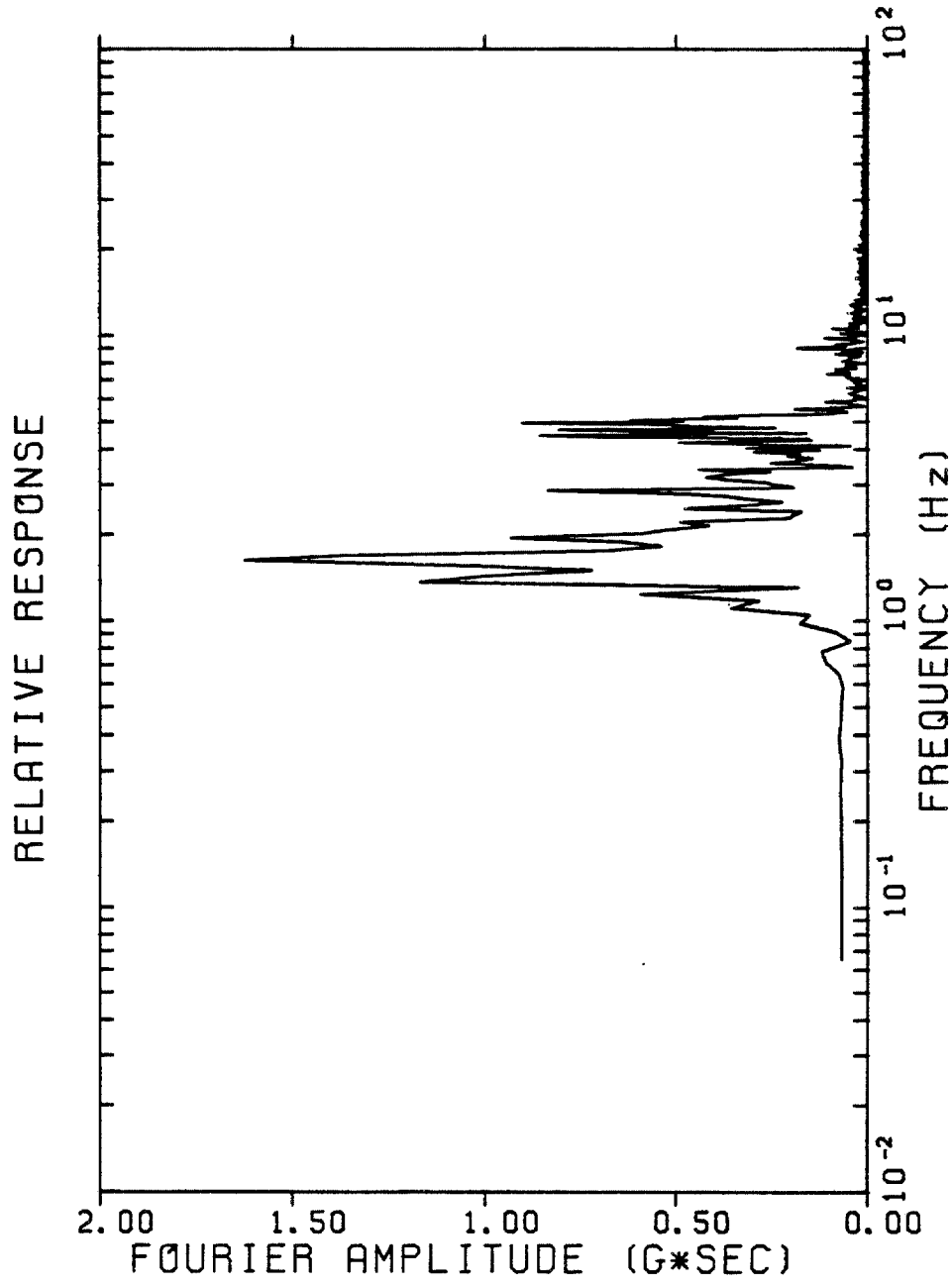


Figure 5.5 Fourier amplitude spectrum of acceleration for response at roof of test structure.

modal restoring force h^r are estimated directly by the nonparametric identification technique outlined in Section 3.4.3.

The optimal modal effective participation factor β^r is considered determined when the difference between the model and system response is minimized. The difference is quantified by an error function P , called the prediction error. As defined in Section 2.5, P is the ratio of the r.m.s. difference at the system response peaks and corresponding model response to the maximum response of the system. The response quantity used in this study is the relative acceleration since it has the richest high frequency content and therefore allows more reliable estimation of the parameters of the high frequency modes. Also, the acceleration time history has relatively more peaks than the velocity and displacement.

Only a two-mode model is determined herein because the signal of the higher modes is very small, as can be observed from Figure 5.5. The optimal model parameters identified by acceleration matching are presented in Table 5.1, including the prediction error P . It is seen from the table that after the second mode has been identified, the prediction error P based on acceleration peaks is 0.146. This indicates a fairly good acceleration match. The negative sign of a_2^1 and a_2^2 indicates the softening behavior of the system stiffness. The equivalent viscous damping increases with velocity amplitude as a consequence of the positive sign of a_4^1 and a_4^2 .

Figure 5.6 illustrates the identified generalized restoring force diagram for the first and second modes. These diagrams exhibit softening stiffness and nonlinear damping behavior which are consistent with the previous observations based on the sign of a_i^r , $i = 1, 2, 3, 4$. Observe that the generalized restoring force for the second mode is comparable to that of the first mode in amplitude. However, the second mode has relatively small generalized displacement.

The test roof response relative to the base is compared with its counterpart

predicted by the identified two-mode model in Figures 5.7-5.9. The solid line is the test response and dashed line represents the response predicted by the model. The quality of the acceleration match of the two mode-model is illustrated in Figure 5.7. Some of the high frequency discrepancies are due partly to the control and measurement errors during the test. Figure 5.8 shows that a fairly good velocity match is obtained even when the model is determined by matching accelerations. It is of interest that the model does not estimate well the peaks of the measured displacement, as observed from Figure 5.9. This cannot be accounted for in the two-mode model solely from the control and measurement errors or from the exclusion of higher modes. A possible explanation for this discrepancy is the hysteretic nature of the response, especially the permanent displacement, which is not identified at all by the model.

In summary, it is seen from the results that the four-parameter nonparametric model with a small number of modes gives a good nonhysteretic estimate of the response time history. However, some discrepancies in the time history, especially in the displacement, are observed. This cannot be explained solely by the experimental errors or the exclusion of higher modes in the model. It is thought that the main reason is that the hereditary nature of the structural response has not been identified since the model employed herein has no mechanism with which the hystertic behavior can be modeled.

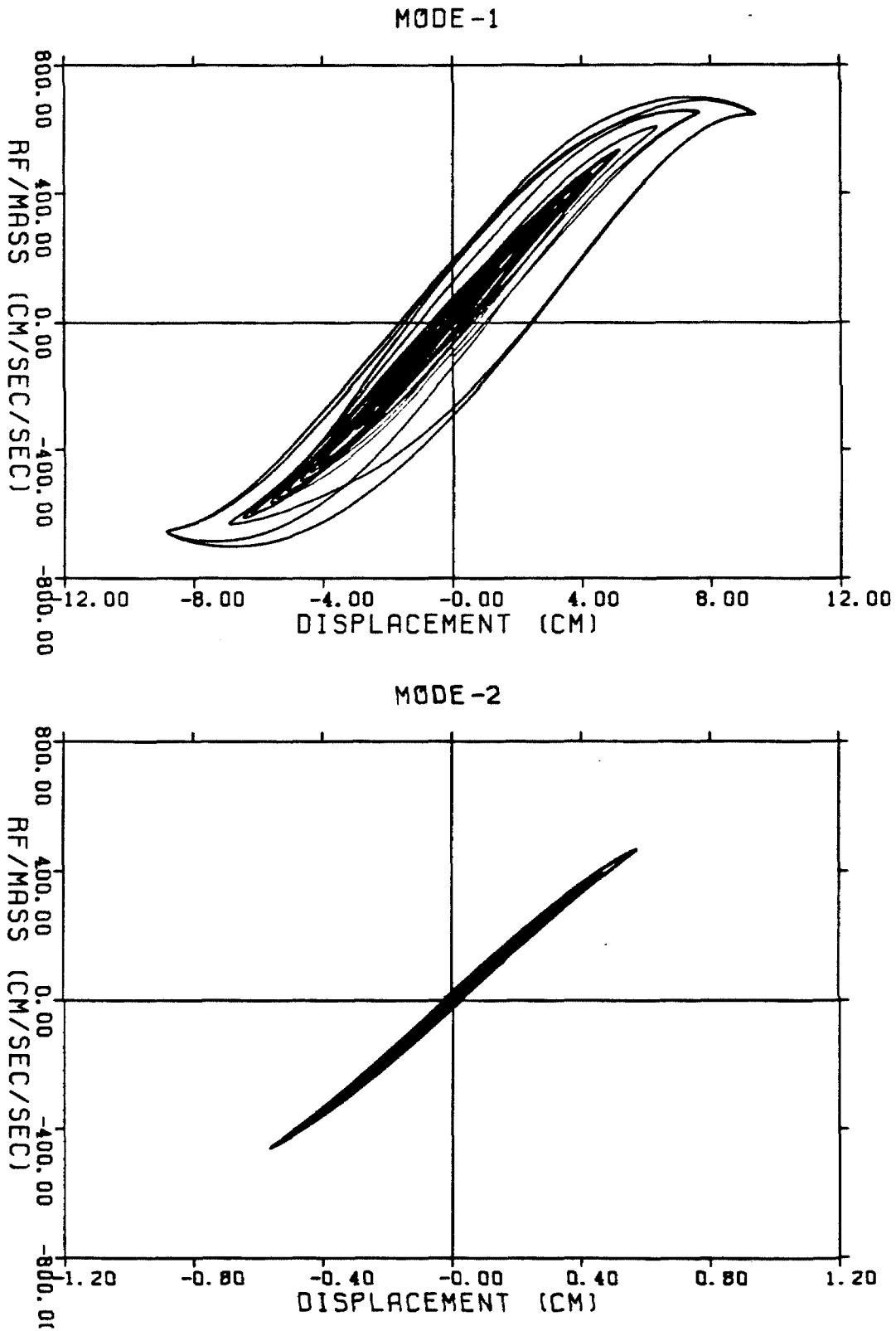


Figure 5.6 Generalized modal restoring force diagrams for identified four-parameter nonhysteretic model of test structure.
(a) First mode.
(b) Second mode.

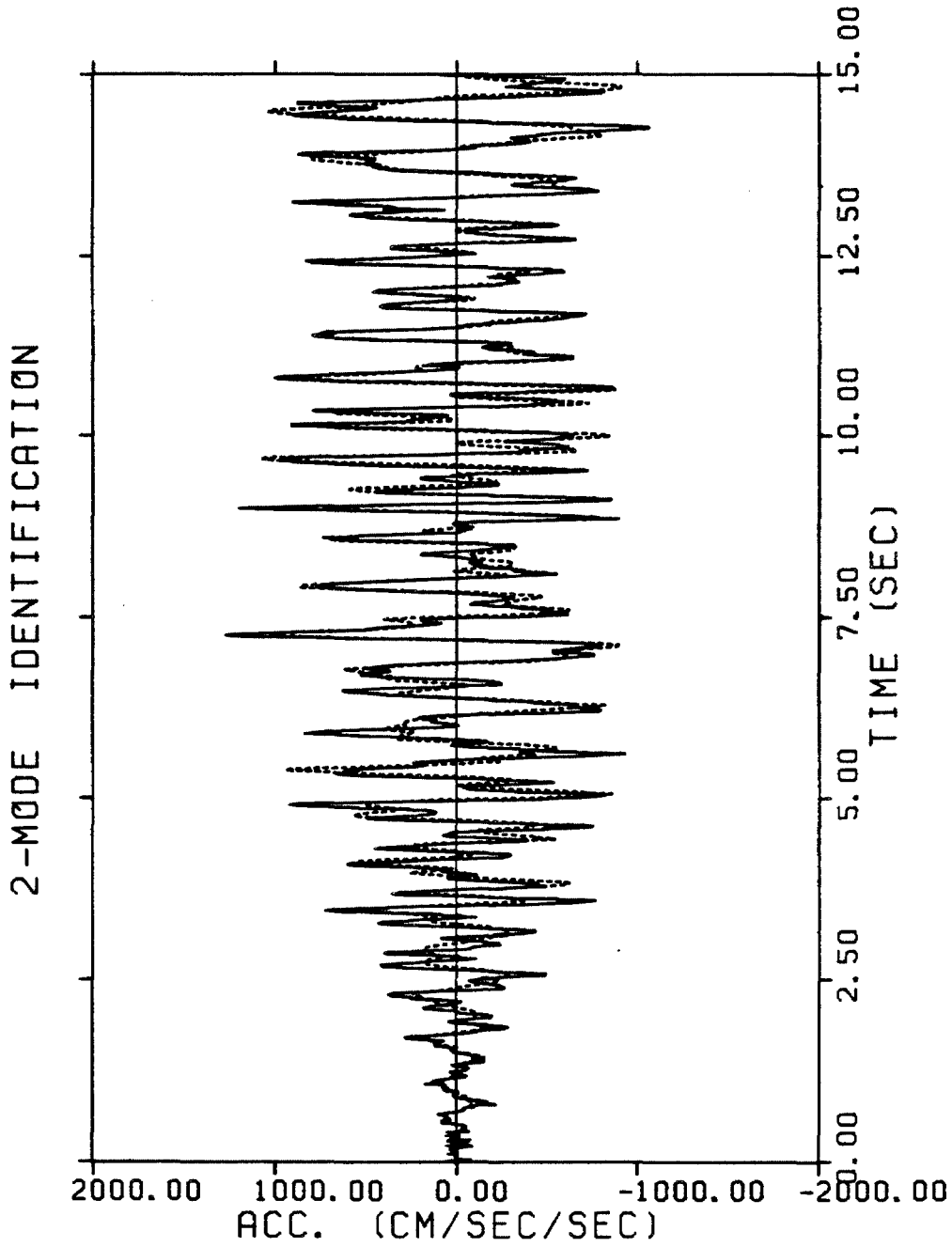


Figure 5.7 Identification of relative acceleration at roof of test structure. Pseudo-dynamic response (—), optimal four-parameter nonhysteretic model with two modes (- - -).

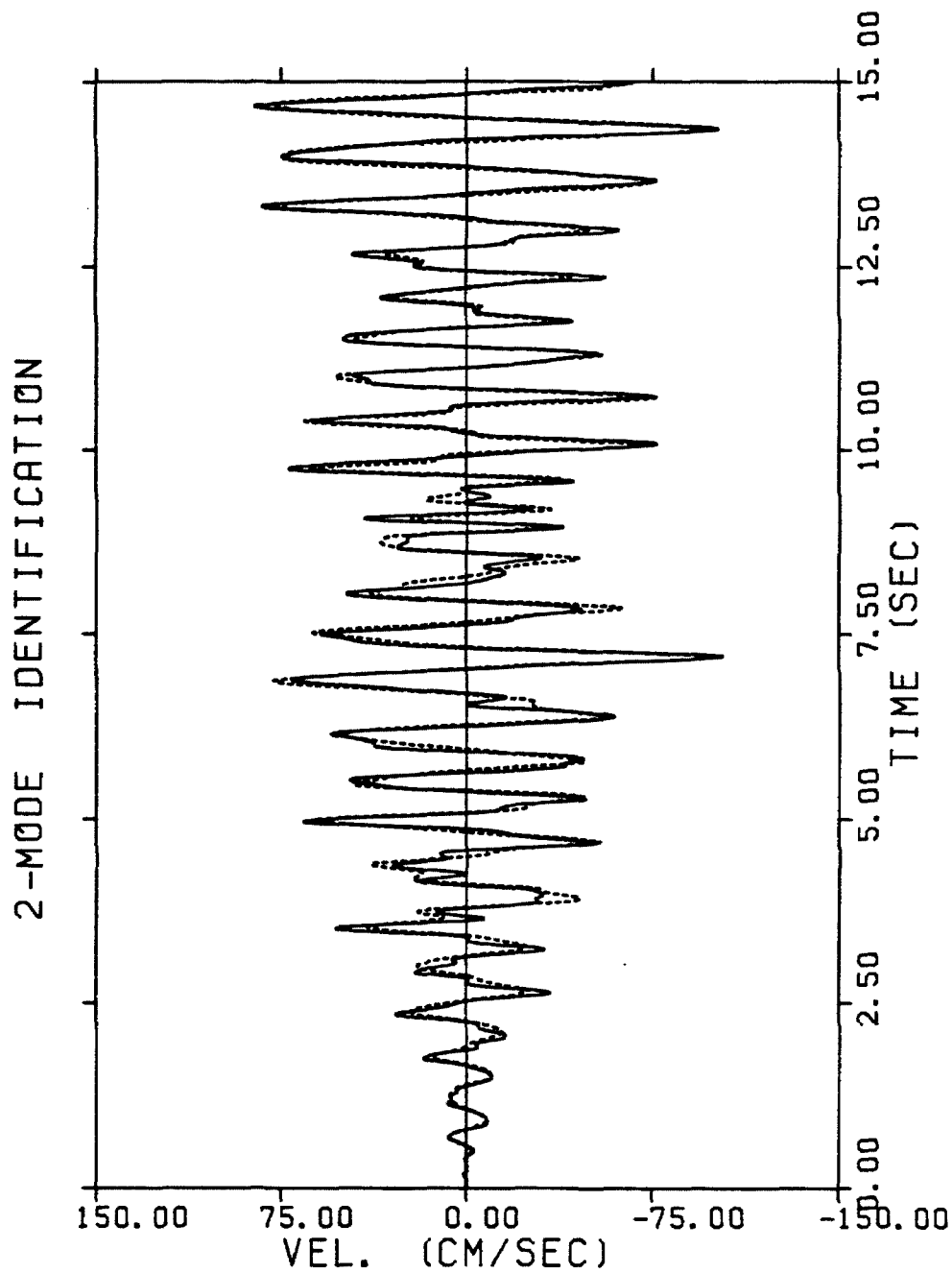


Figure 5.8 Identification of relative velocity at roof of test structure. Pseudo-dynamic response (—), optimal four-parameter nonhysteretic model with two modes (- - -).

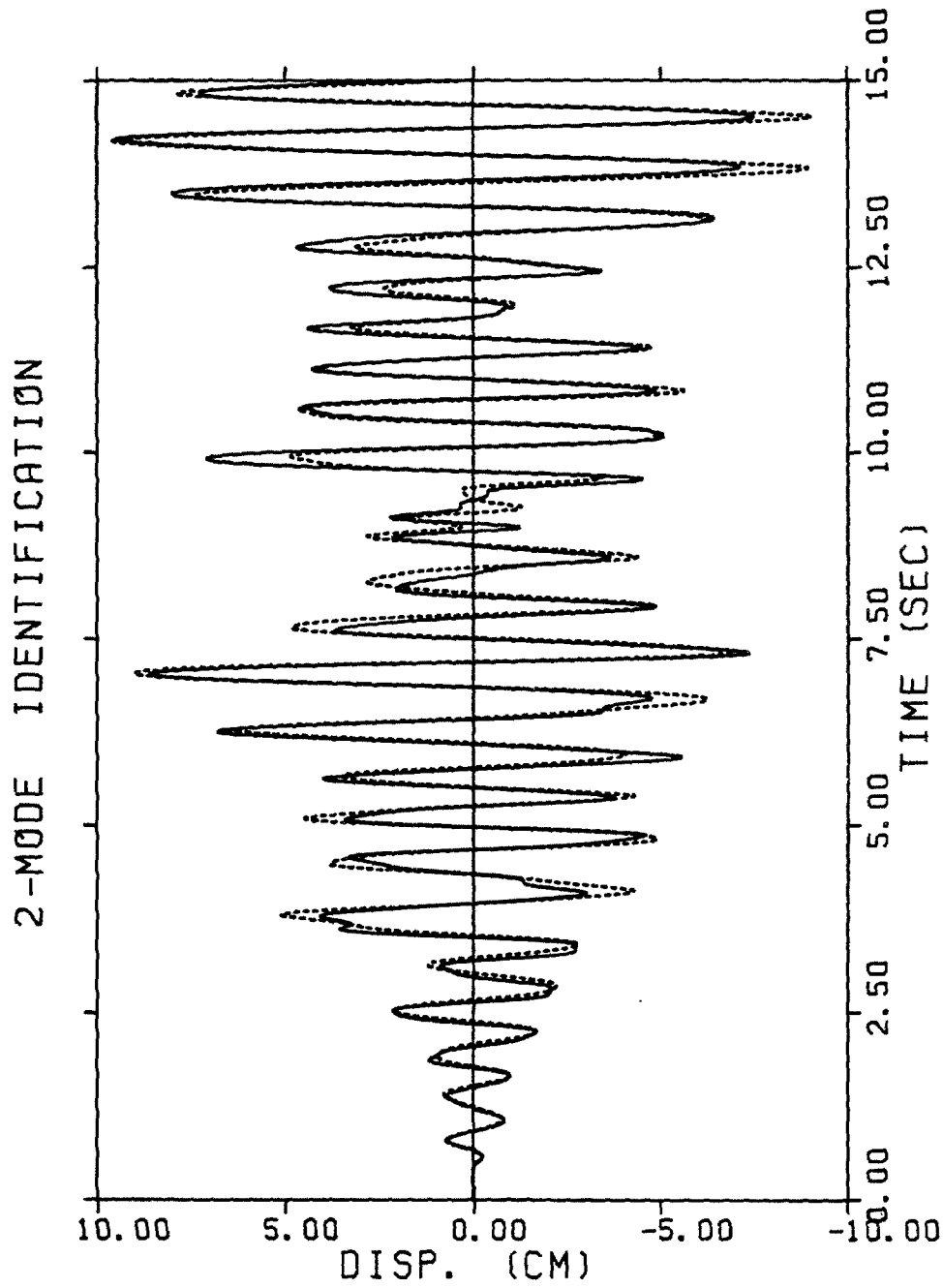


Figure 5.9 Identification of relative displacement at roof of test structure. Pseudo-dynamic response (---), optimal four-parameter nonhysteretic model with two modes (—).

5.5 Two-Parameter Hysteretic Model

In order to identify the hysteretic behavior of the test structure, the two-parameter distributed-element model (4.8) is employed in the generalized modal identification method to obtain the final hysteretic model. This is done to extract the hysteretic nature of the response and to improve the agreement with the test response, especially the displacement. The identification approach when used with simulated data has been presented in Chapter 4.

The same pseudo-dynamic test data and values of frequency band for the first two dominant modes are chosen as in the nonparametric identification. These values are used to estimate the uncoupled modal response as described in Section 2.6.2. In this study, the modal responses are identified by the two-parameter distributed-element model.

The general identification procedure of Section 2.6 is followed. The value for the effective participation factor β^r is optimized as outlined in Section 2.6.4. For given β^r , the parameters b_i^r , $i = 1, 2$, for the generalized modal restoring force h^r are estimated by a parametric identification technique outlined in Section 4.4.4. However, the efficiency and convergency of the parameter optimization process are greatly improved because some parameters can be estimated from the results of the previous nonparametric identification.

The results for the optimal two-mode model determined by matching the relative acceleration are summarized in Table 5.2 and compared with previous nonparametric identification results herein. It is seen that the model parameters identified during the initial stage of nonparametric identification are generally very close to the optimal parameters of the parametric model. This supports the point made above regarding the closeness of the optimal model parameters and their initial estimates obtained from the nonparametric identification.

The softening stiffness behavior of the backbone curve is indicated by the sign

of the parameter b_2^2 for both modes. This is also shown in the identified generalized modal restoring force diagrams of Figure 5.10. The general features of the hysteresis loops are quite similar to those of the four-parameter nonparametric model shown in Figure 5.6.

The actual roof time history is compared with its counterpart predicted by the hysteretic model in Figure 5.11-5.13. In general, the agreement in response, especially in displacement, is better than previous results. This is due to the fact that the hysteretic nature of the response can be identified by the hysteretic model employed herein.

Based on the identified generalized restoring force and linear mode shape of the first mode, an estimation of the inter-story restoring force behavior is attempted. The mass distribution and the mode shape of the first mode from references [17,22] are used. The values from the roof to the first floor are:

$$m_i = 0.077, 0.090, 0.090, 0.090, 0.090, 0.095 \text{ ton}$$

$$\phi_i^1 = 1.40, 1.22, 1.01, 0.78, 0.53, 0.30 .$$

Inter-story restoring force diagrams obtained from the pseudo-dynamic test are compared with the estimated diagrams in Figures 5.14-5.15. The estimated hysteresis in general is acceptable.

All the results clearly show that the two-parameter distributed-element model gives an improved representation of the nonlinear response of the test structure and offers a means to estimate the hysteretic behavior of the inter-story restoring forces. The discrepancy in the time history of response, especially in the displacement, is reduced. Considering the fact that the two-parameter distributed-element model has less number of parameters than does the four-parameter nonparametric model, it is thought that the main reason for this improvement is that the hysteretic nature of the response has been identified.

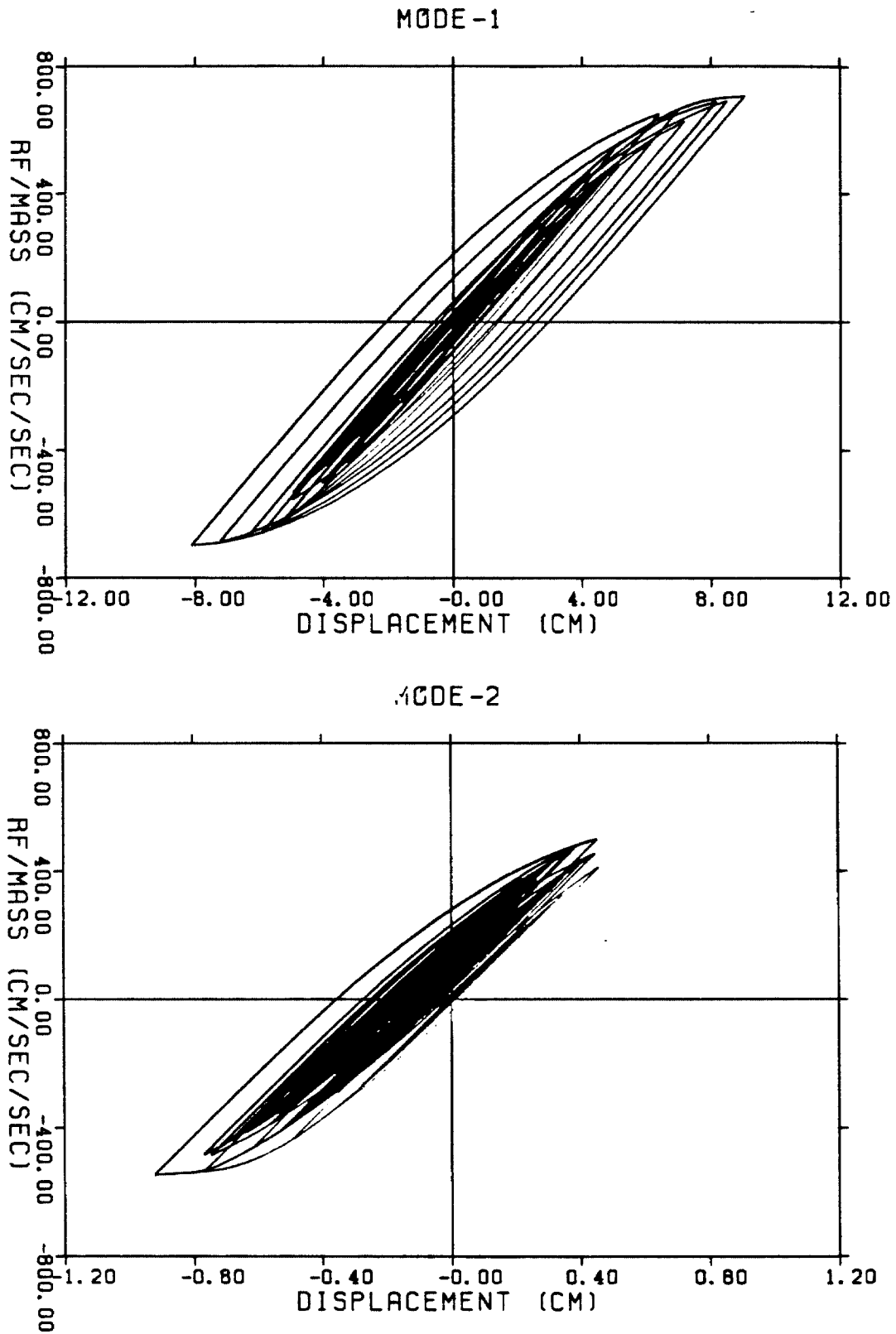


Figure 5.10 Generalized modal restoring force diagrams for identified two-parameter distributed-element hysteretic model of test structure.
(a) First mode.
(b) Second mode.

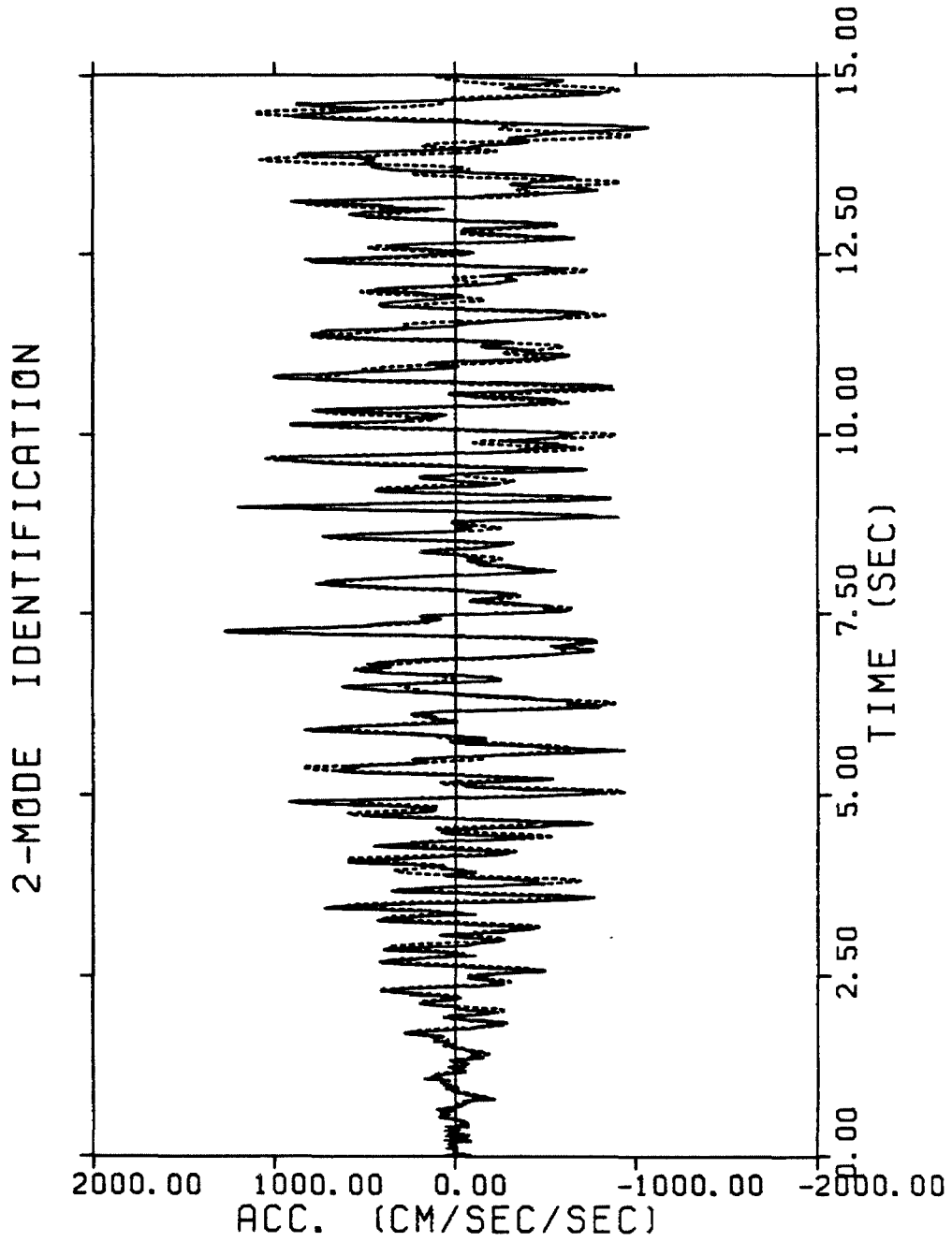


Figure 5.11 Identification of relative acceleration at roof of test structure. Pseudo-dynamic response (—), optimal two-parameter distributed-element hysteretic model with two modes (- - -).

2-MODE IDENTIFICATION

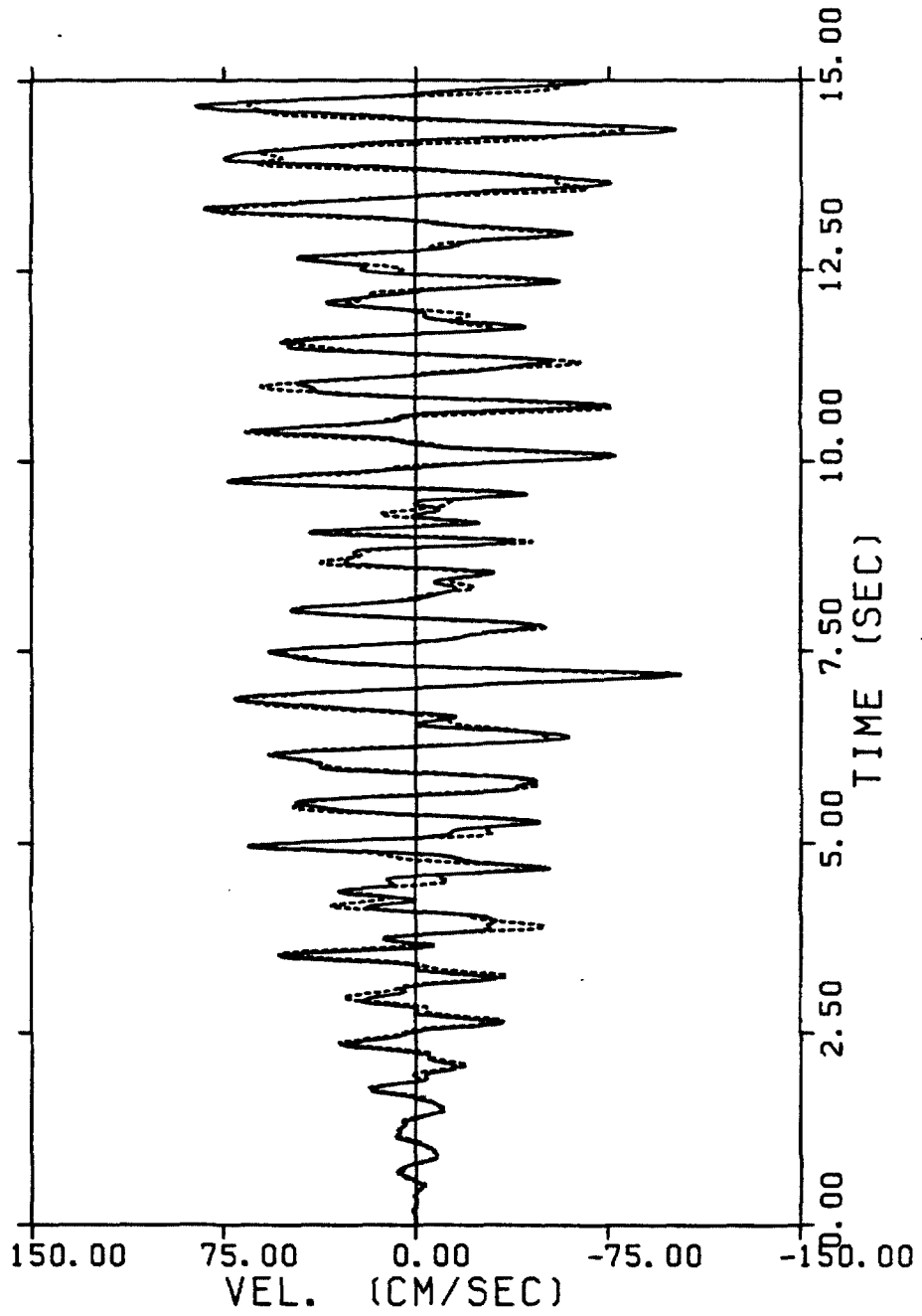


Figure 5.12 Identification of relative velocity at roof of test structure. Pseudo-dynamic response (—), optimal two-parameter distributed-element hysteretic model with two modes (- - -).

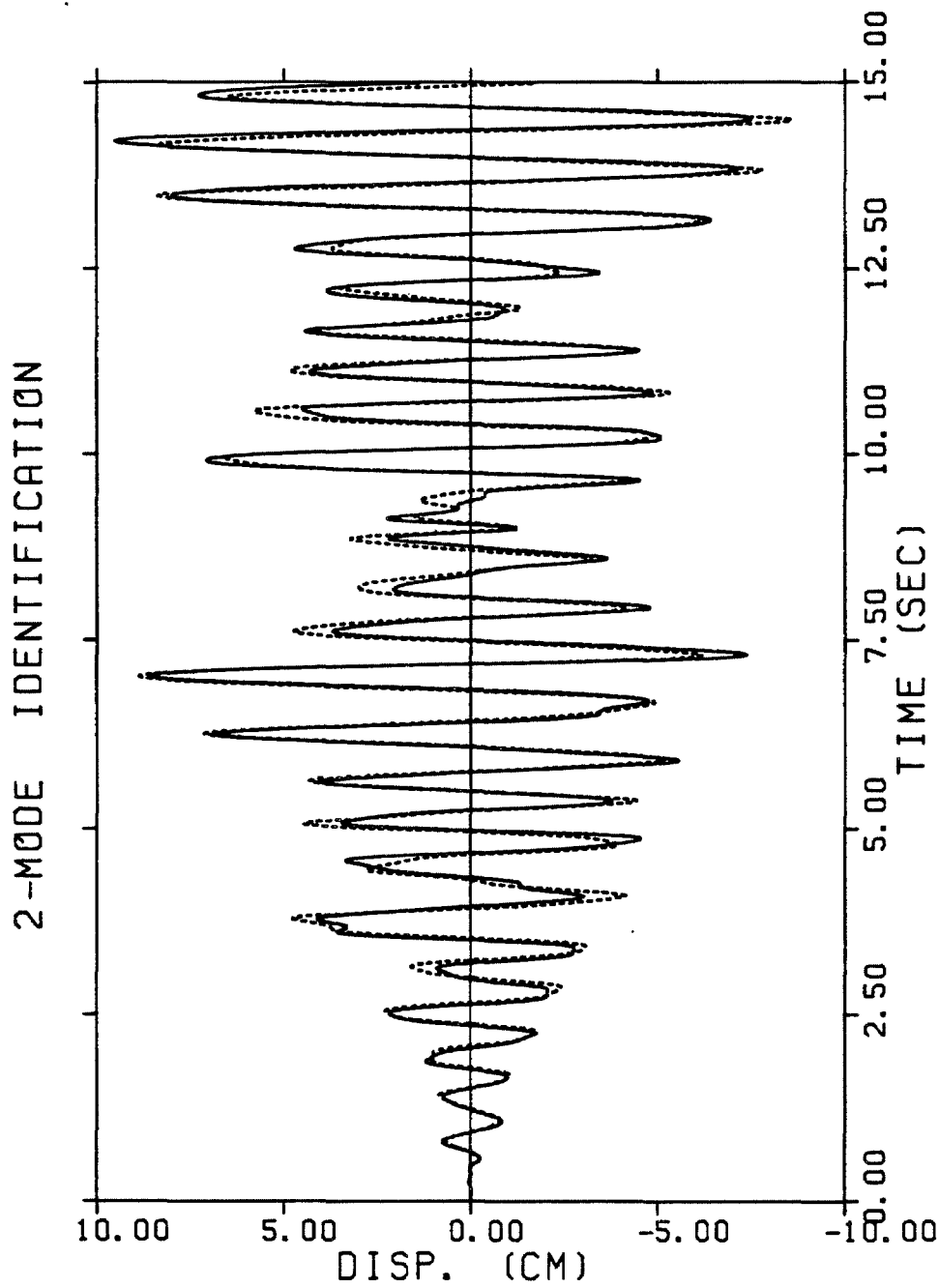


Figure 5.13 Identification of relative displacement at roof of test structure. Pseudo-dynamic response (---), optimal two-parameter distributed-element hysteretic model with two modes (- - -).

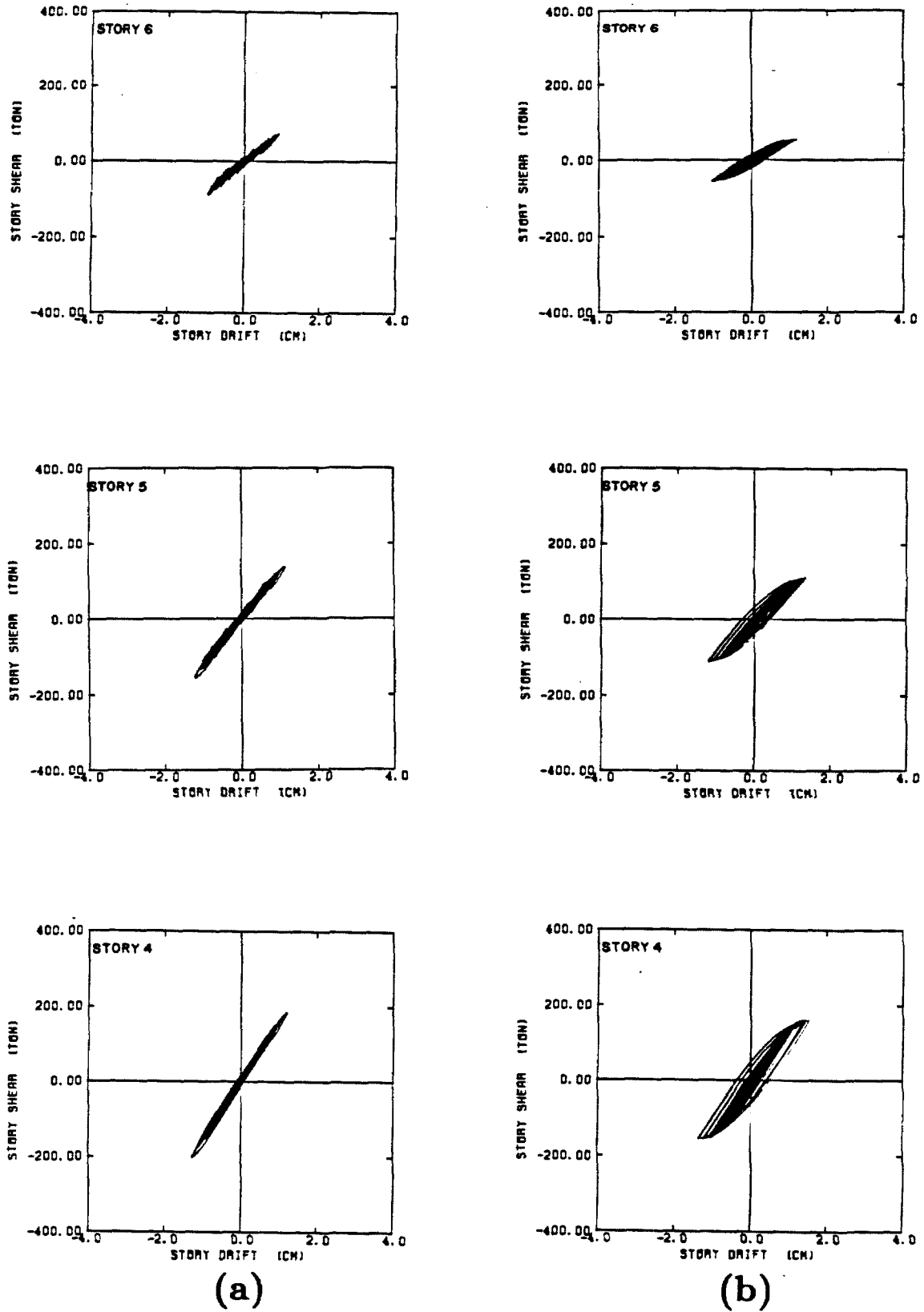


Figure 5.14 Comparison of inter-story restoring force behavior.
(a) Experimental hysteresis loops [17].
(b) Estimated hysteresis loops.

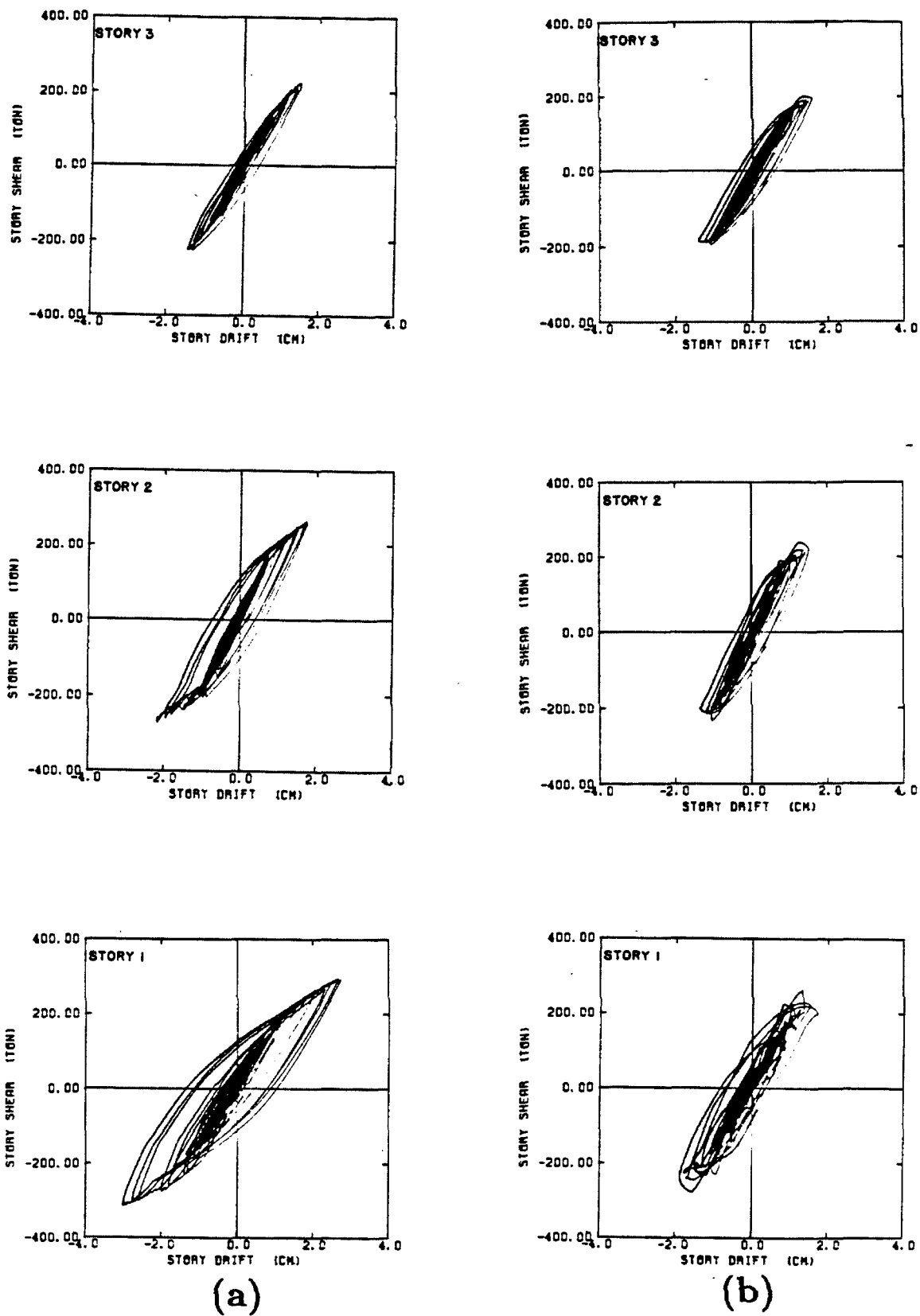


Figure 5.14 (continued) Comparison of inter-story restoring force behavior.
(a) Experimental hysteresis loops [17].
(b) Estimated hysteresis loops.

Mode	Frequency Band (Hz)	a_1^r (1/sec ²)	a_2^r 1/(cm · sec) ²	a_3^r (1/sec)	a_4^r (sec/cm ²)	β^r	P
1	0.0-3.2	1.17×10^2	-5.56×10^{-1}	$.470 \times 10^{-1}$	2.84×10^{-4}	1.218	1.81×10^{-1}
2	3.2-6.5	9.15×10^2	-3.11×10^2	1.05×10^0	1.83×10^{-3}	-0.345	1.46×10^{-1}

Table 5.1 Identification Results of the Four-Parameter Nonhysteretic Model Using Pseudo-Dynamic Test Data

Mode	Frequency Band (Hz)	b_1^r (1/sec ²)		b_2^r 1/(cm · sec) ²		β^r		P
		Initial	Optimal	Initial	Optimal	Initial	Optimal	
1	0.0-3.2	1.17×10^2	1.20×10^2	-5.56×10^{-1}	-5.46×10^{-1}	1.218	1.114	1.80×10^{-1}
2	3.2-6.5	9.15×10^2	1.00×10^3	-3.11×10^2	-5.43×10^2	-0.345	-0.537	1.60×10^{-1}

Table 5.2 Identification Results of the Two-Parameter Distributed-Element Hysteretic Model Using Pseudo-Dynamic Test Data

5.6 Summary

Inelastic pseudo-dynamic test data are analyzed using the generalized modal identification method incorporating two simple nonlinear models, in order to examine the applicability of the method and the models to a real structure. In marked contrast to most nonlinear system identification methods developed so far, only two test records, one at the base of the structure and the other at the roof, are used to determine the optimal nonlinear models. The final hysteretic model exploits the results from nonparametric identification as an initial estimate for the model parameters. This approach greatly improves the efficiency and convergence of the subsequent nonlinear optimization process.

Of the two simple models identified to describe the nonlinear response of the steel structure tested by the pseudo-dynamic method, the better agreement is achieved by the use of a two-parameter distributed-element hysteretic model. Due to two more parameters in the nonhysteretic model, the four-parameter nonparametric model fits the acceleration slightly better. However, this model is not capable of duplicating the displacement response nearly so well as the hysteretic model. The nonhysteretic model does give maximum response close to those observed in this particular test, however, due to the fact that the hysteretic nature of the system is not identified, its use might not provide valid information in predicting the response of the hysteretic system to other excitations.

On the basis of all the results in this chapter, it was shown that the simple two-parameter relationship for the backbone of the distributed-element model is sufficient to capture the essential features of the hysteretic behavior of the generalized modal restoring force for the steel structure. Also, the two-parameter distributed-element model with a small number of modes provides a fully hysteretic structural model which characterizes the nonlinear response of the test structure.

References

- [1] K. Takanashi, et al., "Nonlinear Earthquake Response Analysis of Structures by a Computer-Actuator On-Line System," *Bulletin of Earthquake Resistant Structure Research Center*, No. 8, Institute of Industrial Science, University of Tokyo, Japan, December 1974.
- [2] K. Takanashi, K. Udagawa and H. Tanaka, "A Simulation of Earthquake Response of Steel Buildings," *Proceedings of the 6th World Conference on Earthquake Engineering*, New Delhi, India, January 1977.
- [3] K. Takanashi, K. Udagawa and H. Tanaka, "Earthquake Response Analysis of a 1-Bay 2-Story Steel Frame by Computer-Actuator On-Line System," *Bulletin of Earthquake Resistant Structure Research Center*, No. 11, Institute of Industrial Science, University of Tokyo, Japan, December 1977.
- [4] K. Takanashi, K. Udagawa and H. Tanaka, "Pseudo-Dynamic Tests on a 2-Story Steel Frame by Computer-Load Test Apparatus Hybrid System," *Proceedings of the 7th World Conference on Earthquake Engineering*, Istanbul, Turkey, September 1980.
- [5] K. Takanashi, K. Udagawa and H. Tanaka, "Pseudo-Dynamic Tests on Frames Including High Strength Bolted Connections," *Proceedings of the 7th World Conference on Earthquake Engineering*, Istanbul, Turkey, September 1980.
- [6] E. P. Popov, "Experiment as an Aid to Structural Seismic Design," *Experimental Mechanics*, Vol. 26, No. 2, June 1986.
- [7] P-S B. Shing and S. A. Mahin, "Experimental Error Propagation in Pseudo-dynamic Testing," Report No. UCB/EERC 83/12, Earthquake Engineering Research Center, University of California, Berkeley, California, June 1983.
- [8] P-S B. Shing and S. A. Mahin, "Pseudo-Dynamic Test Method for Seismic Performance Evaluation: Theory and Implementation," Report No. UCB/EERC 84/01, Earthquake Engineering Research Center, University of California, Berkeley, California, January 1984.
- [9] S. A. Mahin and P-S B. Shing, "Pseudodynamic Method for Seismic Testing," *ASCE Journal of Structural Division*, Vol. 111(7), July 1985.
- [10] P-S B. Shing and Stephen A. Mahin, "Computational Aspects of a Seismic Performance Test Method Using On-Line Computer Control," *International Journal of Earthquake Engineering and Structural Dynamics*, Vol. 13, 1985.
- [11] P-S B. Shing and Stephen A. Mahin, "Cumulative Experimental Errors in Pseudo-Dynamic Tests," *International Journal of Earthquake Engineering and Structural Dynamics*, Vol. 15, May 1987.

- [12] P-S B. Shing and Stephen A. Mahin, "Elimination of Spurious Higher-Mode Response in Pseudo-Dynamic Tests," *International Journal of Earthquake Engineering and Structural Dynamics*, Vol. 15, May 1987.
- [13] D. A. Foutch, et al., "Construction of Full Scale Six Story Steel Test Structure," 4th U.S.-Japan Joint Technical Coordinating Committee Meeting, Tsukuba, Japan, June 1983.
- [14] H. Yamanouchi, et al., "Experimental Results on a K-Braced Steel Structure under Seismic Loading Utilizing Full-Scale Six-Story Test Structure," Proceedings of Annual Technical Session of SSRC, San Francisco, California, 1984.
- [15] S. Okamoto, et al., "Techniques for Large Scale Testing at BRI Large Scale Structure Test Laboratory," Research Paper No. 101, Building Research Institute, Ministry of Construction, May 1983.
- [16] G. Askar, S. J. Lee and L-W Lu, "Design Studies of the Six Story Steel Test Building: U.S.-Japan Cooperative Earthquake Research Program," Report No. 467.3, Fritz Engineering Laboratory, Lehigh University, Bethlehem, Pennsylvania, June 1983.
- [17] P. Jayakumar, "Modeling and Identification in Structural Dynamics," Report No. EERL 87-01, Earthquake Engineering Research Laboratory, California Institute of Technology, Pasadena, California, May 1987.
- [18] J. L. Beck and P. Jayakumar, "Analysis of Elastic Pseudo-Dynamic Test Data from a Full-Scale Steel Structure Using System Identification," *Proceedings of the 6th Joint Technical Coordinating Committee Meeting*, U.S.-Japan Cooperative Research Program Utilizing Large-Scale Testing Facilities, Maui, Hawaii, June 1985.
- [19] J. L. Beck and P. Jayakumar, "System Identification Applied to Pseudo-Dynamic Test Data: A Treatment of Experimental Errors," *Proceedings of the 3rd ASCE Engineering Mechanics Specialty Conference on Dynamic Response of Structures*, University of California, Los Angeles, California, April 1986.
- [20] J. L. Beck and P. Jayakumar, "Application of System Identification to Pseudo-Dynamic Test Data from a Full-Scale Six-Story Steel Structure," *Proceedings of the International Conference on Vibration Problems in Engineering*, Xian, China, June 1986.
- [21] J. L. Beck and P. Jayakumar, "Pseudo-Dynamic Testing and Model Identification," *Proceedings of the 3rd U.S. National Conference on Earthquake Engineering*, Charleston, South Carolina, August, 1986.
- [22] M. K. Boutros and S. C. Goel, "Pre-Test Analysis of the Six-Story Eccentric-Braced Steel Test Building," *Proceedings of the 5th Joint Technical Coordinating Committee Meeting*, U.S.-Japan Cooperative Research Program Utilizing

Large-Scale Testing Facilities, Tsukuba, Japan, February 1984.

Chapter 6

Conclusions

A relatively simple and accurate system identification method has been presented in this thesis that is suitable for use with multi-degree-of-freedom nonlinear hysteretic dynamic systems under the action of base motion. The method considers the situation in which only the base input and the response of a small number of degrees-of-freedom in the system are measured. The main objective of this study has been the identification and modeling of the behavior of structural dynamic systems in the nonlinear hysteretic response regime. Once a model for the system has been identified, it is intended to use this model to assess structural damage and to predict response of the structure to future excitations. A general synopsis of the work performed in the preceding chapters is presented herein.

In Chapter 2 a new methodology, called the generalized modal identification method, is formulated for determining an optimal model of a general nonlinear dynamical system from its measured base excitation and response. The method is based on the separation of the response into "modes" which are analogous to those of a linear system. Once the response of each mode has been estimated and the participation factor assumed, the generalized restoring force for each mode is readily obtained.

Various nonparametric or parametric models can be used to extract the unknown nature of system nonlinearity, hysteretic or nonhysteretic. By matching the obtained restoring force directly, the solution of nonlinear differential equations of motion may be avoided at this stage of the identification. Consequently, the methodology reduces the identification problem to the determination of the effective participation factor for each mode. This can be performed by means of any simple one-dimensional optimization scheme. The difficulties of multi-variable

nonlinear optimization are thereby avoided.

The optimality criterion employed throughout is based on minimizing the r.m.s. of the difference between the actual system and model response at the peaks of time histories only. By satisfying this criterion, the model identified is one which best describes the peaks of system response which are generally the points of greatest engineering significance in the response time history.

The new identification methodology proposed results in considerable computational efficiency without sacrificing accuracy. The information obtained is useful for characterizing the nonlinear behavior of structures and for predicting structural response to future excitations.

The main features of this identification methodology are:

- (1) Various restoring force models can be incorporated in the method to identify virtually any type of nonlinear system characteristics. Hysteretic systems, which pose problems for most identification techniques, can be easily handled by the present approach in a unified framework.
- (2) In marked contrast to most nonlinear system identification methods, the measurements required are the base motion and response at only one location in the system. Furthermore, the method requires no information regarding the estimates of mass distribution and pertinent "mode shapes" of the system.
- (3) Convergence of the associated nonlinear optimization algorithm is fast because the problem has been reduced to determining only an optimal estimate of the effective modal participation factor. This process can be performed with any simple one-dimensional nonlinear optimization scheme with resulting computational efficiency.
- (4) The computational requirements, both in terms of CPU time as well as storage, are very small for the characterization of a general nonlinear system.

- (5) There is no practical limitation on the nature of probing signal that can be used for identification.
- (6) The identified generalized modal restoring force models allow one not only to obtain valuable physical insight into the nonlinear stiffness and energy dissipation behavior of the system but also to assess the condition of the system and to predict its response to other excitations.
- (7) The identification results obtained are relatively insensitive to measurement noise due to the use of r.m.s. error measure based on response peaks since at these points the signal to noise ratio is relatively high.

Chapter 3 is concerned with the generalized modal identification method incorporating nonhysteretic restoring force models. Based on model simplicity and computational considerations, a particular nonlinear nonhysteretic model with only four terms is introduced. This model, called the four-parameter nonparametric model, is a truncated form of a more general class of nonparametric models. The simplicity of the model makes it easy to illustrate the role of nonparametric techniques in the preliminary identification studies of hysteretic systems.

The parameters of the model are determined by approximating the generalized modal restoring force in the sense of least-squares. This identification technique involves no iterative nonlinear optimization process and requires no solution of nonlinear equations of motion. Hence, additional computational saving is attained.

The validation of the identification algorithm and the model are performed with simulated data. Three different scaled earthquake accelerograms are selected as a broad-band base excitation to generate response data for a nonlinear hysteretic system. The first accelerogram is used to identify the system. The second and third are used to study the prediction capability of the identified model. The characteristics of the third scaled earthquake are selected to be quite different from those of the first and second excitations and the corresponding response exhibits

more significant hysteretic behavior.

From the results of the verification study, it is demonstrated that the nonhysteretic model has only limited capability for predicting the hysteretic features in the nonlinear response; for example, the permanent displacement of the response. However, the identified model provides a good estimate of the nonlinear stiffness and energy dissipation behavior of the system. Hence, the nonparametric identification results can be exploited to suggest the parametric form of the final hysteretic model which should be used and to provide a priori estimates of the model parameters which should be selected.

Motivated by the above observations, in Chapter 4 the generalized modal identification method incorporating hysteretic restoring models is studied. A physically motivated model, called the two-parameter distributed-element model, is proposed. The backbone relationship of the model is characterized by only two parameters which are based on insight obtained from the previous nonparametric studies.

The relationship between the backbone and hysteresis loops are determined by the physical nature of the model which is consistent with Masing's hypothesis. Thus, no mathematical rules are necessary to assure the physical behavior of hysteresis under various loading histories.

This model employs the results of the previous nonparametric identification as an initial estimate for the model parameters. Since the nonhysteretic estimate of the model parameters obtained from the nonparametric identification study using the four-parameter model is generally very close to the optimal estimate, this approach greatly improves the convergence and efficiency properties of the subsequent parameter optimization process.

The identification algorithm together with the model are verified using the same simulated data as in Chapter 3. The model predictions for the hysteretic features of the response time histories, including the permanent displacement, are

greatly improved. The excellent identification/prediction capability of the present approach emphasizes the importance of choosing an appropriate hysteresis model in the generalized modal identification method to extract the hysteretic nature of a nonlinear system.

In Chapter 5, the generalized modal identification method is applied to the analysis of inelastic response data obtained from the U.S.-Japan cooperative pseudo-dynamic test of a full-scale six-story steel-frame structure. The analysis employs only two test records, one at the base of the structure and the other at the roof. Both four-parameter nonhysteretic and two-parameter distributed-element hysteretic models are identified. The latter model exploits the results from the former as an initial estimate for the model parameters. This approach again results in considerable saving of computational effort to find appropriate starting values for the optimization process.

From the identification results, it is shown that a better description of the hysteretic response is obtained with the use of a two-parameter hysteretic model. Without extracting the hysteretic nature of the system, the identified nonhysteretic model will not provide valid predictions of the response to other excitations. In contrast, the identified hysteretic model will have better capability for response prediction.

This application example shows that the simple two-parameter backbone relationship is sufficient to capture the main hysteretic behavior of the generalized modal restoring force for a real steel structure. Furthermore, the two-parameter distributed-element model with a small number of modes gives an accurate representation of the hysteretic behavior of the structure.

Based on the verification and application studies performed in this thesis, the new system identification method has been found to be both accurate and computationally efficient. It is believed that it will provide a useful tool for the analysis

of structural response data.